Investigating the Role of Nuclear Import Protein, Karyopherin β1 Secreted by Cancer Cells

Alex Whitehouse

WHTALE010

Dissertation submitted in fulfillment of the requirements for the degree of

MSc (Med) in Medical Biochemistry

In the Division of Medical Biochemistry and Structural Biology

Department of Integrative Biomedical Sciences

Faculty of Health Sciences

University of Cape Town

May 2024

Plagiarism Declaration

1. I know that plagiarism is wrong. Plagiarism is to use another's work and pretend that it is one's own.
2. I have used the Nature convention for citation and referencing. Each contribution to, and quotation in, this thesis from the work(s) of other people has been attributed, and has been cited and referenced. Any section taken from an internet source has been referenced to that source.
3. This thesis is my own work, and is in my own words (except where I have attributed it to others).
4. I have not allowed, and will not allow, anyone to copy my work with the intention of passing it off as his or her own work.
5. I acknowledge that copying someone else's assignment or essay, or part of it, is wrong, and declare that this is my own work.

Signed by candidate

Signed: 7 May 2024

Acknowledgements

A Masters research project is not something that can be undertaken alone, and especially not a project that has been as challenging as this one. As Marie Curie once said, “The way of progress was neither swift nor easy”, so I would like to acknowledge the people who have supported me throughout, even when it was not swift or easy.

My thanks go to my supervisor, Professor Leaner for her insight and advice. To Dr van der Watt for her invaluable assistance. To the students in Lab 6.01 for making a collaborative and supportive workplace. To Mrs Guzgay and the lab staff for keeping the lab efficiently run. To D-CYPHER, AMI and the Lang imaging facility for the assistance. To the University of Cape Town for funding my Masters studies.

A special thanks must go to my parents, for always supporting my passion for science and to all my loved ones for listening to me talk about my research – even if it’s not something they could relate to or understand.

Finally I would like to thank Henrietta Lacks and all the other patients whose cells have made all this work possible.

Contents

Abbreviations

5-UTR 5’	Untranslated Region
ACTB	Actin cytoplasmic 1, N-terminally processed
ALYREF	THO complex subunit 4
AMF	Autocrine Motility Factor
ATP51F1A	ATP Synthase subunit alpha
BCA	Bicinchoninic Acid
BSA	Bovine Serum Albumin
CCAR1	Cell Division Cycle and Apoptosis Regulator Protein 1
CRM1	Exportin 1
DAF	Decay-Accelerating Factor
DAPI	4′,6-Diamidino-2-Phenylindole
dH_2O	Distilled water
DMEM	Dulbecco’s Modified Eagle Medium
DNA	Deoxyribonucleic Acid
EV	Extracellular Vesicle
FUBP1	Far Upstream Element Binding Protein 1
GAPDH	Glyceraldehyde 3-Phosphate Dehydrogenase
GFP	Green Fluorescent Protein
HCl	Hydrochloric Acid
HIFCS	10% Heat Inactivated Foetal Calf Serum
HIV	Human Immunodeficiency Virus
HPV	Human Papillomavirus
Hsp70	Heat Shock Protein 70
IgG	Immunoglobulin G
IP-MS	Immunoprecipitation Mass Spectrometry
Kpnβ1	Karyopherin Beta 1
Kpnα2	Karyopherin subunit alpha 2
MFG-E8	Milk fat globule-EGF factor 8 protein
mRNA	Messenger RNA
MTT	Methylthialazole Tetrazolium
NF-κB	Nuclear Factor kappa B
NLS	Nuclear Localisation Sequence

NPC	Nuclear Pore Complex
Pap	Papanicolaou
PBS	Phosphate Buffered Saline
PI	Phosphatase inhibitor
Ran	Ras-related nuclear protein
RIPA	Radio-Immunoprecipitation Assay
RNA	Ribonucleic acid
SDS-PAGE	Sodium Dodecyl-Sulfate Polyacrylamide Gel Electrophoresis
SDS	Sodium Dodecyl Sulfate
SEM	Standard Error of the Mean
SILAC	Stable Isotope Labelling by Amino Acids in Cell Culture
SMARCE1	SWI/SNF-related matrix-associated actin-dependent regulator of chromatin subfamily E member 1
STAT3	Signal transducer and activator of transcription 3
TBST	Tris-buffered saline with 0.1% Tween 20 detergent
tRNA	Transfer RNA

%	Percent
°C	Degrees Celsius
kD	Kilodalton
M	Molar
µg	Microgram
mg	Milligram
g	Gram
mL	Millilitre
µL	Microlitre
nm	Nanometre
pH	Potential of Hydrogen
RPM	Revolutions Per Minute
V	Volts
x g	times Gravity

Abstract

Previous studies in our laboratory have shown that the nuclear transport protein Importin 1 (Kpnβ1) is upregulated in several types of cancer and is crucial to cancer cell survival. Recent findings from our laboratory showed that Kpnβ1, amongst other proteins is secreted into the extracellular space by cancerous and non-cancerous cells. Whilst the role of endogenous Kpnβ1 has been relatively well described in the literature; little is known of the role of secreted Kpnβ1 in the extracellular space.

Proteins secreted into the extracellular space have been reported to play a role in intercellular signaling that may have an impact on the biology of the cell type of origin or on cells of different origin, referred to as autocrine or paracrine respectively. This study is aimed at investigating the effect of Kpnβ1 bound to enhanced Green Fluorescent Protein (Kpnβ1-eGFP) containing secreted protein isolates obtained from cervical cancer cell lines on the biology of cell lines of cervical cancer and non-cancer origin. Conditioned media collected from control, eGFP-expressing or Kpnβ1-eGFP expressing HeLa and CaSki cervical cancer cells was used to treat recipient cells, both cancerous and non-cancerous. This was followed by monitoring the uptake of Kpnβ1-eGFP and effects on biological phenotypes including proliferation and migration. Our study observed that the internalisation of Kpnβ1-eGFP from conditioned media treatments varied across the cell lines used. The treatment of cervical cancer cell lines with conditioned media (control and Kpnβ1-eGFP containing) in an autocrine manner resulted in an increase in cell proliferation and migration. These effects however, appeared independent of Kpnβ1 as the Kpnβ1-eGFP-containing conditioned media did not confer a growth or migratory advantage to the cancer cell lines when compared to the eGFP-containing conditioned media. The effect on non-cancerous epithelial or fibroblast cells had cell line specific effects that appeared dependent on the origin of the secreted Kpnβ1-eGFP, with the non-cancerous epithelial cell line showing increased cell migration whilst the non-cancerous fibroblasts showed an increase in proliferation in response to treatment with Kpnβ1-eGFP-containing conditioned media obtained from CaSki cells.

As Kpnβ1 is a nuclear transport protein that binds to and transports a variety of cargo proteins, we postulated that secreted Kpnβ1 could also be bound to cargo proteins in the extracellular space. These cargo proteins, if any, may also affect the biology of cells targeted by conditioned media treatments. In this study, we thus investigated Kpnβ1 binding partners in the secretome of cancer cell lines. Previous studies in the literature identified endogenous Kpnβ1 binding partners and found that many of these are involved in protein synthesis amongst other cellular processes and are localised in the nucleus, cytoplasm or ribosome. An analysis of these studies identifying endogenous Kpnβ1-binding partners found that the use of immunoprecipitation mass spectrometry (IP-MS) identified a high number of proteins compared to other methods. As such our study made use of immunoprecipitation of secreted Kpnβ1 to identify Kpnβ1-binding partners in the extracellular space. Two approaches were used; firstly, the use of Western blot analysis to determine if previously described endogenous Kpnβ1-binding partners could be identified as bound to Kpnβ1 the extracellular space and secondly using IP-MS to identify novel Kpnβ1-binding partners in the extracellular space. Western blot analysis for the immunoprecipitated Kpnβ1 revealed that Kpnβ1 is bound to Exportin 1 (CRM1) in the secretome of cancerous and non-cancerous cells. It also showed that Kpnβ1 secreted from CaSki, WHCO5, Kyse30 and hTERT RPE-1 is bound to a Kpnβ1 adaptor protein, Karyopherin subunit alpha 2 (Kpnα2). IP-MS of Kpnβ1's binding partners secreted from cancerous and non-cancerous cells, although having a relatively low yield, identified Histones, an Actin protein (Actin cytoplasmic 1, N-terminally processed (ACTB)) and Laminin β. These binding partners have known functions in the extracellular space that may play a role in intercellular signaling.

In conclusion, this study shows that the secretome of cervical and oesophageal cancer cells contain Kpnβ1 and Kpnβ1-binding partners. An analysis of secreted Kpnβ1's binding partners suggest possible mechanistic pathways that may have a role in intercellular communication. Our results suggest that secreted cellular fractions containing overexpressed Kpnβ1 has cell line specific effects, with some biological features of non-cancerous cells possibly being affected.

Chapter One: Literature Review

1.1 Burden of cancer

Cancer is a disease that affects a large variety of people and does not discriminate between age, sex or race. The risk factors for cancer include genetic predisposition or exposure to environmental mutagens which can cause a healthy cell in the body to mutate. Any cell type can mutate and as such cancer can affect any tissue or organ in the body [1]. When the healthy cell mutates it loses its encoded regulatory procedures and begins to proliferate uncontrollably forming masses which can interrupt the healthy functioning of the tissue or organ affected [1]. The cancer cells can also leave the original tumour site and relocate to another tissue or organ. This migration leads to metastasising cancer that can spread quickly throughout the patient's body [1]. Cancer is a highly prevalent disease with over nineteen million new cases reported in 2020 [2]. It is also a lethal disease in many cases, causing nearly ten million deaths worldwide in 2020 alone [2].

1.1.1 Cervical cancer

A particularly prevalent type of cancer in low to middle income countries is cervical cancer. This cancer affects the cervix uteri, located in the female reproductive system, and was reported to be responsible for 3.1% of new cancer cases in 2020 totaling over six hundred thousand new cases globally [2]. Cervical cancer is associated with a high mortality rate, with over three hundred and forty thousand reported deaths in 2020 [2], illustrated below in Figure 1.1.

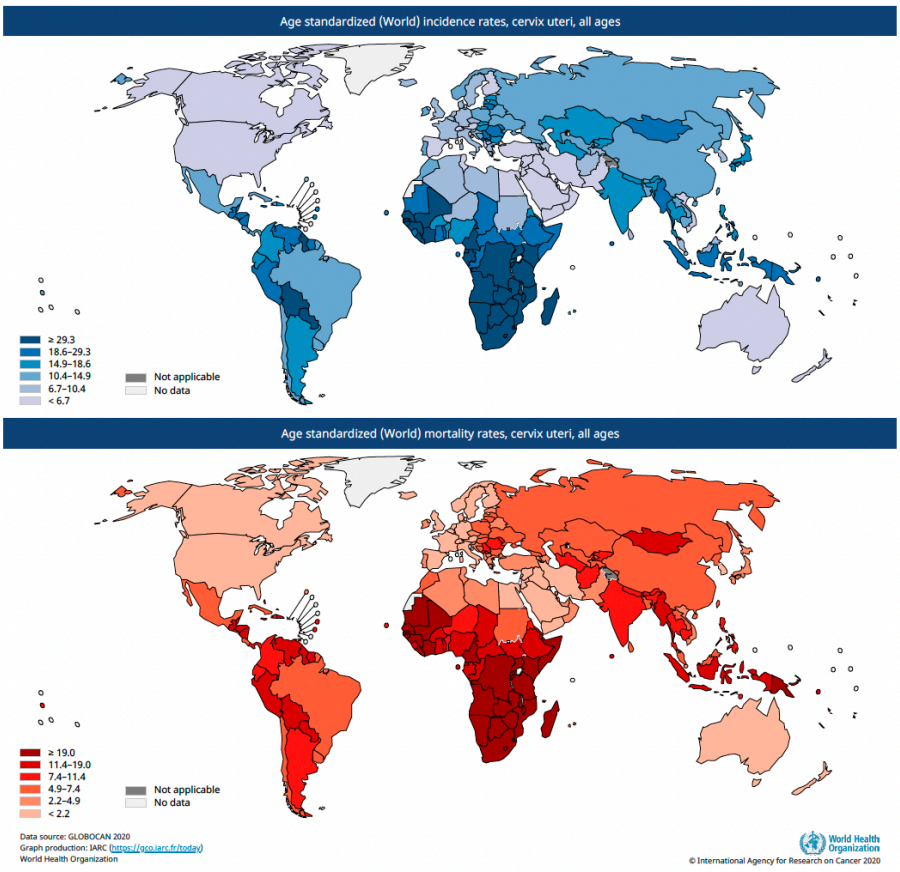

Figure 1.1: Incidence and mortality of cervical cancer. World map showing colour-coded age-standardised incidence rates (top) and mortality rates (bottom) of cervical cancer. World Health Organisation GLOBOCAN data source (2020) [3]

Figure 1.1 also highlights the disproportionately high incidence and mortality rates in low to middle-income countries. The highest incidence and mortality rates in these regions are in Sub-Saharan Africa [4]. A notable cause for the increased incidence rates observed in Sub-Saharan Africa, which are as much as ten times higher than in some higher-income countries, is the high rate of infection with Human Papillomavirus (HPV)[5]. HPV is a sexually transmitted disease that is categorised as a carcinogen [6] and plays a causative role in the onset of cervical cancer [7,8]. Worth noting is the role of Human Immunodeficiency Virus (HIV), which is also at a high incidence in Sub-Saharan Africa [9]. HIV lowers the body's immune response and alongside a HPV infection has been linked to increased cervical carcinogenesis [10].

The mortality rate associated with cervical cancer in Sub-Saharan Africa is twice as high as in some high-income countries [4] and this is partially due to the large number of cases that present at a late stage, which results in a lower chance of survival.

Mitigating the risk of cervical cancer depends on an early diagnosis, and this can be achieved by having regular Papanicolaou (Pap) smears to detect any abnormal cervical cells. In addition to screening for cervical cancer, there are vaccines available against several carcinogenic HPV types, the use of which may reduce a person's risk of cervical cancer by 40% [11]. Unfortunately providing regular cervical cancer screening and HPV vaccines is a costly endeavour for a public health system and low to middle-income countries may lack the funds and the infrastructure to put these measures into place.

1.1.2 Oesophageal cancer

Oesophageal cancer caused 3,1% of new cancer cases and 5,5% of cancer-related deaths in 2020 [12]. The incidence and mortality rates are illustrated in Figure 1.2.

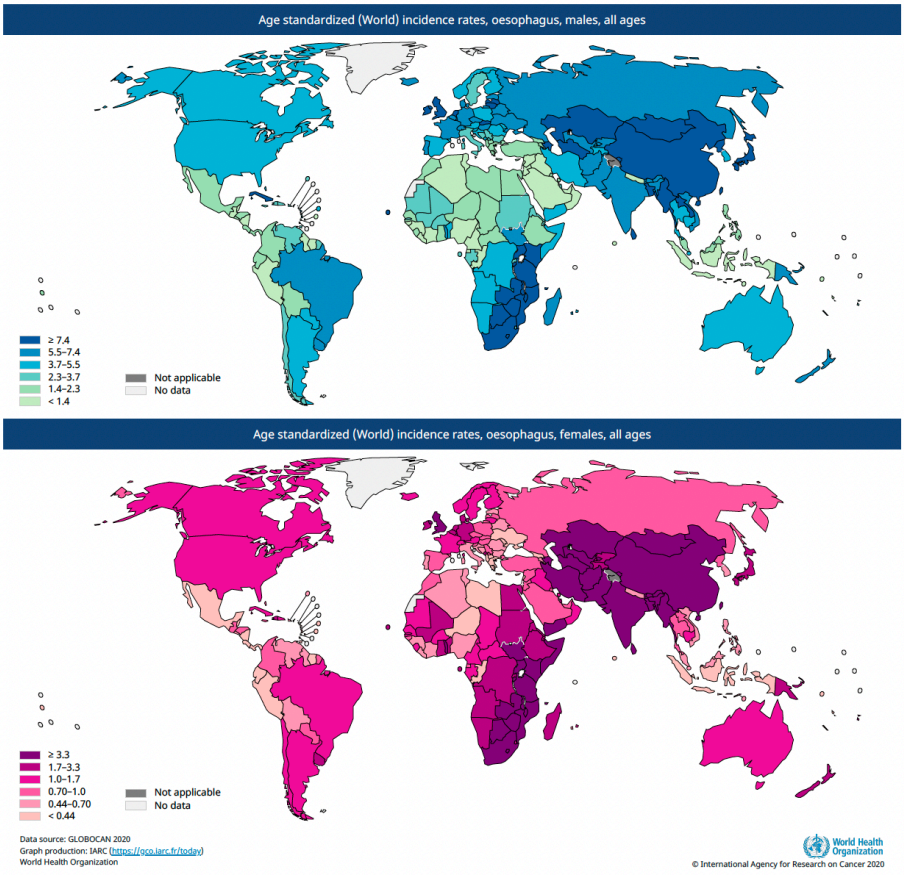

Figure 1.2: Incidence and mortality of oesophageal cancer. World map showing colour-coded age-standardised incidence rates (top) and mortality rates (bottom) of oesophageal cancer. World Health Organisation GLOBOCAN data source (2020) [12]

Similarly to the distribution of cervical cancer oesophageal cancer is especially prevalent in low to middle-income countries, including Sub-Saharan Africa [12] (Figure 1.2). Smoking, drinking alcohol and a poor diet has been reported to increase the likelihood of oesophageal cancer [13–15]. These factors likely influence the high incidence rates in Sub-Saharan Africa. The high mortality rates, as observed for cervical cancer, are in part due to late diagnosis which would lower the patient's chance of survival.

The disproportionate incidence and mortality rates of cervical and oesophageal cancer in Sub-Saharan Africa compared to higher-income countries [12] is a concern.

Continued work in the field of cancer research has been aimed at gaining a greater understanding of cellular factors that associate with cancer, potentially allowing for the identification of new treatments and diagnostic tools. A branch of cancer research that is anticipated to contribute to both diagnosis and treatment is the identification of cancer biomarkers. Genomic, proteomic and bioinformatic approaches may be used to identify differentially expressed proteins or genes present in cancer cells. These differentially expressed proteins or genes may then be targeted for using novel treatments or used to aid in diagnosis [16].

A previous study in our laboratory used microarray analysis to identify differentially expressed genes between normal cervical tissue and cancerous tissue samples. The study identified several genes as differentially expressed in cervical cancer, of which multiple proteins associated with nuclear transport pathways, in particular the nuclear import protein Karyopherin Beta 1 (Kpnβ1) became of interest as a novel cancer target[17].

1.2 Nuclear transport proteins

Nuclear transport proteins function to transport cargo proteins into or out of the nucleus that are too large to diffuse through the nuclear membrane unassisted [18]. As such nuclear transport proteins support several crucial processes in the cell, including Deoxyribonucleic Acid (DNA) replication, protein synthesis and cellular replication [19].

1.2.1 Karyopherin Beta 1

The Karyopherin protein group make up the majority of nuclear transport proteins in the cell [19]. A member of this protein family, Karyopherin β1 (Kpnβ1), otherwise referred to as Importin β1, is an importin protein, responsible for trafficking cargo into the nucleus. Cargo proteins containing a nuclear localisation sequence (NLS) are recognised by Karyopherin subunit alpha, also known as Importin α (Kpnα), an adaptor protein, that will then bind to Kpnβ1 forming a complex able to enter the nucleus because of Kpnβ1's subsequent interaction with the nuclear pore complex (NPC). This process is known as the classical transport pathway, illustrated in Figure 1.3 [20]. An alternate non-classical pathway where Kpnβ1 binds cargo proteins directly and independent of an adaptor protein may also be used [18].

While the primary role of Kpnβ1 is to transport cargo into the nucleus it also functions to assist spindle assembly in mitosis, supporting cellular replication [21,22].

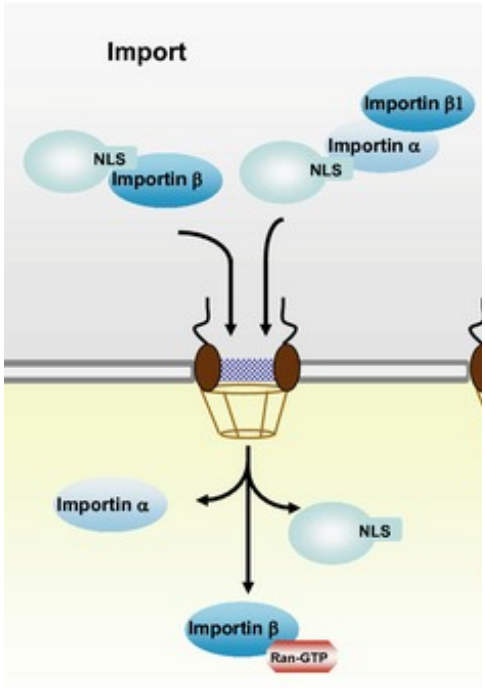

Figure 1.3: The pathway of nuclear transport. Kpnβ1 (Importin β1) binds to the cargo protein containing a NLS with the adaptor protein Kpnα (Importin α) in the classical pathway, or without in the non-classical pathway. The complex then travels through the NPC into the nucleus where the complex disassembles. Diagram adapted from Sekimoto, Toshihiro and Yoneda, Yoshihiro (2012) [20].

Kpnβ1 is responsible for a significant portion of the transport into the nucleus that occurs in the cell. An increase in the concentration of Kpnβ1 has been shown to increase the rate of nuclear transport in the cell by at least ten times, often more [23]. This highlights the importance of this protein and the role it plays as well as suggesting that an overexpression of Kpnβ1 and other karyopherin proteins results in altered nuclear transport rates.

1.2.2 Nuclear transport proteins in cancer

Several members of the Karyopherin protein family have been reported to be upregulated in cancerous cells compared to non-cancerous cells, including Kpnβ1[17,24]. Cancer cells have an increased rate of DNA synthesis, cellular replication and protein synthesis and as a result are more dependent on upregulated nuclear transport proteins [25] amongst other protein functions. The nuclear transport proteins may therefore support the cancer development as they aid the cancer in sustaining proliferation, which is a hallmark of cancer [26]. There are other hallmarks of cancer that nuclear transport proteins have been linked to, including invasion and metastasis [27,28]. The dependence of cancer cells on nuclear transport proteins highlights their importance in cancer cell biological processes and overall functioning [25].

While the importance of nuclear transport proteins in cancer is appreciated there are also some roles of nuclear transport proteins that are not yet understood. Previous studies in our lab have shown that Kpnβ1 and other nuclear transport proteins are secreted by cancer cells into the extracellular space, and their role, if any, in the extracellular space is undetermined [29,30]. This may have significance as not only do intracellular activities contribute to the development and progression of cancer, but factors in the extracellular space have also been reported to contribute to the cancer phenotype in both an autocrine and paracrine manner.

1.3 Autocrine and paracrine signalling as contributors to cellular function

Intercellular signalling is the process by which cells can communicate with one another, affecting the subsequent actions of the cell to which the signal was transmitted. It functions via the actions of molecules external to or secreted into the extracellular space [31]. Cells secrete proteins to remove debris, in which case the protein is waste, or as molecules required for cell-cell communication. The secreted protein or signalling molecule either binds to a cell surface receptor or is endocytosed, inducing a chain reaction through which gene expression, and thus the behavior of the cell, is affected [31]. Intercellular signalling represents an important mode of control a cell can direct over itself or other cells.

Intercellular signalling can be separated into two categories: autocrine and paracrine signalling. Autocrine signalling occurs when an external molecule affects the biological function of the cell that it originated from (Figure 1.4 A). Paracrine signalling occurs when the molecule affects a cell that it was not secreted from, which could be in the surrounding cells or even in a different tissue [32] (Figure 1.4 B).

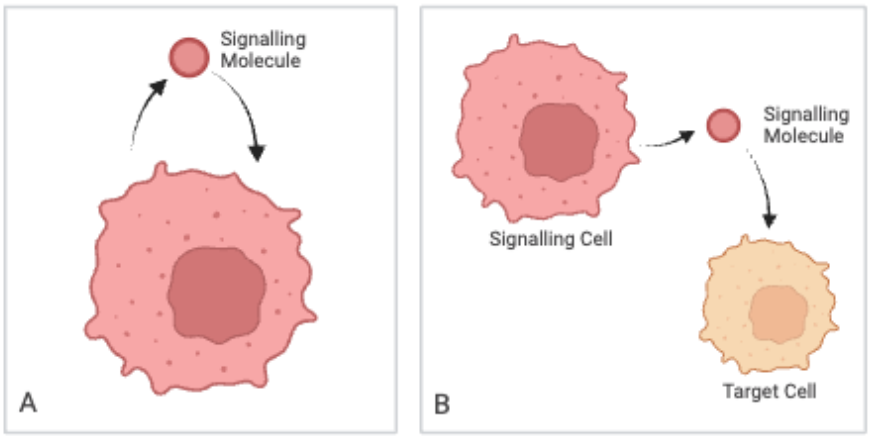

Figure 1.4: Autocrine and paracrine signalling. Autocrine signalling (A) where the signalling molecule secreted from the cell acts on the cell it was secreted from, and paracrine signalling (B) where the secreted signalling molecule acts on a cell it was not secreted from. Created with BioRender.com

1.3.1 Cellular signalling associated with exosomes

A specific type of intercellular communication involves signalling that associates with exosomes located in the extracellular space. Exosomes are microvesicles that range

from 30nm to 150nm [33]. These microvesicles originate from inside of a cell and bud off the plasma membrane to enter the extracellular space [34]. The exosome is made up of a lipid bilayer that has maintained the transmembrane protein topography of the original cell, including the cell receptors and markers. Contained in the exosome is cytosol with lipids, proteins, DNA and Ribonucleic Acid (RNA) that originated from inside the cell [33,35,36].

Exosomes are able to facilitate intercellular communication. Once secreted exosomes can travel to a target cell and trigger a signal transduction cascade in an autocrine or in a paracrine manner [37,38]. To transmit the signal to the target cell exosomes can bind receptor proteins on cell surface of target cells or be internalised through endocytosis, micropinocytosis or phagocytosis (Figure 1.5) [39–42]. The contents of exosomes can then be released through the target cell's endosomal pathway and deliver proteins, lipids and nucleic acids to various parts of the cell [43,44]. The subsequent actions of the cell can be affected by molecules taken up by the cell, and as such exosomes have been reported to indirectly regulate the function of cells [35]. Exosomes can travel through bodily fluids hence intercellular signalling in the exosomal pathway may have long rage effects and affect multiple cell types [36].

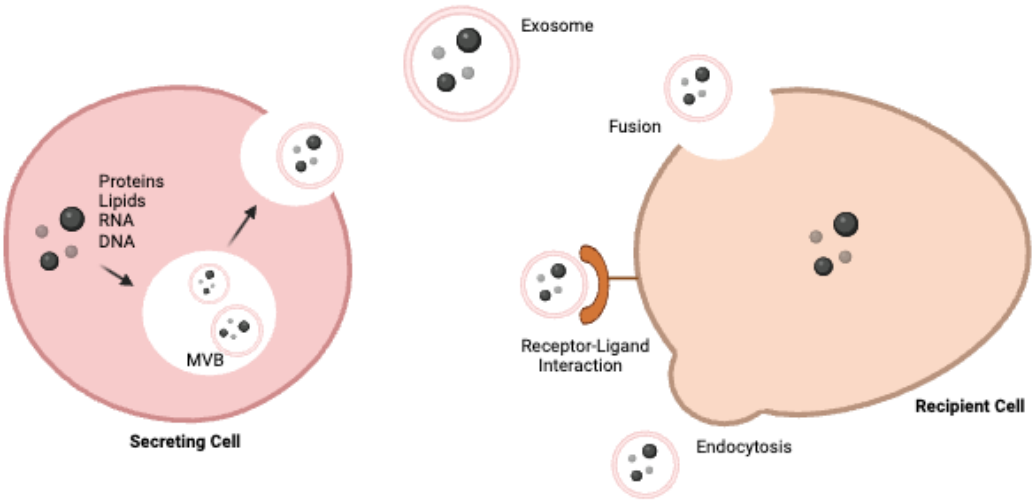

Figure 1.5: Exosomal signalling. Exosomes are synthesised in the multivescular body (MVB) inside the cell before budding out into the extracellular space. The exosomes then travel to the target cell where it may bind to a cellular receptor or be taken up into the target cell, where the contents of the exosome are then released. Diagram adapted from Dilsiz, N. (2020) [45]. Created with BioRender.com

1.3.2 Intercellular signalling in cancer

Intercellular signalling is important for the functioning of non-cancerous cells as well as cancerous cells. Autocrine and paracrine signalling can play a role in cancer cell functioning and has been reported to support the cancer phenotype [46]. Growth factors, for example, that act in a paracrine or autocrine manner can increase the proliferation of cancer cells. Signalling molecules can also influence the tumour microenvironment by stimulating angiogenesis, reducing the immune response and increasing the motility of cancer cells, which can lead to metastasis [46,47].

Exosomal signalling, more specifically, has also been implicated in influencing cancer progression and morphology. Exosomes from cancer cells can influence angiogenesis, vascular permeability, tumour immunity, axonogenesis, Epithelial-Mesenchymal-Transition and increased cell motility, thereby contributing to metastasis [33,35–37,48–51]. The exosomes originating from cancer cells contain proteins from the cytosol of the cancer cell and so frequently contain proteins upregulated in cancer cells compared to the exosomes of non-cancerous cells [52–54]. This may have an effect on cancer development, for example Heat shock protein 70 (Hsp70), Milk fat globule-EGF factor 8 protein (MFG-E8), and Decay-accelerating factor (DAF) proteins found to be upregulated in the exosomes of prostate cancer have also been shown to modulate the immune response in tumours, assisting cancer development [54].

In our laboratory, we showed that proteins in the nuclear transport protein family are upregulated in cervical, oesophageal, and other cancer types, and are required for cancer biology [17,55]. We have also shown that several of the nuclear transport proteins can be detected in the secreted fraction of cancer cells, in particular in cancer exosomes [56].

1.4 Nuclear transport proteins secreted by cancer cells

Little is known of the role of secreted nuclear transport proteins, if any, in cellular communication and cell biology. Our laboratory has evidence that the nuclear import

protein Kpnβ1 is secreted by cancer cells and has potential as both a therapeutic and diagnostic target. A potential role for secreted Kpnβ1 in cancer cell biology and whether secreted Kpnβ1 is bound to cargo proteins is not known as yet.

In its role as a nuclear transport protein, Kpnβ1 functions directly or with multiple binding partners. For example, it binds the adaptor protein, Kpnα, various cargo proteins that contain an NLS, and the proteins of the NPC. It has also been shown to bind Ras-related nuclear protein bound to Guanosine Triphosphate (Ran-GTP), which facilitates the transport of Kpnβ1 out of the nucleus once Kpnβ1 has successfully transported and then detached from its cargo [57–60]. Kpnβ1 also binds Ran-GTP in its role in mitotic spindle formation [21]. Kpnβ1 has many binding partners, of which some are cargo proteins, as a result of its role as a nuclear transport protein. Some experimentally determined Kpnβ1 binding partners include Signal transducer and activator of transcription 3 (STAT3) and Nuclear Factor kappa B (NF-κB) transcription factors and proteins involved in protein synthesis [61–63]. Okpara *et al*. (2022) in our laboratory used immunoprecipitation mass spectrometry (IP-MS) to identify cellular Kpnβ1 binding partners in cancerous and non-cancerous cells, including Karyopherin subunit alpha 2 (Kpnα2), Ran, CRM1, Cell division Cycle and Apoptosis Regulator protein 1 (CCAR1) and Far Upstream element Binding Protein 1 (FUBP1), which have been validated using Western blot analysis [62].

1.4.1 Significance

Secreted proteins may have functions in the extracellular space but may also be used for cancer diagnosis though liquid biopsies. This diagnostic process uses a body fluid obtained from a patient to determine the presence of specific molecular biomarkers, from RNA to protein, that could be present at elevated levels in cancer patients in comparison to that in healthy patients. Liquid biopsies are less invasive than tissue biopsies as often only a blood sample is required which will also make any repeat biopsies less painful [64]. This diagnostic method also has the capability of identifying cancer even when the cancer is located in a position that a tissue biopsy could not

reach, making it a useful tool. Exosomal proteins are ideal candidates for liquid biopsies [64,65] as exosomes can be found in blood [66].

Determining the identity of proteins present in the extracellular space of cancerous cells could validate existing biomarkers or aid in the discovery of new ones that can be found in bodily fluids and subsequently be used in the diagnosis of cancer.

1.5 Project Aims

The aims of this study are:

1. To determine the effect of secreted protein fractions containing elevated Kpnβ1 levels from cervical cancer cell lines on the biology of cancer and non-cancer cells.
2. To identify the Kpnβ1-binding partners in the secreted fraction of cancer cells.

Chapter Two: Materials and Methods

2.1 Materials

2.1.1 Cell lines

Human cervical carcinoma cancer cell lines, HeLa and CaSki, and a human telomerase-immortalized retinal pigmented epithelial 1 non-cancerous cell line, hTERT RPE-1, were acquired from the American Type Culture Collection (ATCC, Rockville, MD, USA). A skin fibroblast non-cancerous cell line, FG0, was acquired from the Department of Medicine, UCT. A human oesophageal squamous cell carcinoma cancer cell line, WHCO5, was acquired from Professor Rob Veale at the University of Witwatersrand. Another human oesophageal squamous cell carcinoma cancer cell line, KYSE30, was acquired from Deutsche Sammlung von Mikroorganismen und Zellkulturen (DSMZ) (Berlin, Germany).

The HeLa Kpnβ1-eGFP Pool 2, CaSki Kpnβ1-eGFP Pool 3, HeLa eGFP and CaSki eGFP cell lines were generated by Sarah Carden, UCT. These cell lines were generated using a pEGFP-Kpnβ1 plasmid acquired from Patrizia Lavia, Institute of Molecular Biology and Pathology, National Research Council of Italy, (Rome, Italy), and a pEFIRES plasmid acquired from Yosef Shaul, Weizmann Institute of Science, (Israel).

All the cell lines except hTERT RPE-1 were kept in a media composed of Dulbecco's Modified Eagle Medium (DMEM) with 10% Heat Inactivated Foetal Calf Serum (HIFCS), Penicillin (100 µg/ml) and Streptomycin (100 µg/ml). The cell lines that contained a plasmid; HeLa Kpnβ1-eGFP Pool 2, CaSki Kpnβ1-eGFP Pool 3, HeLa eGFP and CaSki eGFP, had the addition of Puromycin (0,5 µg/ml) to ensure that only cells containing the plasmid were present.

The hTERT RPE-1 cells were kept in a media composed of DMEM with an additional nutrient mixture (DMEM/F-12) with 10% HIFCS, Penicillin (100 µg/ml) and Streptomycin (100 µg/ml). Cells were incubated at 37 °C with 5% carbon dioxide.

2.2 Methods

2.2.1 Cellular protein extraction

The media was removed from the cells and placed in a 14 mL tube. The cells were then washed twice with 1 mL of cold 1X Phosphate Buffered Saline (PBS), this was then added to the 14 mL tube containing the media and was centrifuged to isolate the floating cells. The cells adhered to the cell culture dish were treated with 60 µL of complete radio-immunoprecipitation assay (RIPA) and collected into an eppendorf tube using a cell scraper. The pellet containing the floating cells was also treated with 60 µl of complete RIPA and pooled into the eppendorf. The sample was then sonicated for approximately 10 seconds and then centrifuged for 10 minutes (4 °C at 10 000 RPM) to remove cellular debris. The supernatant was then removed from the pellet and placed in a clean eppendorf and the pellet was discarded.

2.2.2 Extracellular protein extraction

When the cells were between 70%-80% confluency the media was removed and the cells were washed twice with serum-free media (DMEM, Penicillin (100 µg/ml) and Streptomycin (100 µg/ml)) before 5 mL of serum-free media was added and the cells were left to incubate for twenty-four hours. Once the incubation period had elapsed the conditioned media was collected, pooled, and centrifuged for 10 minutes (3000 RPM) to remove any cellular debris. The supernatant was then transferred to an Amicon Ultra-15 centrifugal filter unit (Merck Millipore) and centrifuged for 30 minutes (4 °C and 1000 RPM), distilled water (dH_2O) was then added to aid in protein concentration and the sample was centrifuged again. This was then repeated once more for a total of 3 rounds of centrifugation. The filtration unit retained proteins of 30 kDa and above. The concentrated protein was then placed in a clean eppendorf.

2.2.3 BCA Assay

To quantify the collected protein samples the Thermo Scientific Pierce Bicinchoninic Acid (BCA) Protein Assay Kit was used. Protein samples were added to a 96-well plate, alongside bovine serum albumin (BSA) standards that ranged from 2 mg/mL to

0 mg/mL, in duplicate. A volume of 25 µL of each protein standard was used. The cellular protein samples were diluted 1:10 with distilled water to 25 µL, the extracellular protein samples were not diluted and 25 µL was used. A volume of 200 µL of the BCA solution was added to each well and left to incubate at 37 °C for 30 minutes. The plate was then read with a spectrophotometer (BioTek EL800) at a wavelength of 595 nm. Protein will reduce the copper ions present in the BCA reagent and produce a purple colour [67], which can be quantified and used to create a standard curve and calculate the protein concentration of the samples.

2.2.4 SDS-PAGE

A 7.5% or 12% acrylamide resolving gel and a 4% acrylamide stacking gel were made in a 1.5 mm plate. The protein samples were prepared by adding 30 µg of protein and dH_2O for a total volume of 10 µL. Where this was not possible due to protein availability or concentration a consistent mass of the protein samples was added to dH_2O for a maximum volume of 30 µL. The 4X loading dye, containing 10% β-mercaptoethanol, is added to make up a quarter of the total volume. The samples are then heated to 90 °C for 5 minutes before being loaded into the wells of the gel. A protein standard ladder is used (New England Biolabs), and a total of 3 µL is loaded. The tank is filled with a 1X Running buffer and the gel is run at 160 V for approximately 70 minutes, or until the loading dye has reached the bottom of the gel.

2.2.5 Immunoblotting

To transfer the proteins from a SDS-PAGE to a HyBond™-ECL™ nitrocellulose membrane (Amersham) a 1X Transfer Buffer is used at 100 V for 70 minutes. The membrane was then cut horizontally, in line with the relevant marker on the protein ladder. This is to separate the area containing the protein of interest from the area containing the loading control, as each will need separate antibodies. The individual pieces of the membrane are then blocked in 5% milk in tris-buffered saline with 0.1% Tween 20 detergent (TBST) for 1 hour. The respective primary antibodies are then put on the membranes and left to block in the cold room overnight. Following that the membrane will be washed with TBST for 5-minute periods 3 times before the

secondary antibody is added. The membrane is blocked with the secondary antibody at room temperature for 1 hour. The membrane is then washed for 5-minute periods three times in TBST. All of the blocking and washing periods take place on a shaker to ensure even distribution. To visualise the blot a LumiGLO Chemiluminescent Substrate Kit (KPL) is used in a 1:1 ratio and the image is captured using the iBright 1500 (Invitrogen).

Table 2.1: Antibody conditions used for Western Blot

Primary antibody	Primary antibody conditions	Secondary antibody	Secondary antibody conditions
Kpnβ1 (97 kDa) (ab45938,Abcam)	1:5000 in TBST	Goat anti-rabbit (#1706515, Biovac)	1 in 5000 in TBST
CCAR1 (130 kDa) (NB500-186, Novus Biologicals)	1:500 in TBST	Goat anti-rabbit (#1706515, Biovac)	1 in 5000 in TBST
CRM1 (115 kDa) (sc-5595, Santa Cruz Biotechnology)	1:1000 in TBST	Goat anti-mouse (#1706516, Biovac)	1 in 5000 in TBST
FUBP1 (69 kDa) (NBP2-16543, Novus Biologicals)	1:1000 in TBST	Goat anti-rabbit (#1706515, Biovac)	1 in 5000 in TBST
NFκB (65 kDa) (sc-7151, Santa Cruz Biotechnology)	1:500 in 1% Milk	Goat anti-rabbit (#1706515, Biovac)	1 in 5000 in TBST
Kpnα2 (52 kDa) (14372S, Cell Signalling)	1:1000 in 2,5% Milk	Goat anti-rabbit (#1706515, Biovac)	1 in 5000 in TBST
cJun (39 kDa) (sc-44, Santa Cruz Biotechnology)	1:250 in TBST	Goat anti-rabbit (#1706515, Biovac)	1 in 5000 in TBST
β-tubulin (55 kDa) (sc-5274, Santa Cruz Biotechnology)	1:5000 in TBST	Goat anti-rabbit (#1706515, Biovac)	1 in 5000 in TBST
GAPDH (36 kDa) (G9545, Sigma Aldrich)	1:5000 in TBST	Goat anti-rabbit (#1706515, Biovac)	1 in 5000 in TBST

2.2.6 Stripping nitrocellulose membrane

The membrane that has been previously probed with a primary and secondary antibody is washed for 12 minutes in 1 M Glycine (pH 2.5) to remove any antibodies attached to the membrane. The membrane is then washed 3 times in TBST for 5 minutes. The newly stripped membrane is then blocked in 5% milk for 2 hours. The membrane is now ready to be probed with a new primary antibody.

2.2.7 Generation of conditioned media

Cells from which the conditioned media was obtained, the donor cells, were plated in an equal amount and volume to the cells that were treated with the conditioned media, the recipient cells. The cells then had twenty-four hours to adhere to the plate before the media was aspirated. The cells were then washed twice with serum-free media (DMEM, Penicillin (100 µg/ml) and Streptomycin (100 µg/ml)), after which the final volume of serum-free media required was added to the cells. The cells were then incubated for twenty-four hours in the serum-free media. After this twenty-four hour period had elapsed the media is now considered to be conditioned media as it would contain all the proteins, among other molecules, the cells have secreted in that period.

2.2.8 Treatment with conditioned media

Twenty-four hours after the donor cells, those from which the conditioned media will be collected, are plated the recipient cells, those to be treated with the conditioned media, are plated and given twenty-four hours to adhere to the plate. The media is aspirated from the recipient cells and are washed twice with serum-free media before treatment. The conditioned serum-free media is then transferred to the recipient cells. The treated cells are left for twenty-four or forty-eight hours, as necessary.

2.2.9 MTT Assay

Cells to be treated were plated in a 96-well plate in 100 µl of media and left to adhere to the plate for twenty-four hours. Cells with a higher proliferation rate, specifically HeLa, WHCO5 and Kyse 30 were plated with 5000 cells per well and those with a

slower proliferation rate, CaSki, hTERT RPE-1 and FG0 cells were plated with 7500 cells per well. The cells were then treated with conditioned media and then left for twenty-four or forty-eight hours. At the end of the treatment period the cells were then treated with 10 µl of 5 mg/ml Methylthialazole Tetrazolium (MTT) from Sigma. After 4 hours they were treated with 100 µl of solubilisation buffer (10% SDS and 0.01 M HCl). Any actively metabolizing cells present will reduce the MTT to formazan, resulting in a colour change from yellow to purple [68].After an incubation of approximately 16 hours the plates were read using a spectrophotometer (BioTek EL800), obtaining the absorbance values at 595 nm for each well. The absorbance values will indicate how much of the MTT was reduced and allow the viability and proliferation of the cells to be determined.

Experiments were run in triplicate with a blank and were repeated at least 3 independent times.

2.2.10 Scratch assay

To investigate the migration of cells 0.25 x 10^6 cells per well were added to a 6-well plate and left to adhere for twenty-four hours. Mitomycin C was then added at a concentration of 5 µg/ml to prevent protein synthesis and thus cellular replication, so that any change seen would be due to cell migration [69]. A concentration 1 µg/ml of Mitomycin C was used for CaSki cell lines due to their increased sensitivity. A scratch was then made across the well using a pipette tip. The scratch was imaged at the time of the scratch as well as twenty-four and forty-eight hours later. The area of the scratch was then calculated using *ImageJ* and the relative percentage of the original scratch remaining was used as a measure of migration ability. This assay was repeated 3 independent times.

2.2.11 Cell fixing and DAPI staining

Cells were plated on sterilised coverslips in 6-well plates and treated twenty-four hours later using conditioned media. Twenty-four or forty-eight hours later the cells were fixed by adding 1 mL of methanol that was left on for 10 minutes to dehydrate the cells. The methanol was then removed and the fixed cells were washed twice using 2 mL of

PBS-Tween. To block the cells 1.6 mL of 1% BSA in PBS was added and the cells were left to incubate at room temperature for 30 minutes. This was followed by 2 washes in 1X PBS before 4′,6-Diamidino-2-Phenylindole (DAPI) was added (1 mL, 100 ng/mL in PBS) and left at room temperature for 10 minutes. The cells were washed twice in 1X PBS and then mounted onto a slide using Mowiol.

2.2.12 Brightfield and fluorescent microscopy

Images of the prepared slides were captured using either an EVOSTM M5000 Imaging System (Invitrogen), an Axioscan 7 (ZEISS) or a LSM 880 Confocal (ZEISS) Microscope. Images captured on the Confocal microscope were focused on the interior section of the cells to focus on internalised proteins and exclude any that were surface bound. The fluorescent images were processed using *ImageJ* to correct for autofluorescence.

2.2.13 Immunoprecipitation

In order to isolate Kpnβ1 and it's binding partners 1 mg of extracellular protein was equally distributed into 2 clean eppendorf tubes. A volume of 50 µL of Protein A Agarose (High-Affinity) beads (Abcam) was added to each tube to preclear the sample and was incubated at 4°C for 45 minutes with gentle rocking. The samples were then centrifuged (4 °C, 18 000 x g) for 10 minutes before the supernatants were placed in clean eppendorf tubes. Anti-Karyopherin β1 (H-7) AC agarose conjugated antibody (Santa Cruz Biotechnology) was added to a tube (50 µg added, 500 µg/ml, 25% agarose) and 50 µL of Protein A Agarose (High-Affinity) beads alongside 15 µL of Rabbit (DA1E) mAb IgG isotype control (Cell Signalling technology) was added to the other. The sample with the Kpnβ1 antibody should attach to any Kpnβ1 present in the sample, allowing subsequent isolation, where the sample with the IgG antibody will non-selectively bind, acting as a control. The samples were then incubated overnight at 4 °C with gentle rocking. The incubated samples were then centrifuged (4 °C, 18 000 x g) for 3 minutes before the supernatant was removed and discarded. The beads underwent 5 washes where the samples were centrifuged, supernatants

discarded and 500 µL 1X PBS and 50 µL 1X Phosphatase inhibitor (PI) were added, until 5 cycles had been completed.

To run the samples on a SDS-PAGE the beads were resuspended in 35 µL of 2X loading dye without bromophenol blue, boiled at 95 °C for 5 minutes and then centrifuged for 5 minutes (18 000 x g). The supernatants were then taken and 1 µL of 1% bromophenol blue was added prior to being loaded into the gel. Veriblot for IP detection agent (Abcam) was used in place of a secondary antibody when visualising the immunoprecipitation Western blot (1:2500 in 5% milk)

2.2.14 Mass Spectrometry

Immunoprecipitated samples were sent for examination at the D-CYPHER proteomic core facility. A Q-Exactive quadrupole-Orbitrap Mass Spectrometer (Thermo Fisher Scientific, USA) coupled with a Dionex Ultimate 3000 nano-UPLC system was used. *Xcalibur* (Version 4.1.31.9), *Chromeleon* (Version 6.8), *Orbitrap MS* (Version 2.9) and *Thermo Foundations* (Version 3.1) were used to acquire data and peptides were identified using *Byonic* (Version 3.8.13), with a human reference proteome sourced from UniProt. Proteins with less than 2 unique peptides and those with a false discovery rate of above 0.05 were excluded. Results were received in the form of a *Microsoft Excel* document.

2.2.15 Data analysis

Densitometry of Western blots, fluorescent image processing and analysis were completed using *ImageJ* (Version 2.14.0). *Microsoft Excel* was used for calculation as well as determining the standard error of the mean (SEM) and running student's t-tests. A p-value of less than 0.05 was considered statistically significant.

Chapter 3: Determining the Effect of Secreted Kpnβ1 in an Autocrine and Paracrine Manner

3.1 Introduction

Autocrine and paracrine signalling plays an important role in cellular functioning, allowing cells to communicate with each other and affect the operations of the target cells. Autocrine and paracrine signalling has also been shown to affect cell morphology and mobility in cancer cells, as well as impacting other biological processes [46,47]. Intercellular signalling thus represents a way by which cancer cells can exert control over their microenvironment and progression by affecting the functioning of surrounding cells and tissues. Investigating the role of intercellular signalling in cancer and isolating the effects of specific proteins as signalling molecules could aid in better understanding cancer functioning and potentially identifying promising drug targets that would block the subsequent effects of the intercellular signalling.

Our laboratory previously showed that cancer cells have elevated expression of members of the nuclear transport protein family, including Kpnβ1, and secrete members of this protein family into the extracellular space [24,56,70]. There is evidence in the literature that nuclear transport proteins in the extracellular space may be acting as signalling molecules, for example Exportin 1 (CRM1) has been implicated in intercellular signalling, shuttling Ras-related nuclear protein bound to Guanosine Triphosphatase (Ran-GTPase) between cells [71]. The detection of nuclear import proteins such as Kpnβ1 in the extracellular space is a relatively recent observation and the functional role secreted Kpnβ1 may play, if any, in the intercellular signalling of cancer cells has not been investigated to date. Kpnβ1 has several functional roles inside of the cell but its purpose and activity in the extracellular space has not been determined. A previous study showed that overexpressing Kpnβ1 in cervical cancer cells resulted in changes in cell morphology, proliferation and the adhesive ability of the cervical cancer cells [72]. Considering that endogenous Kpnβ1 overexpression had effects on the biology of cancer cells, we questioned whether high levels of secreted

Kpnβ1 plays a role in intercellular signalling that may result in changes in biological features such as proliferation, morphology and migration of target cells. As intracellular Kpnβ1 plays a vital role in cancer cell proliferation and survival [55,70,73] it may potentially associate with changes in proliferation and migration, among other biological processes, to contribute to cancer progression.

The aim of this chapter is to investigate a potential role for secreted Kpnβ1 in intercellular signalling in cancer cells. To investigate the contribution of specific proteins to the biological features of cells the protein can either be knocked out or overexpressed. Ideally to investigate the effect of a specific protein a knock-out model would be used to determine the individual effect of the protein. Multiple attempts to generate cancer cell lines where Kpnβ1 has been knocked out proved unsuccessful in our laboratory as no viable knock-out clones could be generated. We suspect that could be because Kpnβ1 plays such an essential role in the biology of cancer cells. Cell lines with over-expressing Kpnβ1 has however been generated successfully in our laboratory and are thus used as a model to investigate the effects of enhanced Kpnβ1 levels in cancer cells. The cervical cancer cell lines, HeLa and CaSki, stably transfected with plasmids encoding either enhanced Green Fluorescent Protein (eGFP) on its own as a control, generating HeLa eGFP and CaSki eGFP cell lines, or a Kpnβ1-eGFP fusion protein, generating HeLa Kpnβ1-eGFP and CaSki Kpnβ1-eGFP cell lines are used in this study.

In this chapter, we first describe some of the biological features of Kpnβ1-eGFP expressing cervical cancer cells, followed by investigating the effects of secreted protein fractions containing Kpnβ1-eGFP from cervical cancer cell lines on the biology of cancer and non-cancer cells. Briefly, secreted factors isolated from control and Kpnβ1-eGFP expressing cells were harvested and placed on HeLa and CaSki parental cells, or non-cancerous cell lines, hTERT RPE-1 and FG0, to target the cells originating from the same tissue or those from a different tissue, in an autocrine or paracrine manner. The resultant effects on the target cell's morphology, protein expression, proliferation and cell migration were investigated.

3.2 Results

3.2.1 Endogenous Kpnβ1 and Kpnβ1-eGFP in stabling expressing HeLa and CaSki cells.

HeLa and CaSki cell lines with stable expression of eGFP or Kpnβ1-eGFP were previously generated [72] and grown in cell culture for the isolation of secreted proteins. To confirm endogenous Kpnβ1 and Kpnβ1-eGFP expression cellular protein was harvested from the different cell lines and analysed by Western blot analysis. Western blot analysis using 3 biological repeats confirmed that HeLa Kpnβ1-eGFP and CaSki Kpnβ1-eGFP show an additional band at the expected size of approximately 129.7 kD which is representative of the Kpnβ1-eGFP fusion protein that is not present in the control eGFP expressing cell lines (Figure 3.1 A and 3.1 B).

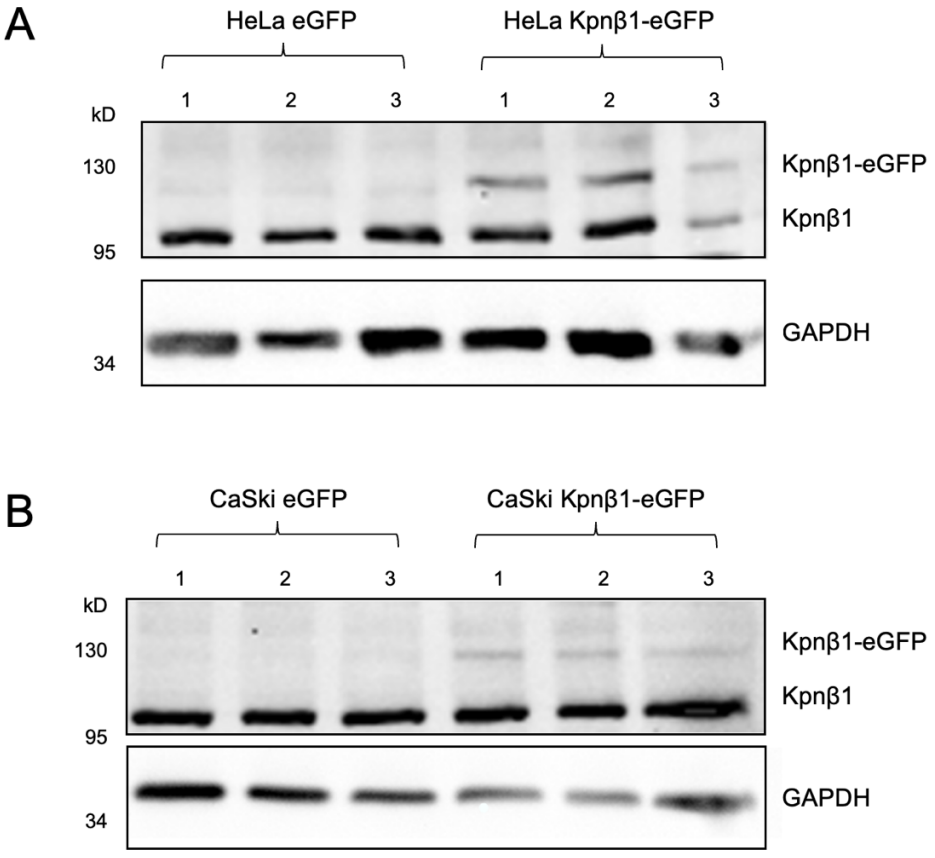

Figure 3.1: Endogenous Kpnβ1 and Kpnβ1-eGFP in stably expressing eGFP and Kpnβ1-eGFP HeLa and CaSki cells. (A) Western blot analysis of Kpnβ1 in HeLa eGFP and HeLa Kpnβ1-eGFP cell lines. (B) Western blot analysis of Kpnβ1 in CaSki eGFP and CaSki Kpnβ1-eGFP cell lines. 30 µg of protein was loaded in each lane and GAPDH was used as a loading control. Three biological repeats are shown for each cell line (1, 2 and 3).

In addition to observing the expression of Kpnβ1-eGFP by Western blot analysis, we also monitored the cells using fluorescent microscopy.

3.2.2 Immunofluorescent analysis to visualise eGFP and Kpnβ1-eGFP expression in HeLa and CaSki cells.

Due to the fluorescent nature of eGFP, HeLa eGFP, HeLa Kpnβ1-eGFP, CaSki eGFP and CaSki Kpnβ1-eGFP cells can be visualised using fluorescent microscopy. Cells were mounted onto slides and stained with DAPI for the concurrent visualisation of nuclei. The images captured were processed using *ImageJ* (Version 2.14.0) where the average fluorescence value of the background, where no cells were present, was determined and then subtracted from the entire image to remove any background fluorescence. This was repeated for both the green and blue channels before the channels were merged.

HeLa eGFP and CaSki eGFP cells produce eGFP that is unbound and anticipated to localise throughout the cell, including in the nucleus, as it is a small protein (less than 40 kDa) that can diffuse into the nucleus without an NLS[74]. Indeed, the fluorescent images show that eGFP is spread diffusely across the cell area and does not appear to concentrate in any specific area or organelle (Figure 3.2). In HeLa and CaSki Kpnβ1-eGFP expressing cell lines, Kpnβ1-eGFP is also detected throughout the cell, including in the cytosol and the nucleus, with an indication of slightly more fluorescence concentrated in a perinuclear localisation (Figure 3.2). This localisation of Kpnβ1-eGFP correlates with the areas where Kpnβ1 is located in the cell. As a nuclear transport protein Kpnβ1 can travel to all areas of the cell to collect cargo, so is present throughout the cell, also on the nuclear envelope from where it transports its cargo into the nucleus.

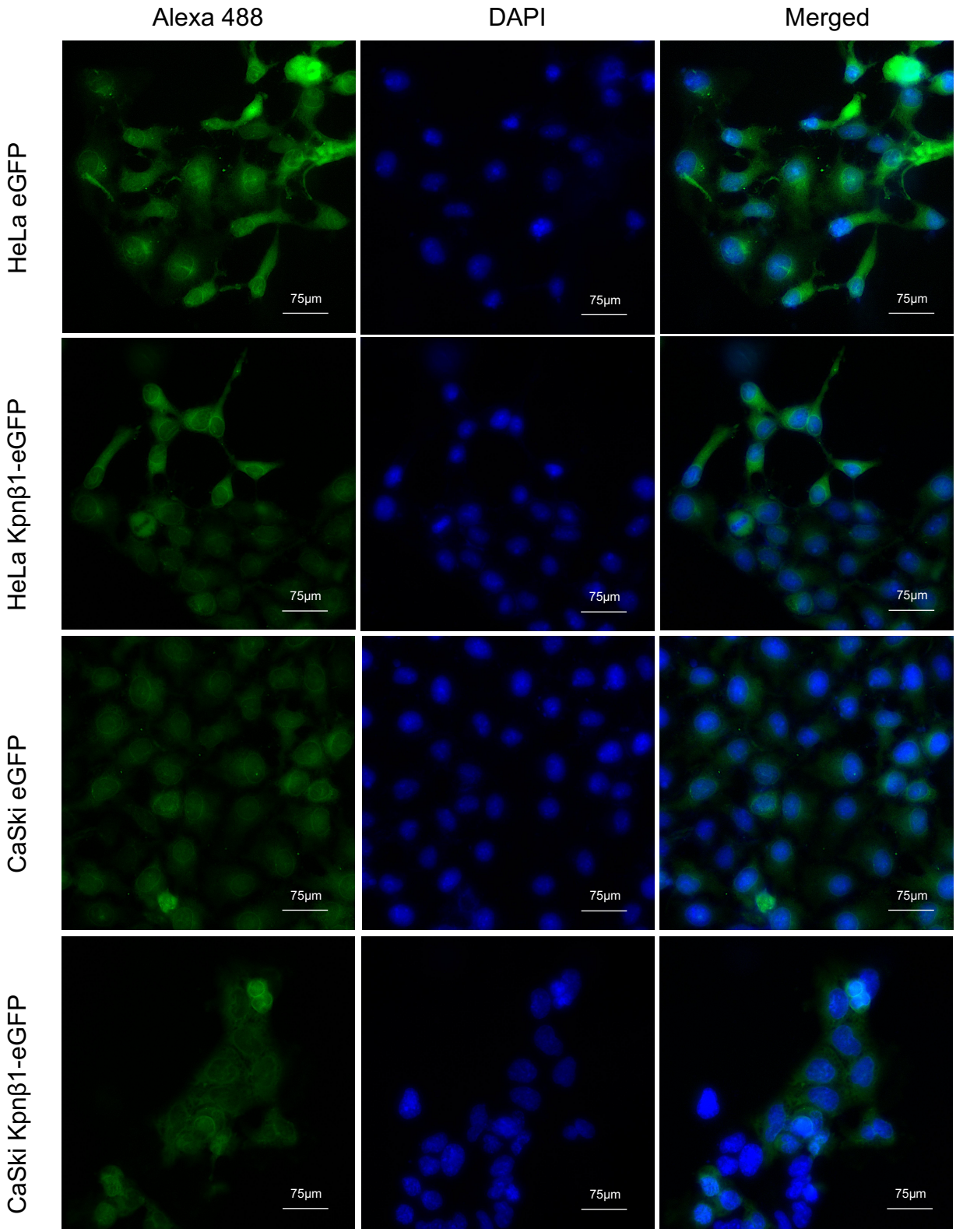

Figure 3.2: Immunofluorescent analysis to detect eGFP and Kpnβ1-eGFP in HeLa and CaSki eGFP and Kpnβ1-eGFP cells. eGFP localisation in HeLa eGFP, HeLa Kpnβ1-eGFP, CaSki eGFP and CaSki Kpnβ1-eGFP cell lines imaged using fluorescent microscopy at a magnification of 40X. Cell nuclei were stained with DAPI.

Having established Kpnβ1-eGFP expression in HeLa and CaSki cell lines, the biological relevance of Kpnβ1 overexpression was next investigated on cellular phenotypes including morphology, proliferation, and migration.

3.2.3 The effect of Kpnβ1 overexpression on the morphology of HeLa and CaSki cells.

To determine the effect of the overexpressed Kpnβ1-eGFP on the morphology of cervical cancer cells, HeLa Kpnβ1-eGFP, HeLa eGFP, CaSki Kpnβ1-eGFP and CaSki eGFP were visualised using phase contrast microscopy.

HeLa eGFP cells show the standard HeLa cell morphology (Figure 3.3 A). The HeLa Kpnβ1-eGFP cells show a different morphology with the cells appearing rounder in shape and more tightly packed, forming clumps of cells (Figure 3.3 B).

The CaSki eGFP cells show the standard CaSki morphology, having a cobblestone appearance and growing close to one another (Figure 3.3 C) and the CaSki Kpnβ1-eGFP cells showed a similar morphology to the CaSki eGFP cells with no obvious difference in shape and size (Figure 3.3 D). Similar to HeLa Kpnβ1-eGFP the CaSki Kpnβ1-eGFP grow close together and form clumps but is not as pronounced a difference when compared to the respective GFP-expressing cells.

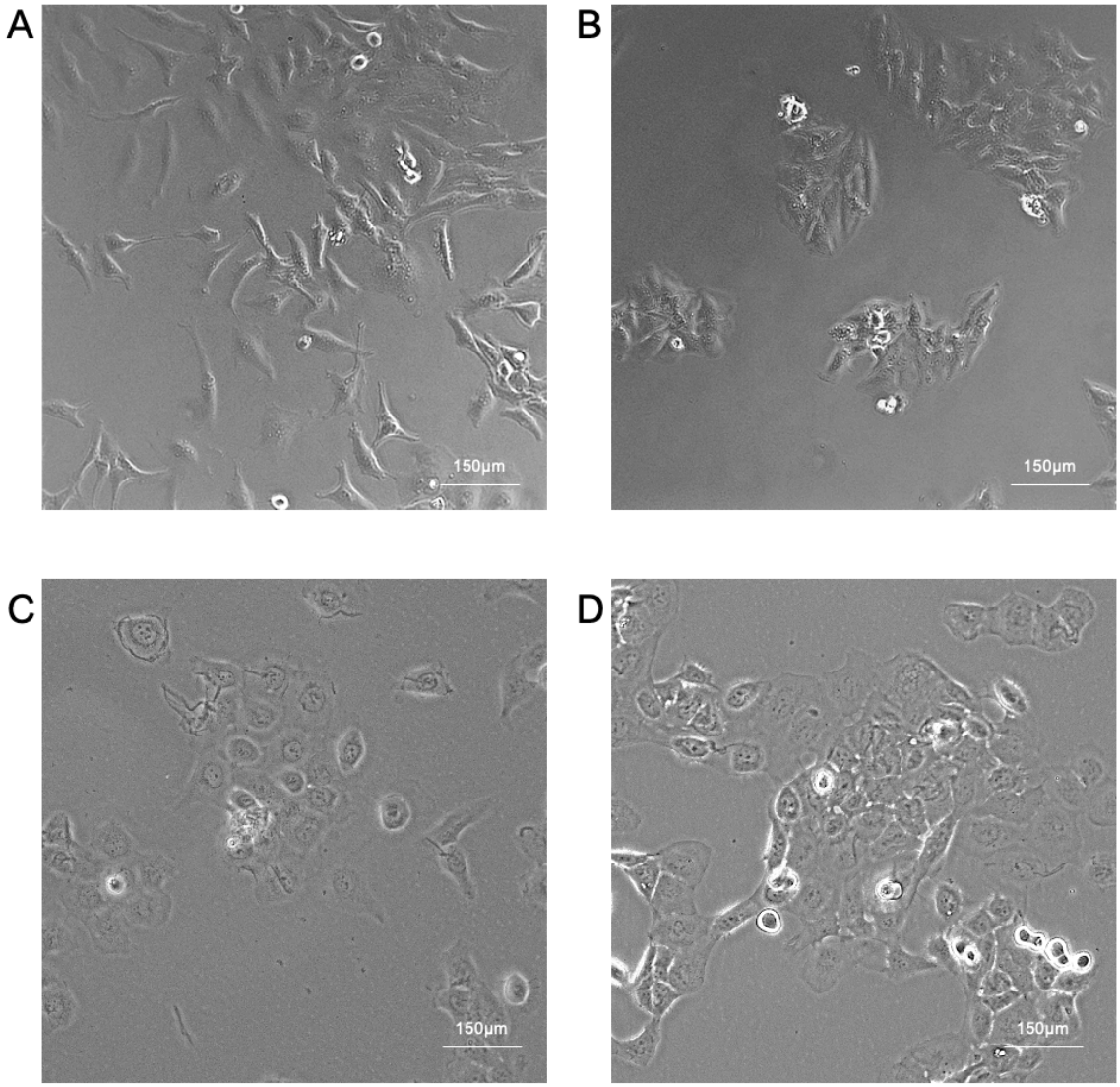

Figure 3.3: Morphology of HeLa and CaSki cells expressing eGFP and Kpnβ1-eGFP. Morphology of (A) HeLa eGFP, (B) HeLa Kpnβ1-eGFP, (C) CaSki eGFP, (D) CaSki Kpnβ1-eGFP cell lines imaged using phase contrast microscopy at a magnification of 20X.

3.2.4 Effect of Kpnβ1 overexpression on the proliferation of HeLa and CaSki cells.

To investigate the effect of the overexpressed Kpnβ1-eGFP on the proliferation of cervical cancer cells, proliferation was monitored using MTT assays. HeLa Kpnβ1-eGFP and HeLa eGFP cell lines showed no statistically significant differences in proliferation up to seventy-two hours, although a trend of increased proliferation in HeLa Kpnβ1-eGFP was observed. Proliferation observed in HeLa Kpnβ1-eGFP overexpressing cells at ninety-six hours was significantly higher than in HeLa eGFP cells (relative proliferation of 16.1 vs 6.5, $p = 0.026$) (Figure 3.4 A). Interestingly, CaSki

Kpnβ1-eGFP cells showed significantly slower proliferation compared to CaSki eGFP at 24 hours (relative proliferation of 1.3 vs 2.3, p = 0.001), 72 hours (relative proliferation of 4.4 vs 5.6, p = 0.006) and 96 hours (relative proliferation of 6.1 vs 9.2, p = 0.010) (Figure 3.4 B).

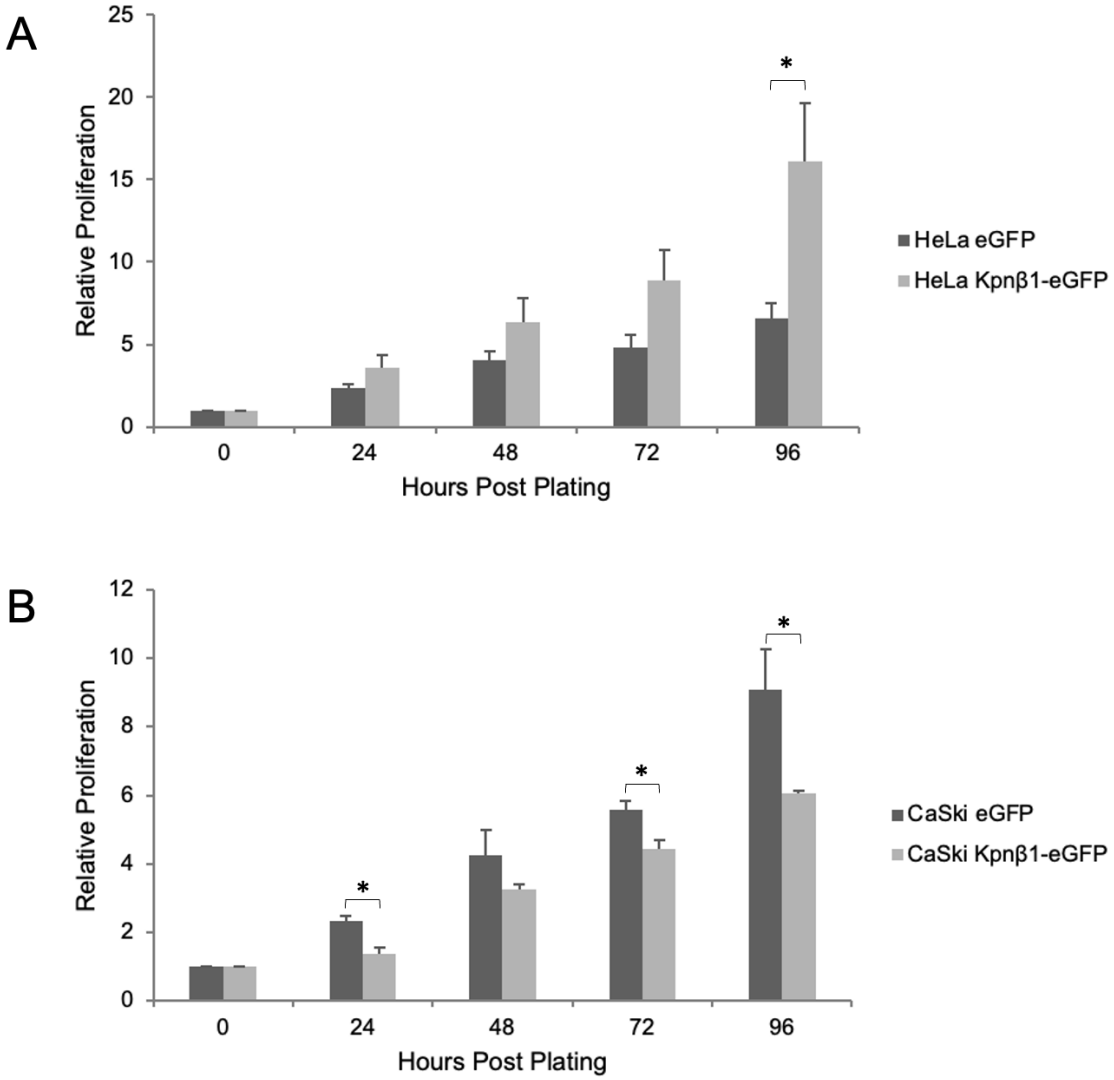

Figure 3.4: Proliferation of eGFP and Kpnβ1-eGFP expressing HeLa and CaSki cells. (A) HeLa eGFP and HeLa Kpnβ1-eGFP and (B) CaSki eGFP and CaSki Kpnβ1-eGFP, cell proliferation over a 96-hour period is shown relative to the number of proliferating cells when plated. Results are represented as the mean ± SEM. Experiments were performed at least three times. Statistically significant values ($p < 0.05$) are represented with an *

3.2.5 Effect of Kpnβ1 overexpression on the migration of HeLa and CaSki cells.

To investigate the effect of Kpnβ1 overexpression on the migratory ability of the cervical cancer cell lines a scratch assay was performed. The relative area of the original scratch still visible after twenty-four and forty-eight hours was determined using *ImageJ* and used as a proxy for cell migration. The area of the scratch remaining relative to the area of the original scratch was calculated and is representative of 3 independent repeat experiments. This method of analysing scratch closure allows comparison between experiments where the scratch closure may be inconsistent, or the original scratch area differed. The cells were treated with Mitomycin C alongside the scratch to inhibit proliferation so that any changes seen could be attributed to the migration of the cells.

The results showed migration over the forty-eight hour period as visualised by cells moving into the vacant area of the scratch (Figure 3.5 A). Both HeLa eGFP and HeLa Kpnβ1-eGFP showed a reduction in the scratch area by approximately 20% at twenty-four hours and approximately 30% by forty-eight hours (Figure 3.5 B). However, there was no significant difference in the migration of the control and Kpnβ1-eGFP overexpressing HeLa cells.

CaSki eGFP and CaSki Kpnβ1-eGFP cells reduced the scratch area by approximately 45% after twenty-four hours (Figure 3.5 A). However, there was no significant difference between the GFP expressing and the Kpnβ1-eGFP expressing CaSki cell lines (Figure 3.5 B). CaSki eGFP and CaSki Kpnβ1-eGFP appeared to be more sensitive to Mitomycin C treatment for periods longer than twenty-four hours so an accurate result at forty-eight hours post scratch could not be obtained.

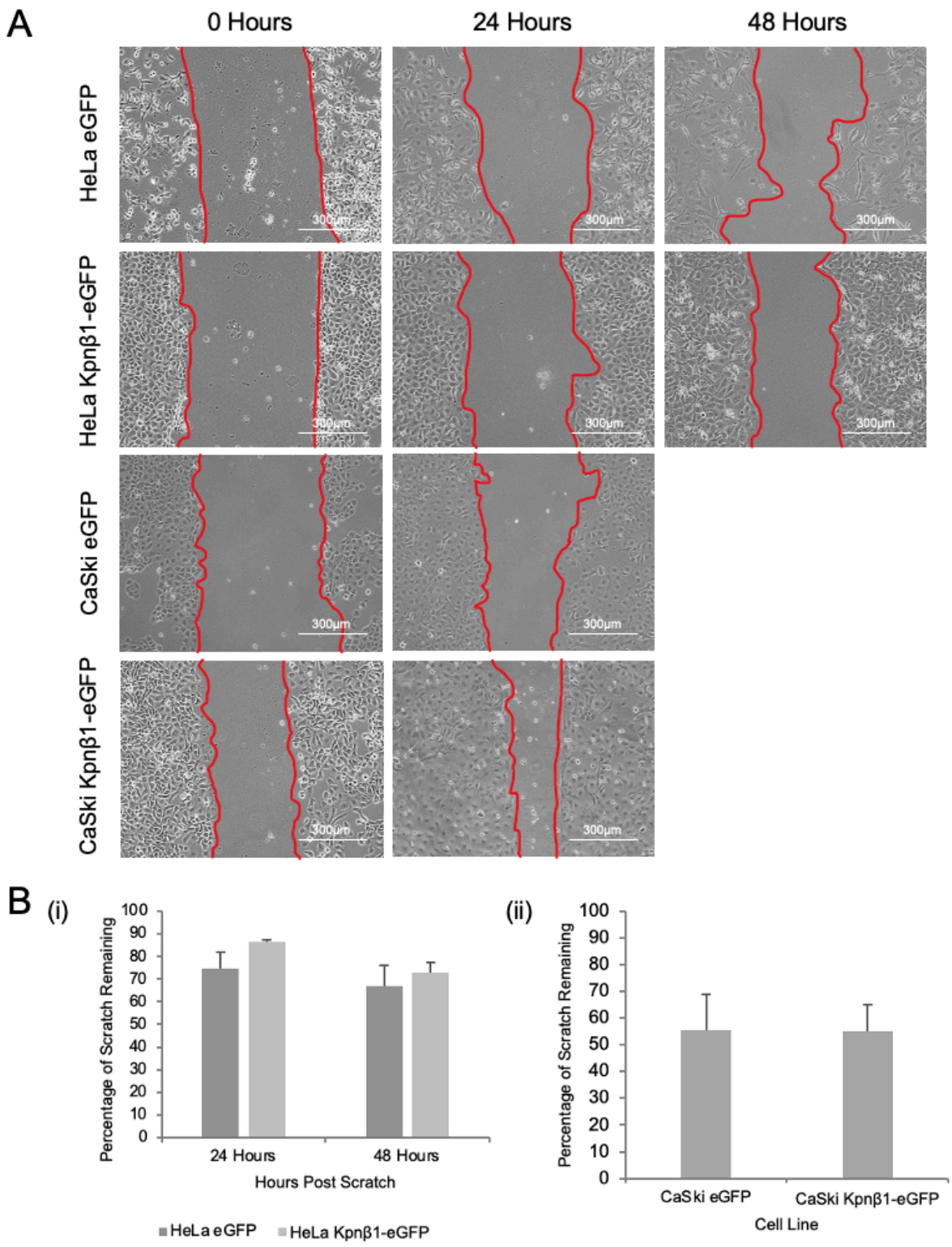

Figure 3.5. Migration of cervical cells expressing eGFP and Kpnβ1-eGFP. (A) Migration of cultured cervical cancer cell lines after the scratch line is drawn. Imaged using phase contrast microscopy at a magnification of 10X. The edge of the scratch is highlighted in red. (B) Percentage of the scratch area remaining after 24 and 48 hours for (i) Hela eGFP and HeLa Kpnβ1-eGFP cell lines and after 24 hours for (ii) CaSki eGFP and CaSki Kpnβ1-eGFP cell lines. Results are represented as the mean ± SEM. Experiments were performed 3 independent times.

We have prior evidence that multiple members of the nuclear transport protein family, including Kpnβ1 are secreted into the extracellular space. We thus next investigated whether exogenous Kpnβ1 was secreted from the cell, and if so, to investigate the effects of secreted Kpnβ1 on the biology of both cervical cancer cells and non-cancerous cells.

3.2.6 Secreted Kpnβ1 and Kpnβ1-eGFP in stabling expressing eGFP and Kpnβ1-eGFP HeLa and CaSki cells.

To determine whether Kpnβ1 and Kpnβ1-eGFP are secreted from stably expressing eGFP and Kpnβ1-eGFP HeLa and CaSki cells, secreted proteins were harvested, quantified and analysed by Western blot analysis.

The Western blot analysis results show that both the eGFP control cells and the Kpnβ1-eGFP expressing cell lines secrete Kpnβ1 into the extracellular space. Interestingly, the additional Kpnβ1-eGFP band at the expected size of 129.7 kD was also detected in the secreted fraction of both HeLa and CaSki cells stably expressing Kpnβ1-eGFP (Figure 3.6 A and B). β-tubulin was analysed in the secreted fractions to exclude cellular contamination of the secreted protein and no β-tubulin was detected. GAPDH, on the other hand, was used as a loading control as it has previously been reported to be secreted from cancer cells [75,76].

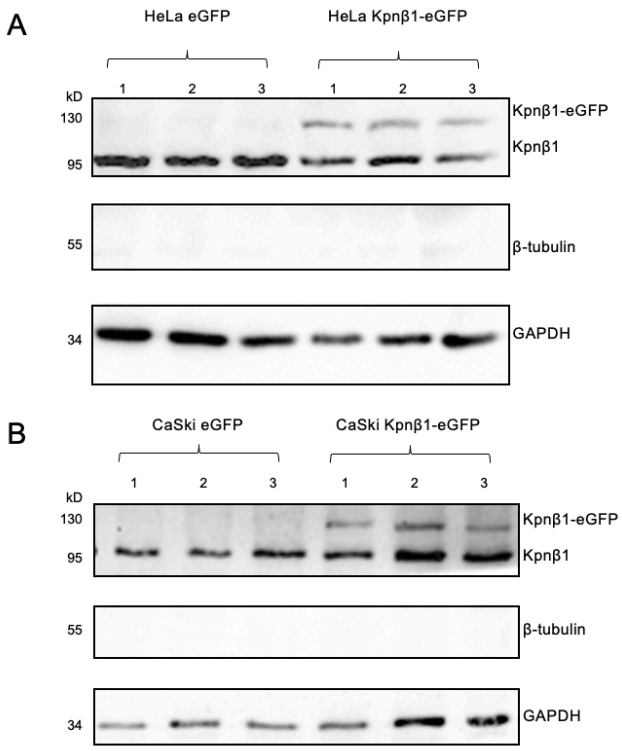

Figure 3.6: Secreted Kpnβ1 and Kpnβ1-eGFP from stably expressing eGFP and Kpnβ1-eGFP HeLa and CaSki cells. Western blot analysis of secreted Kpnβ1 from (A) HeLa eGFP and HeLa Kpnβ1-eGFP cells or (B) CaSki eGFP and CaSki Kpnβ1-eGFP cells. 15 µg of protein was loaded in each lane, β-tubulin was used to detect any contamination with cellular protein and GAPDH was used as a loading control. Three biological repeats are shown for each cell line.

3.2.7 Internalisation of secreted eGFP and Kpnβ1-eGFP by cervical cancer and non-cancer cells.

To mimic intercellular molecule delivery, as is seen in intercellular signalling, conditioned media from control eGFP and Kpnβ1-eGFP overexpressing HeLa and CaSki cell lines was collected after a twenty-four hour incubation in serum-free media. The conditioned media contains the secretome including signalling molecules, proteins, exosomes and other molecules secreted by the cells into the extracellular space. Parental cervical cancer cell lines, HeLa or CaSki, were incubated with the conditioned media from their respective eGFP and Kpnβ1-eGFP expressing counterparts, allowing the secreted protein fractions to target the recipient cells originating from the same tissue in an autocrine manner. hTERT RPE-1 non-cancer epithelial cells or FG0 non-cancer fibroblasts were similarly used as target cells originating from a different tissue type in a paracrine fashion. The cells were incubated with conditioned media containing secreted Kpnβ1 and Kpnβ1-eGFP for twenty-four

or forty-eight hours and association and internalisation of the fluorescent proteins by recipient cells monitored using fluorescent confocal microscopy. The confocal microscope imaged an optical slice of the cells' interior, to focus on internalised proteins and to exclude any that may have been bound to the surface of the cells.

The target cell lines: HeLa, CaSki, hTERT RPE-1 and FG0 do not express either eGFP or Kpnβ1-eGFP, hence fluorescent signals emanating from the cells after incubation with conditioned media should be reflective of eGFP cellular location due to internalisation. To exclude the effects that possible autofluorescence and non-specific fluorescence may have on the interpretation of results, target cells were incubated with conditioned media from HeLa or CaSki cells that do not express the eGFP proteins and imaged alongside the experimental samples. The mean gray value, indicative of pixel intensity, seen in the green channel of these controls was calculated and then subtracted from the images of the experimental samples using *ImageJ* to correct for autofluorescence and background fluorescence.

3.2.7.1 Internalisation of eGFP and Kpnβ1-eGFP in conditioned media by HeLa and CaSki cells.

Autofluorescence corrected images of GFP-Alexa 488 showing the association of eGFP with HeLa and CaSki cells after treatment with conditioned media containing eGFP or Kpnβ1-eGFP is presented in Figure 3.7. DAPI was used as a nuclear stain.

The results show that HeLa cells incubated with conditioned media from HeLa eGFP cells for twenty-four or forty-eight hours had internalised eGFP to varying extents, as evidenced by the green signals associating with some cells, an example of which is indicated by an arrow (Figure 3.7 A). Fluorescent signals associating with cells were also observed in the HeLa cells treated with conditioned media from HeLa Kpnβ1-eGFP cells in the twenty-four and forty-eight hours treatment groups (Figure 3.7 A).
The results for CaSki parental cells treated with conditioned media from CaSki eGFP or CaSki Kpnβ1-eGFP cells similarly, with both the treatment groups at the twenty-four and forty-eight time points, showed punctate fluorescence of eGFP or Kpnβ1-eGFP in some cells (Figure 3.7 B)

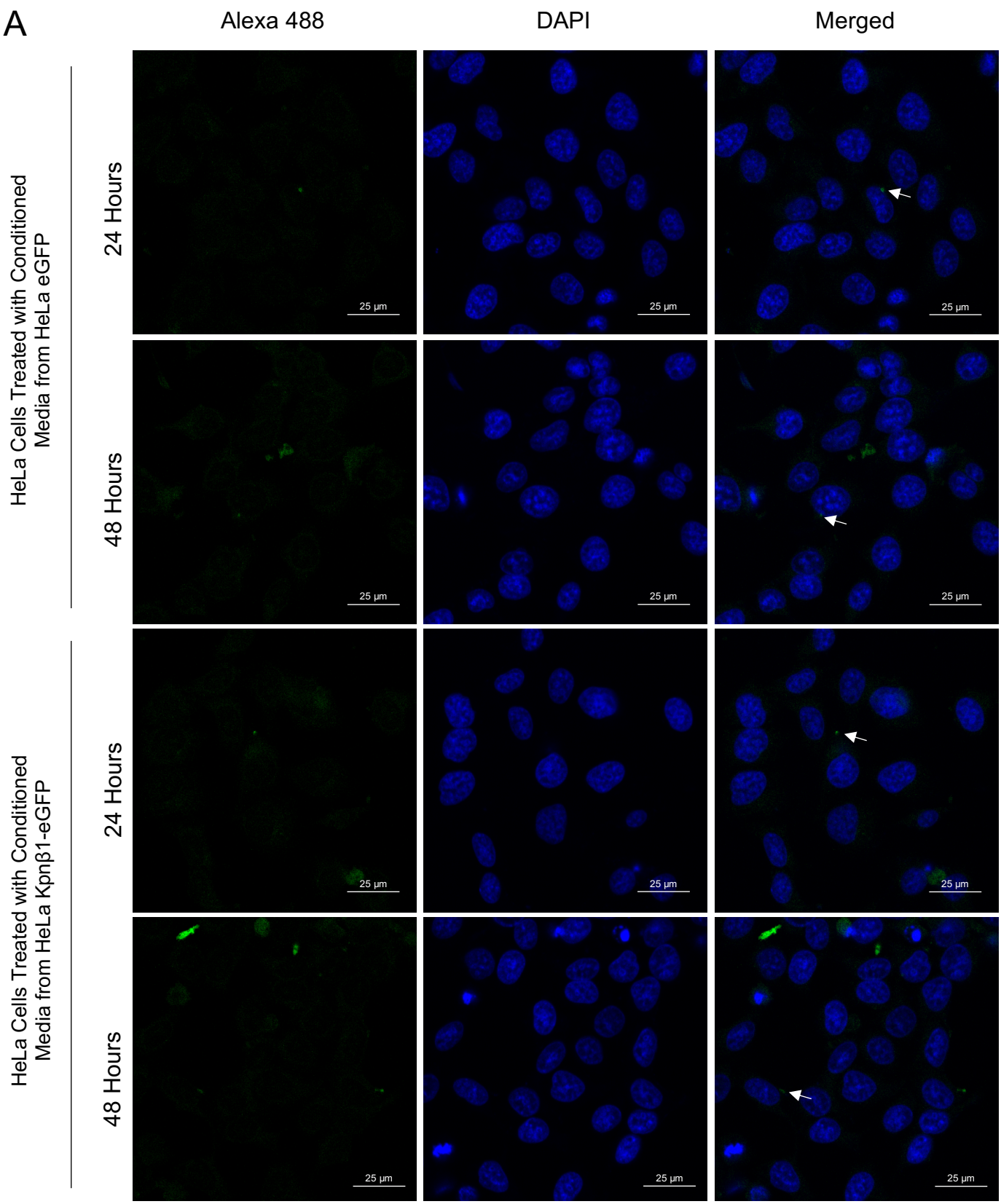
A
Alexa 488
DAPI
Merged
HeLa Cells Treated with Conditioned Media from HeLa eGFP
HeLa Cells Treated with Conditioned Media from HeLa Kpnβ1-eGFP
24 Hours
48 Hours
24 Hours
48 Hours
25 µm

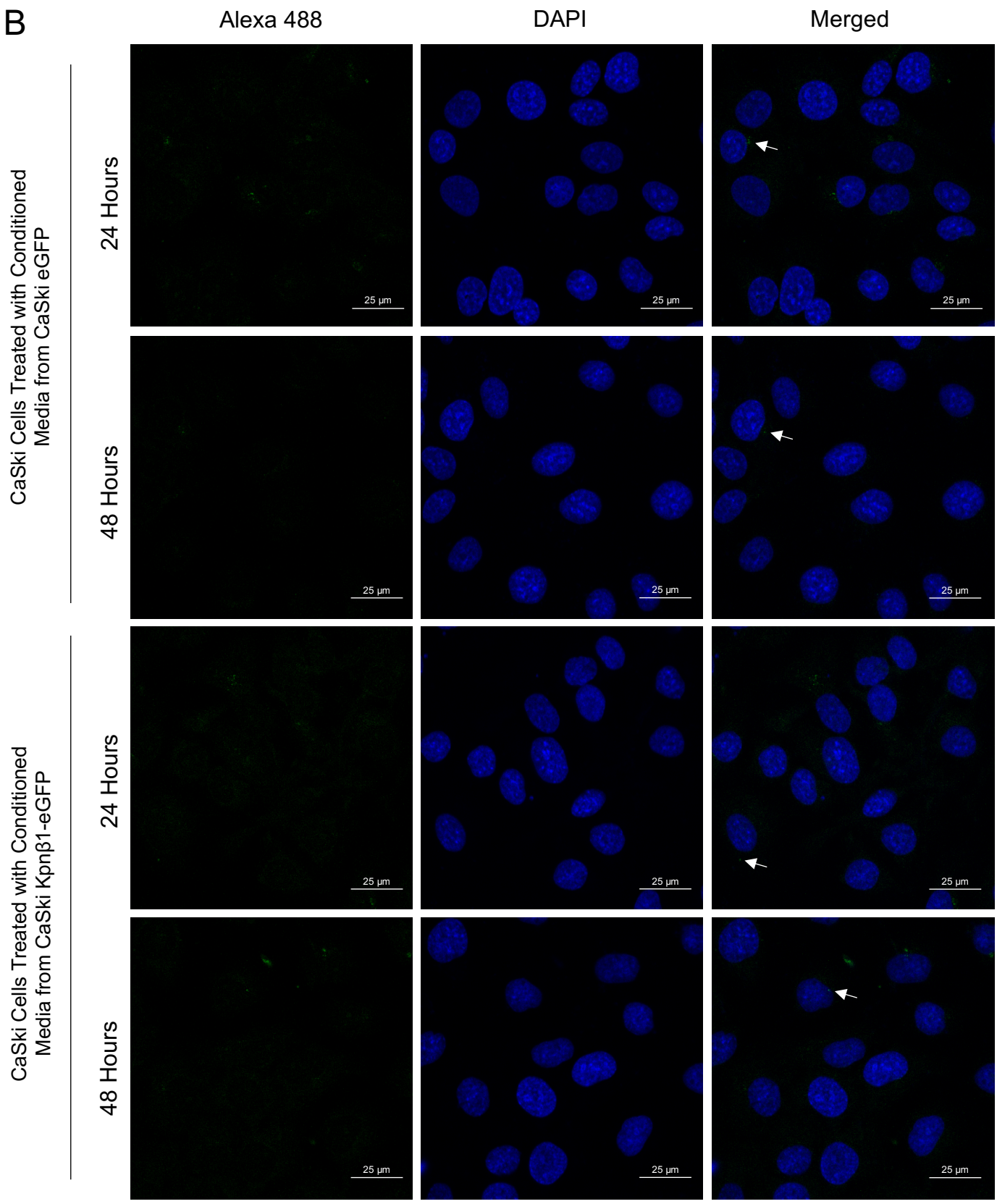

Figure 3.7: Fluorescent analysis of HeLa and CaSki cells incubated with conditioned media containing eGFP or Kpnβ1-eGFP. Representative GFP-Alexa 488 fluorescent images of (A) HeLa and (B) CaSki cells treated with conditioned media from eGFP or Kpnβ1-eGFP expressing HeLa and CaSki cells, respectively. Arrow in the merged images pointing to an area of eGFP internalisation. Images shown were captured at a magnification of 63X.

3.2.7.2 Internalisation of eGFP and Kpnβ1-eGFP from conditioned media by non-cancer hTERT RPE-1 and FG0 cells.

We next tracked the uptake of eGFP and Kpnβ1-eGFP from conditioned media isolated from eGFP and KpnB1-eGFP overexpressing HeLa and CaSki cell lines by non-cancer cell lines including the epithelial cell line hTERT RPE-1 and the fibroblast cell line FG0. Results are shown in Figures 3.8 and 3.9.

Fluorescent signals were detected in non-cancerous hTERT RPE-1 cells treated with conditioned media from HeLa eGFP and HeLa Kpnβ1-eGFP at both twenty-four and forty-eight hours, with more pronounced signals observed at the forty-eight hour time point (Figure 3.8A). As the fluorescence was not spread generally across the cells, this may be indicative of internalisation of the fluorescent proteins into the cytoplasmic space. hTERT RPE-1 cells also showed varying levels of internalised eGFP and Kpnβ1-eGFP from CaSki eGFP and CaSki Kpnβ1-eGFP conditioned media treatments (Figure 3.8B).

The non-cancerous fibroblast cells FG0 showed extensive fluorescent signals associating with the cells, indicative of eGFP and Kpnβ1-eGFP, at both twenty-four and forty-eight hours after treatment with HeLa eGFP and HeLa Kpnβ1-eGFP conditioned media (Figure 3.9 A). The signal was primarily seen in the cytoplasm of the cells. FG0 cells treated with CaSki eGFP and CaSki Kpnβ1-eGFP similarly had extensive fluorescent signals detected primarily in cytoplasmic region the cells, indicative of uptake of eGFP or Kpnβ1-eGFP at both twenty-four and forty-eight hours after treatment (Figure 3.9 B).

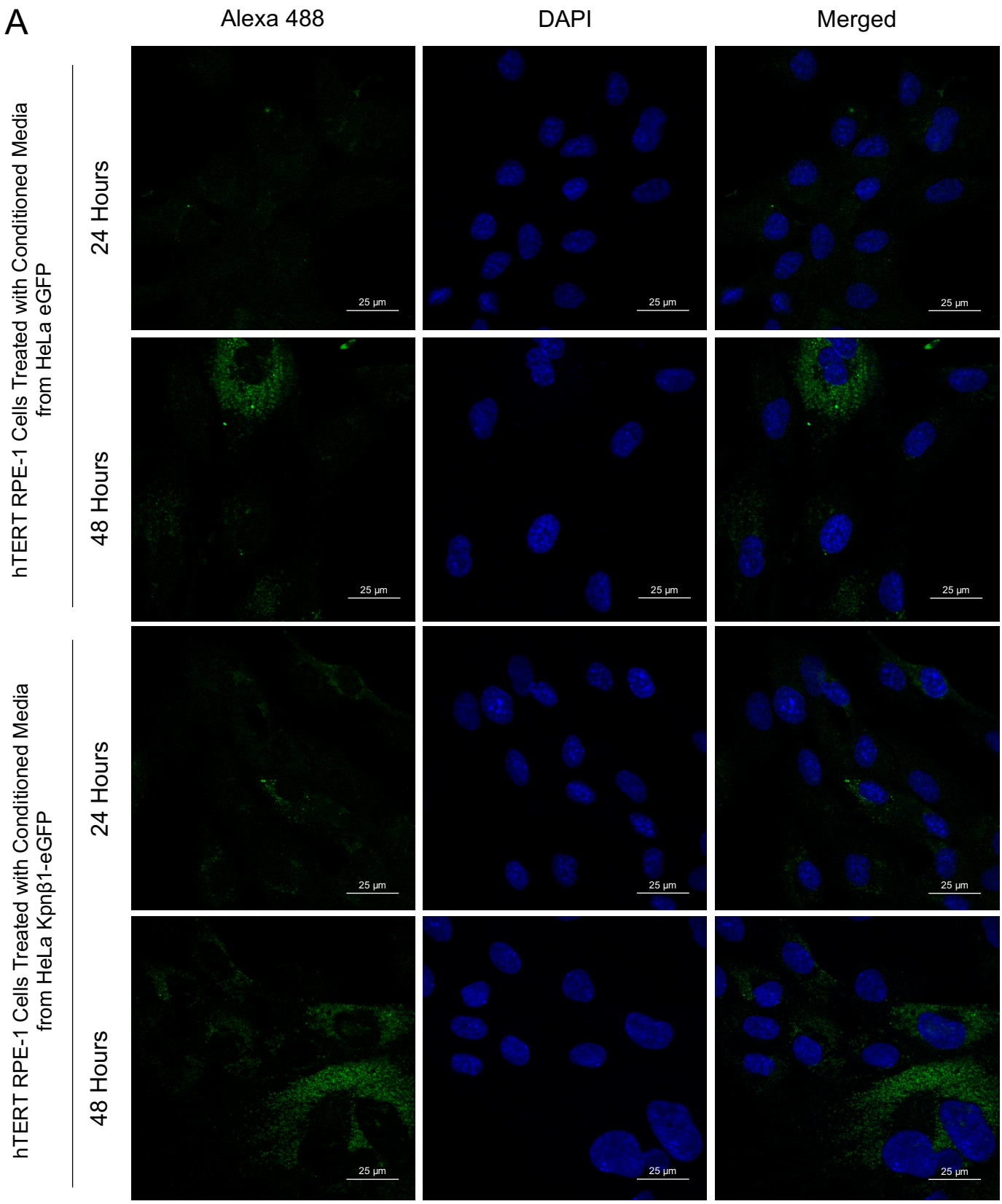
A
Alexa 488
DAPI
Merged
hTERT RPE-1 Cells Treated with Conditioned Media from HeLa eGFP
24 Hours
48 Hours
hTERT RPE-1 Cells Treated with Conditioned Media from HeLa Kpnβ1-eGFP
24 Hours
48 Hours
25 µm

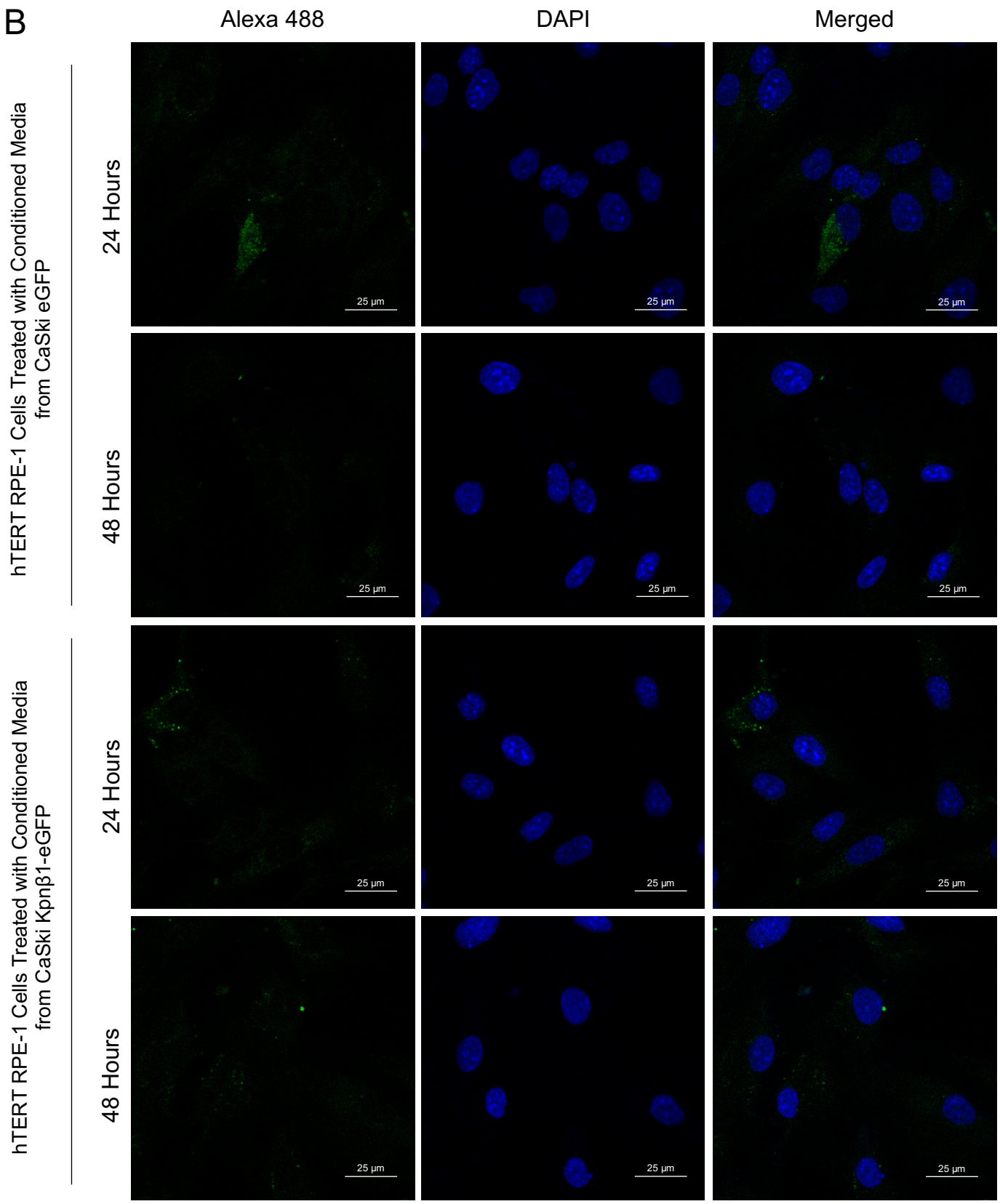

Figure 3.8: eGFP and Kpnβ1-eGFP fluorescence in hTERT RPE-1 cells treated with conditioned media from cervical cancer cell lines Representative fluorescent images of eGFP in hTERT RPE-1 treated with conditioned media from (A) HeLa eGFP and HeLa Kpnβ1-eGFP or (B) CaSki eGFP and CaSki Kpnβ1-eGFP. Imaged using fluorescent microscopy at a magnification of 63X.

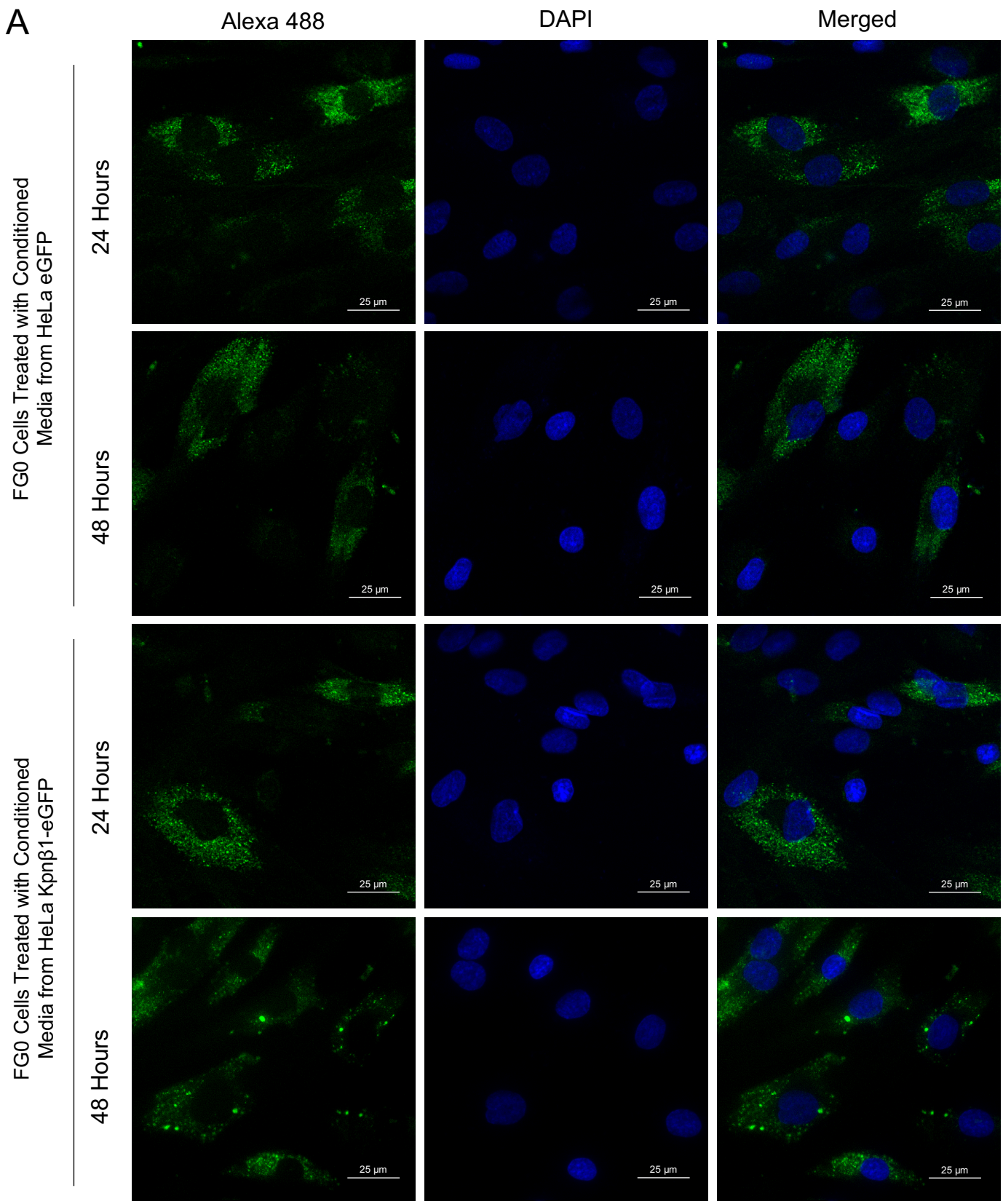
A
Alexa 488
DAPI
Merged
FG0 Cells Treated with Conditioned Media from HeLa eGFP
24 Hours
48 Hours
FG0 Cells Treated with Conditioned Media from HeLa Kpnβ1-eGFP
24 Hours
48 Hours
25 µm

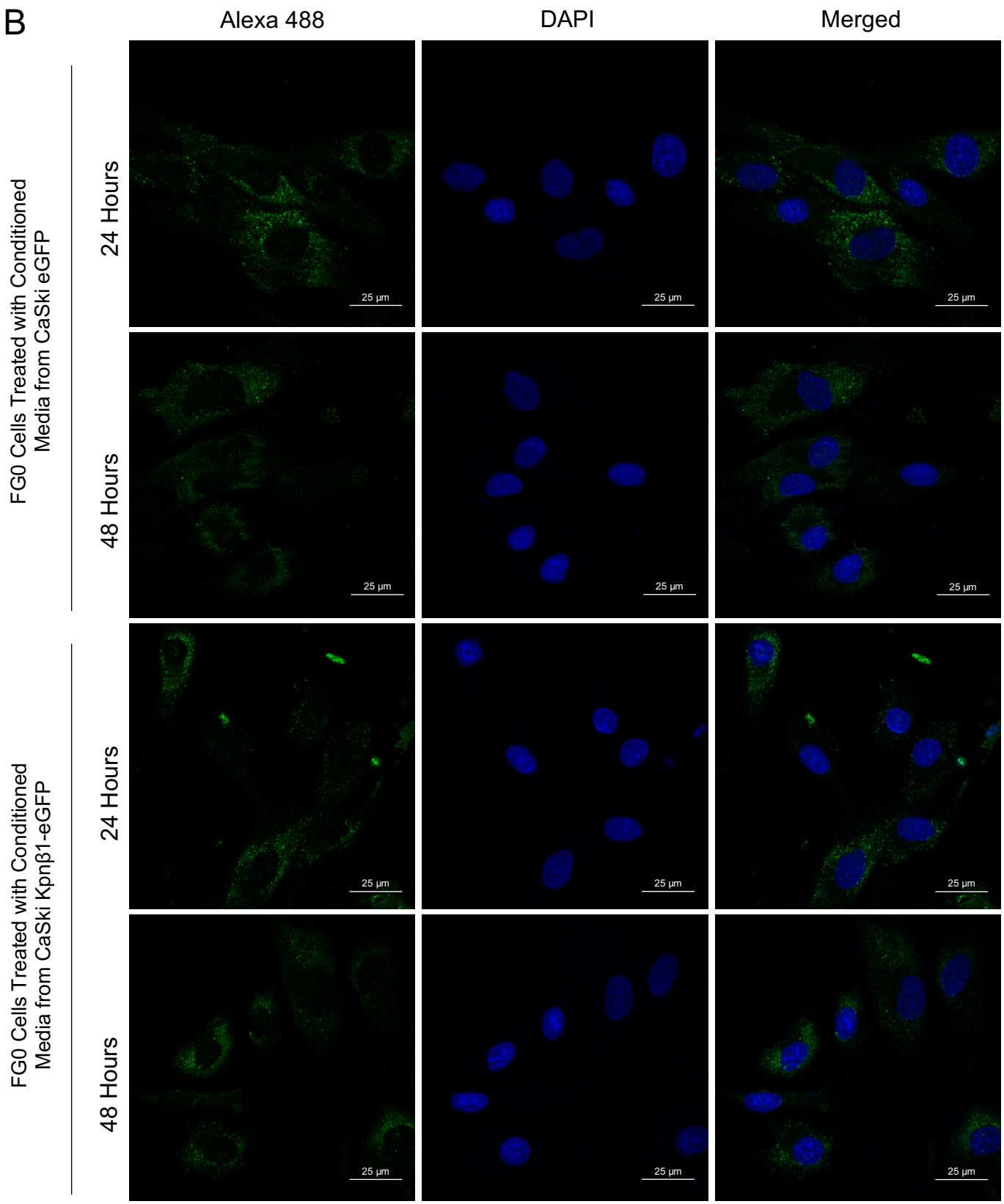

Figure 3.9: eGFP and Kpnβ1-eGFP fluorescence in FG0 cells treated with conditioned media from cervical cancer cell lines. Representative fluorescent images of eGFP in FG0 treated with conditioned media from (A) HeLa eGFP and HeLa Kpnβ1-eGFP or (B) CaSki eGFP and CaSki Kpnβ1-eGFP. Imaged using fluorescent microscopy at a magnification of 63X.

We next sought to determine the possible effects of conditioned media containing secreted Kpnβ1 on the biology of both cervical cancer cells and non-cancerous cells.

3.2.8 Morphology of cells treated with conditioned media from eGFP and Kpnβ1-eGFP expressing HeLa and CaSki cells.

Earlier in the chapter we showed that overexpressing Kpnβ1-eGFP in HeLa and CaSki cells resulted in changes in cell morphology making the HeLa cells appear rounder and both HeLa and CaSki cells appearing more tightly packed. In addition, these cell lines secreted Kpnβ1 and Kpnβ1-eGFP into the extracellular space, which in turn could be internalised by the parental HeLa and CaSki cells as well as non-cancer hTERT RPE-1 and FG0 to varying extents. We next assessed if the conditioned media had any effect on the biological features of target cells, including cell morphology, proliferation and migration.

To monitor effects on cell morphology, HeLa and CaSki parental cells were incubated with eGFP or Kpnβ1-eGFP containing conditioned media for twenty-four and forty-eight hours after which images of cells were captured using phase contrast microscopy. Serum free media was used as a control for comparison.

HeLa cells incubated with conditioned media from HeLa eGFP cells did not appear to have any morphological differences from the control cells at either time point, however, the cells treated with conditioned media from HeLa Kpnβ1-eGFP cells appeared to grow in a marginally more tightly packed manner (Figure 3.10).

CaSki cells similarly did not show any distinct morphological changes between the control and CaSki eGFP and Kpnβ1-eGFP containing conditioned media at twenty-four or forty-eight hours post treatment (Figure 3.10). As CaSki cells generally grow in a more tightly packed manner the effects on cell morphology were more subtle.

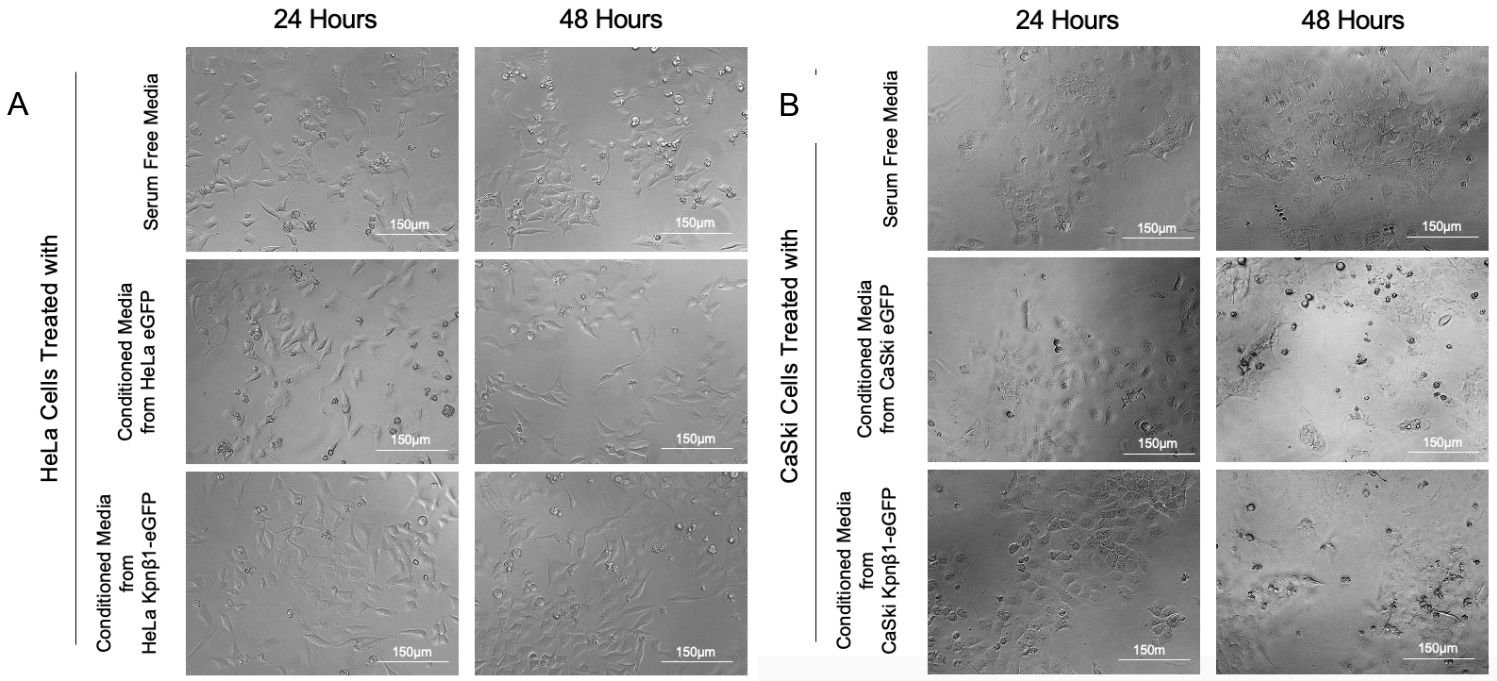

Figure 3.10: Morphology of parental HeLa and CaSki cells treated with conditioned media from eGFP or Kpnβ1-eGFP HeLa and CaSki cells. (A) HeLa cells treated with conditioned media originating from Hela eGFP and HeLa Kpnβ1-eGFP or (B) CaSki cells treated with conditioned media from CaSki eGFP and CaSki Kpnβ1-eGFP cells, with serum free media as a control, were imaged after 24 and 48 hours. Images were captured using phase contrast microscopy at a magnification of 20X.

The morphology of non-cancer epithelial hTERT RPE-1 cells treated with conditioned media from eGFP and Kpnβ1-eGFP expressing HeLa and CaSki cells similarly had no apparent effect on the morphology of hTERT RPE-1 cells at either twenty-four or forty-eight hours (Figure 3.11).

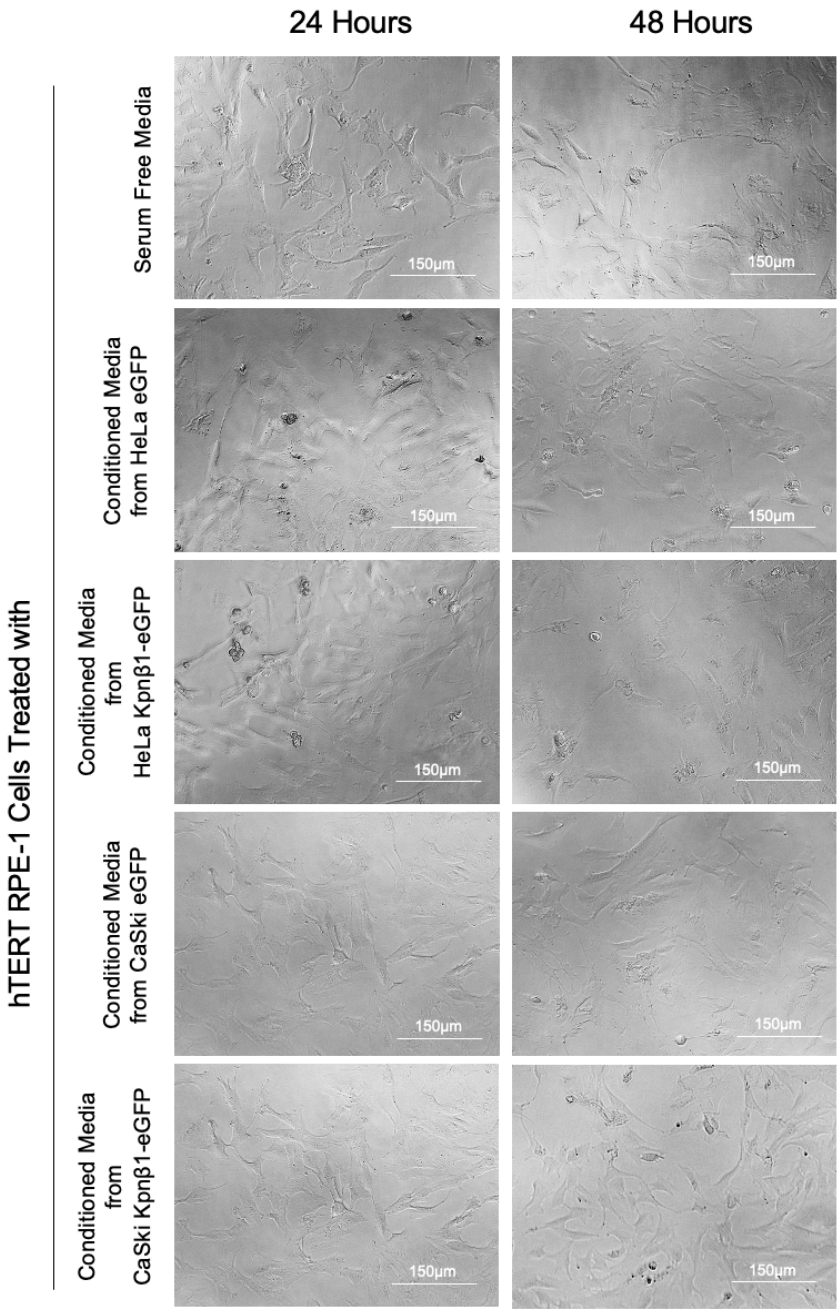

Figure 3.11: Morphology of hTERT RPE-1 non-cancerous cells treated with conditioned media from eGFP and Kpnβ1-eGFP HeLa and CaSki cell lines hTERT RPE-1 were treated with conditioned media originating from Hela eGFP, HeLa Kpnβ1-eGFP, CaSki eGFP and CaSki Kpnβ1-eGFP with serum free media as a control and imaged after 24 and 48 hours. Images were captured using phase contrast microscopy at a magnification of 20X.

FG0 non-cancerous fibroblast cells treated with conditioned media from eGFP and Kpnβ1-eGFP expressing HeLa and CaSki cells appeared to slightly more tightly packed in comparison the serum free media treated controls at both twenty-four and

forty-eight hours (Figure 3.12). No obvious differences were observed between cells treated with eGFP and Kpnβ1-eGFP containing conditioned media.

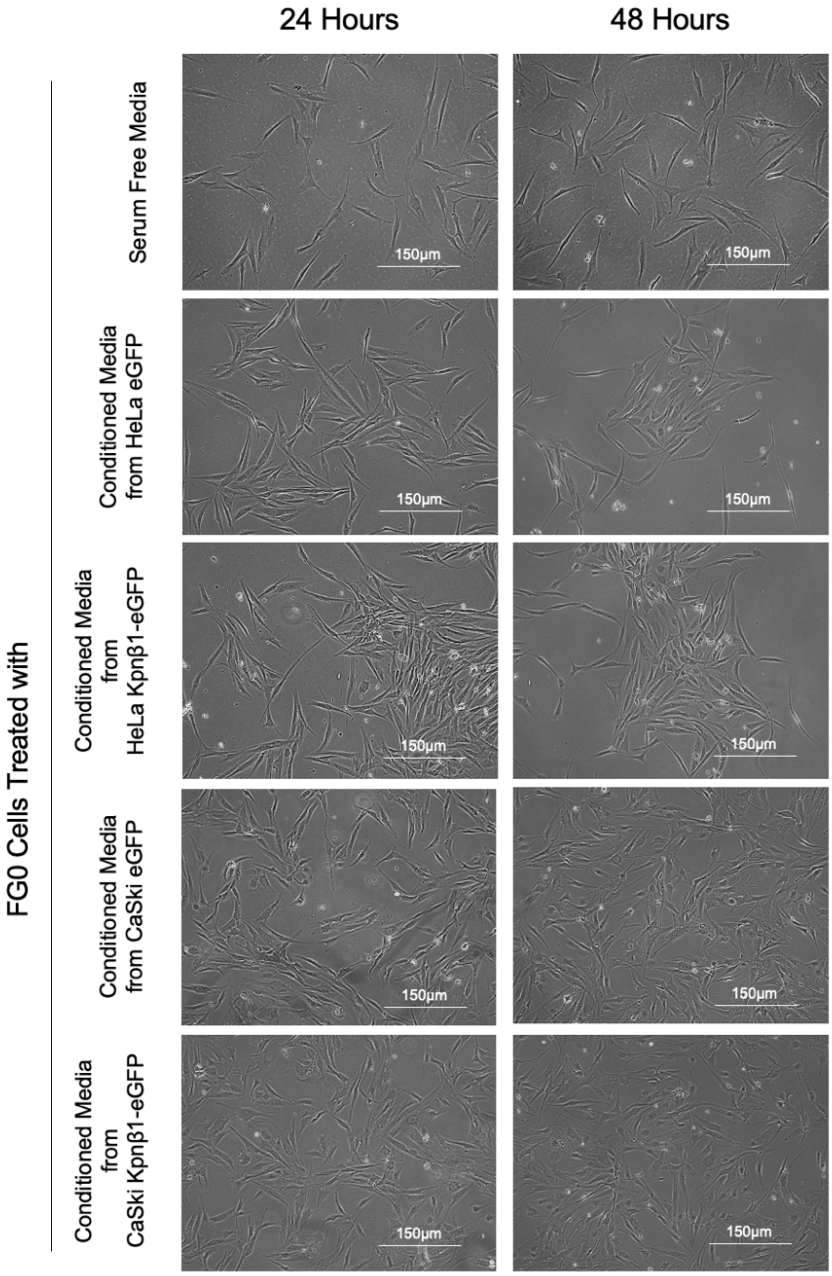

Figure 3.12: Morphology of FG0 non-cancerous cells treated with conditioned media from eGFP and Kpnβ1-eGFP HeLa and CaSki cell lines FG0 cells and treated with conditioned media originating from Hela eGFP, HeLa Kpnβ1-eGFP, CaSki eGFP and CaSki Kpnβ1-eGFP with serum free media as a control were imaged after 24 and 48 hours. Images were captured using phase contrast microscopy at a magnification of 20X.

3.2.9 Determining the effect of conditioned media from eGFP and Kpnβ1-eGFP expressing HeLa and CaSki cells on the proliferation of parental cervical cancer and non-cancer cell lines.

MTT Assays were used to monitor the effect of conditioned media from eGFP-expressing or Kpnβ1-eGFP overexpressing HeLa and CaSki cells on HeLa, CaSki, hTERT RPE-1 and FG0 cell prolifration. Cells grown in serum free media were included as controls.

HeLa cells incubated with conditioned media from HeLa eGFP cells showed an increase in proliferation compared to the cells treated only with serum free media at both twenty-four (relative proliferation of 1.5 vs 1.0, $p = 0.040$) and forty-eight hours (relative proliferation of 2.0 vs 1.0, $p = 0.038$). HeLa cells treated with conditioned media from HeLa Kpnβ1-eGFP showed an increase in proliferation compared to the control group at forty-eight hours (relative proliferation of 2.1 vs 1.0, $p = 0.025$). However, no significant change in proliferation between eGFP and Kpnβ1-eGFP containing HeLa conditioned media was observed (Figure 3.13 A).

CaSki cells incubated with conditioned media from CaSki eGFP cells showed an increase in proliferation compared to cells grown in serum-free media at both twenty-four (relative proliferation of 1.7 vs 1.0, $p = 0.020$) and forty-eight hours (relative proliferation of 1.8 vs 1.0, $p = 0.003$). CaSki cells incubated with conditioned media from CaSki Kpnβ1-eGFP cells also showed an increase in proliferation relative to the control group at both twenty-four (relative proliferation of 1.5 vs 1.0, $p = 0.012$) and forty-eight hours (relative proliferation of 1.8 vs 1.0, $p = 0.011$). There was no significant difference observed between the conditioned media treatment groups (Figure 3.13 B).

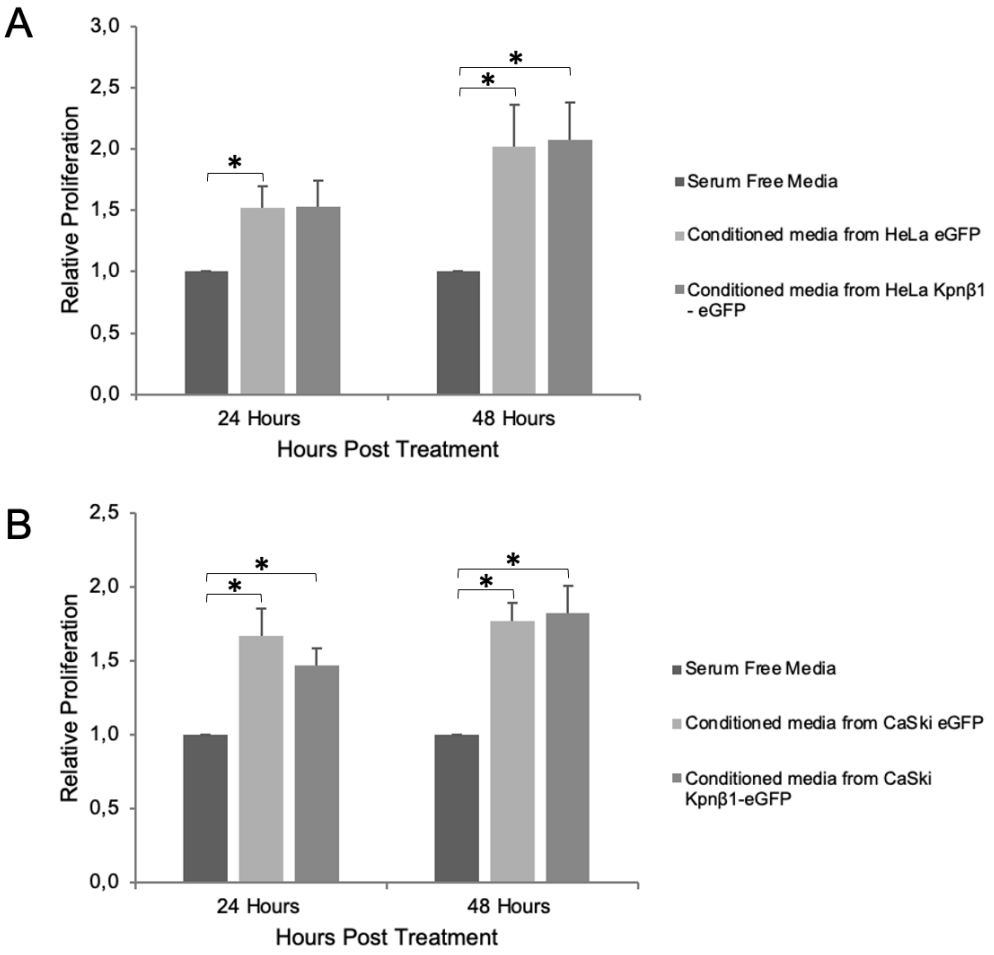

Figure 3.13: Proliferation of HeLa and CaSki cells treated with eGFP or Kpnβ1-eGFP containing conditioned media from HeLa and CaSki cells. The relative proliferation of (A) HeLa cells treated with conditioned media from HeLa eGFP or HeLa Kpnβ1-eGFP and (B) CaSki cells treated with conditioned media from CaSki eGFP or CaSki Kpnβ1-eGFP. Serum free media was used as a control and the MTT results are shown relative to the number of proliferating cells in the control group. Results are represented as the mean ± SEM of experiments performed in triplicate and repeated at least 3 independent times. Statistically significant values ($p < 0.05$) are represented with an *.

The non-cancerous epithelial cell line hTERT RPE-1 similarly showed increased proliferation after treatment with conditioned media from eGFP or Kpnβ1-eGFP expressing HeLa and CaSki cells, with no difference between the conditioned media treatment groups (Figure 3.14 A and B). hTERT RPE-1 cells incubated with conditioned media from HeLa eGFP cells showed an increase in proliferation compared to cells grown in serum-free media at both twenty-four (relative proliferation of 1.9 vs 1.0, $p = 0.005$) and forty-eight hours (relative proliferation of 3.7 vs 1.0, $p = 0.006$). CaSki cells incubated with conditioned media from HeLa Kpnβ1-eGFP cells

also showed an increase in proliferation relative to the control group at both twenty-four (relative proliferation of 1.9 vs 1.0, p = 0.007) and forty-eight hours (relative proliferation of 3.4 vs 1.0, p = 0.003) (Figure 3.14 A)

hTERT RPE-1 cells incubated with conditioned media from CaSki eGFP cells showed an increase in proliferation compared to cells grown in serum-free media at both twenty-four (relative proliferation of 2.4 vs 1.0, p = 0.017) and forty-eight hours (relative proliferation of 2.3 vs 1.0, p = 0.028). CaSki cells incubated with conditioned media from CaSki Kpnβ1-eGFP cells also showed an increase in proliferation relative to the control group at both twenty-four (relative proliferation of 3.3 vs 1.0, p = 0.014) and forty-eight hours (relative proliferation of 2.4 vs 1.0, p = 0.035) (Figure 3.14 B)

FG0 fibroblast cells treated with conditioned media from HeLa eGFP showed a modest increase in proliferation after forty-eight hours compared to the FG0 cells treated with serum free media (relative proliferation of 1.2 vs 1.0, p = 0.018) with no significant differences between the two conditioned media treatment groups (Figure 3.14 C).

FG0 cells incubated with conditioned media from CaSki eGFP cells showed an increase in proliferation compared to cells grown in serum-free media at twenty-four hours (relative proliferation of 1.1 vs 1.0, p = 0.009) and forty-eight hours (relative proliferation of 1.1 vs 1.0, p = 0.001). FG0 cells incubated with conditioned media from CaSki Kpnβ1-eGFP cells also showed an increase in proliferation relative to the control group at forty-eight hours (relative proliferation of 1.5 vs 1.0, p = 0.000) (Figure 3.14D).

FG0 cells treated with conditioned media from CaSki Kpnβ1-eGFP cells had a significant increase of approximately 15% in proliferation compared to those treated with conditioned media from CaSki eGFP at forty-eight hours (relative proliferation of 1.5 vs 1.1, p = 0.006) (Figure 3.14D).

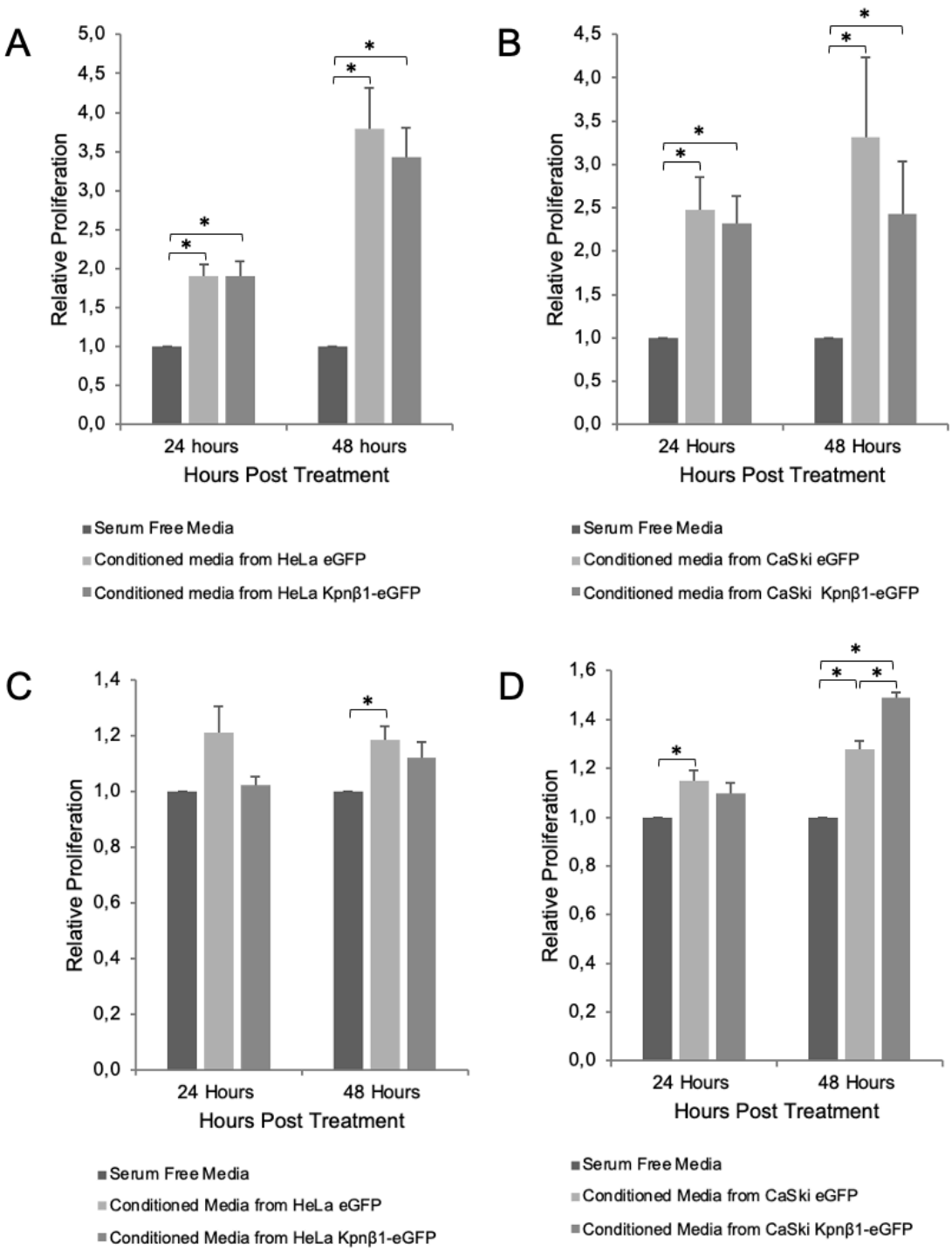

Figure 3.14: Proliferation of non-cancerous cells treated with conditioned media from cervical cancer cell lines. The relative proliferation of hTERT RPE-1 cells treated with conditioned media from (A) HeLa eGFP or HeLa Kpnβ1-eGFP, (B) CaSki eGFP or CaSki Kpnβ1-eGFP or FG0 cells treated with conditioned media from (C) HeLa eGFP or HeLa Kpnβ1-eGFP and (D) CaSki eGFP or CaSki Kpnβ1-eGFP. Serum free media was used as a control and the MTT results are shown relative to the serum-free control group. Results are represented as the mean ± SEM of experiments performed in triplicate and performed at least 3 independent times. Statistically significant values ($p < 0.05$) are represented with an *.

3.2.10 Determining the effect of conditioned media from eGFP and Kpnβ1-eGFP expressing HeLa and CaSki cells on cell migration.

One of the hallmarks of cancer is the ability of cancer cells to migrate from the primary tumour to distant sites [26]. To investigate if conditioned media from eGFP or Kpnβ1-eGFP overexpressing HeLa and CaSki cells affects the migration of parental HeLa and CaSki and non-cancerous hTERT RPE-1 and FG0 cells, scratch assays were used.

Scratch assay results for HeLa cells treated with serum free media, or conditioned media from HeLa eGFP or HeLa Kpnβ1-eGFP cells for twenty-four and forty-eight hours are shown in Figure 3.15 A. Quantification of the scratch area for the HeLa cells shows that the HeLa eGFP conditioned media treatment resulted in a marginal but significant reduction in the scratch area compared to that observed with serum free media at twenty-four hours (scratch area reduction of 14% vs 2%, p = 0,049), but that there was no significant difference between the two treatments (Figure 3.15 B).

CaSki cells treated with serum free media or conditioned media from CaSki eGFP and CaSki Kpnβ1-eGFP cells showed similar migratory ability at twenty-four hours post treatment (Figure 3.15 A). Quantification of the scratch area across the 3 repeats confirmed that there were no significant differences in migratory ability observed across treatments (Figure 3.15 B). As observed in the CaSki eGFP and CaSki Kpnβ1-eGFP cells, CaSki cells were sensitive to Mitomycin C treatments longer than twenty-fours hours hence an accurate result for forty-eight hours after treatment could not be obtained.

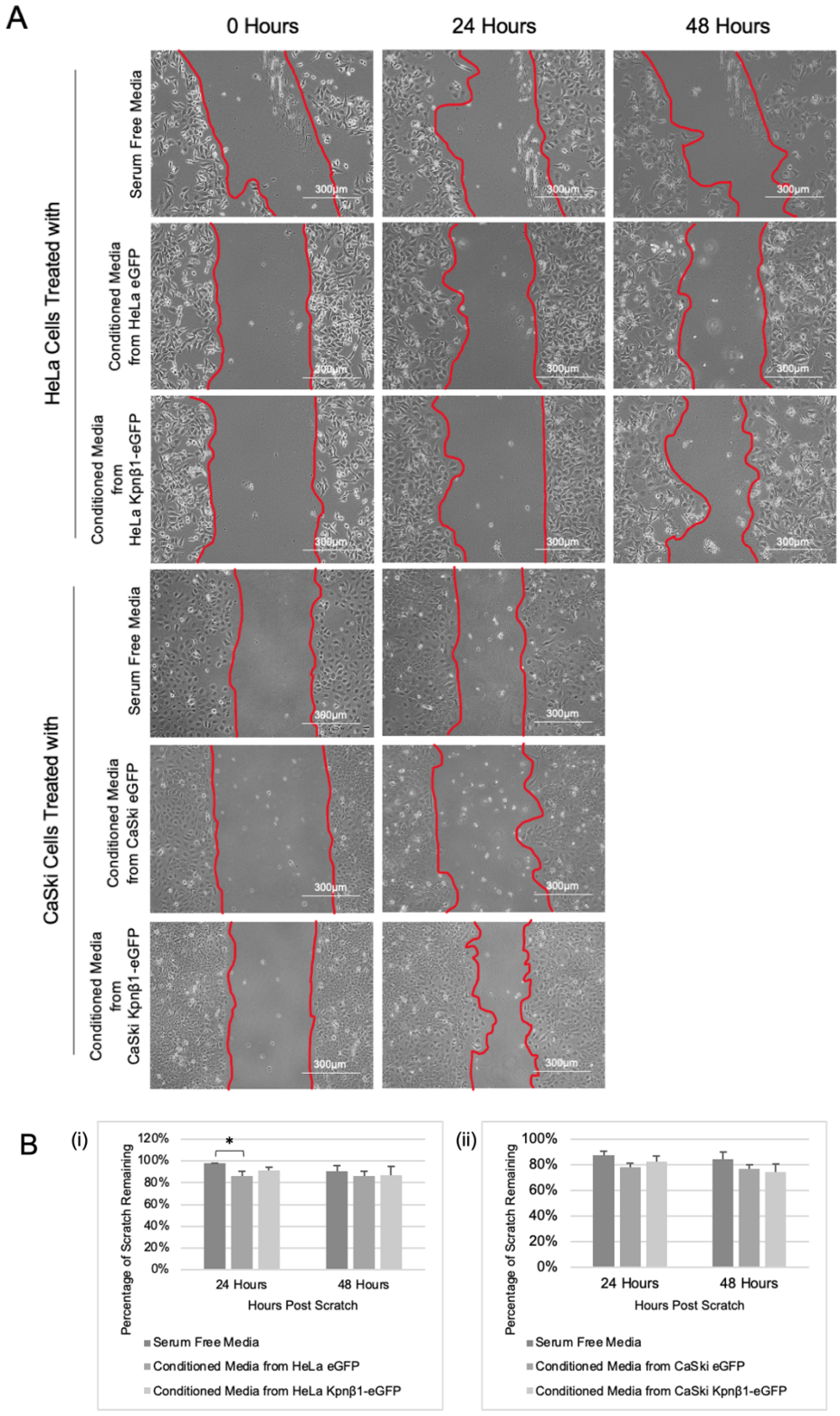

Figure 3.15: Migration of parental HeLa and CaSki cells treated with conditioned media from eGFP and Kpnβ1-eGFP expressing HeLa cells. (A) Migration of cultured HeLa and CaSki cells after the plate is scratched. Images were captured using phase contrast microscopy at a magnification of 10X. (B) Percentage of the scratch area remaining after 24 and 48 hours in (i) Hela cells treated with Hela eGFP and HeLa Kpnβ1-eGFP conditioned media or (ii) CaSki cells treated with CaSki eGFP and CaSki Kpnβ1-eGFP conditioned media. Results are represented as the mean ± SEM. Experiments were performed 3 independent times Statistically significant values ($p < 0.05$) are represented with an *.

The hTERT RPE-1 cells treated with conditioned media from HeLa eGFP or HeLa Kpnβ1-eGFP both show similar migration to the serum-free media treated cells at twenty-four and forty-eight hours (Figure 3.16 A). At forty-eight hours post treatment with the HeLa Kpnβ1-eGFP conditioned media treatment cell migration appeared enhanced compared to the serum free media control but was not statistically significant (Figure 3.16 B).

The treatment with conditioned media from CaSki Kpnβ1-eGFP resulted in a significant increase in migration in the treated hTERT RPE-1 cells twenty-four hours after treatment compared to the CaSki eGFP conditioned media (reduction in original scratch area of 64% vs 48%, $p = 0.009$), or serum free media treatments (64% vs 35%, $p = 0.034$) (Figure 3.16 B). At forty-eight hours post treatment with CaSki eGFP conditioned media migration was increased compared to the control (84% vs 48%, $p = 0.014$), as did the treatment with CaSki Kpnβ1-eGFP conditioned media (84% vs 48%, $p = 0.017$). There did not appear to be a difference between the two treatment groups at forty eight hours (Figure 3.16 A and B).

FG0 cells treated with serum free media, or conditioned media from HeLa eGFP, HeLa Kpnβ1-eGFP, CaSki eGFP or CaSki Kpnβ1-eGFP cells all demonstrated similar migratory ability at both twenty-four and forty-eight hours after treatment (Figure 3.17 A). The FG0 cells appeared to bunch at the scratch edge directly after the scratch was formed, but this did not appear to impede the migration of the cells in the following time points. Quantification of the scratch area across three repeats showed no statistically significant differences in scratch closure across the treatments (Figure 3.17 B). The FG0 cells had almost completely closed the scratch within forty-eight hours making quantification difficult, however the use of *ImageJ* to calculate the area of the scratch remaining allowed as much accuracy as possible.

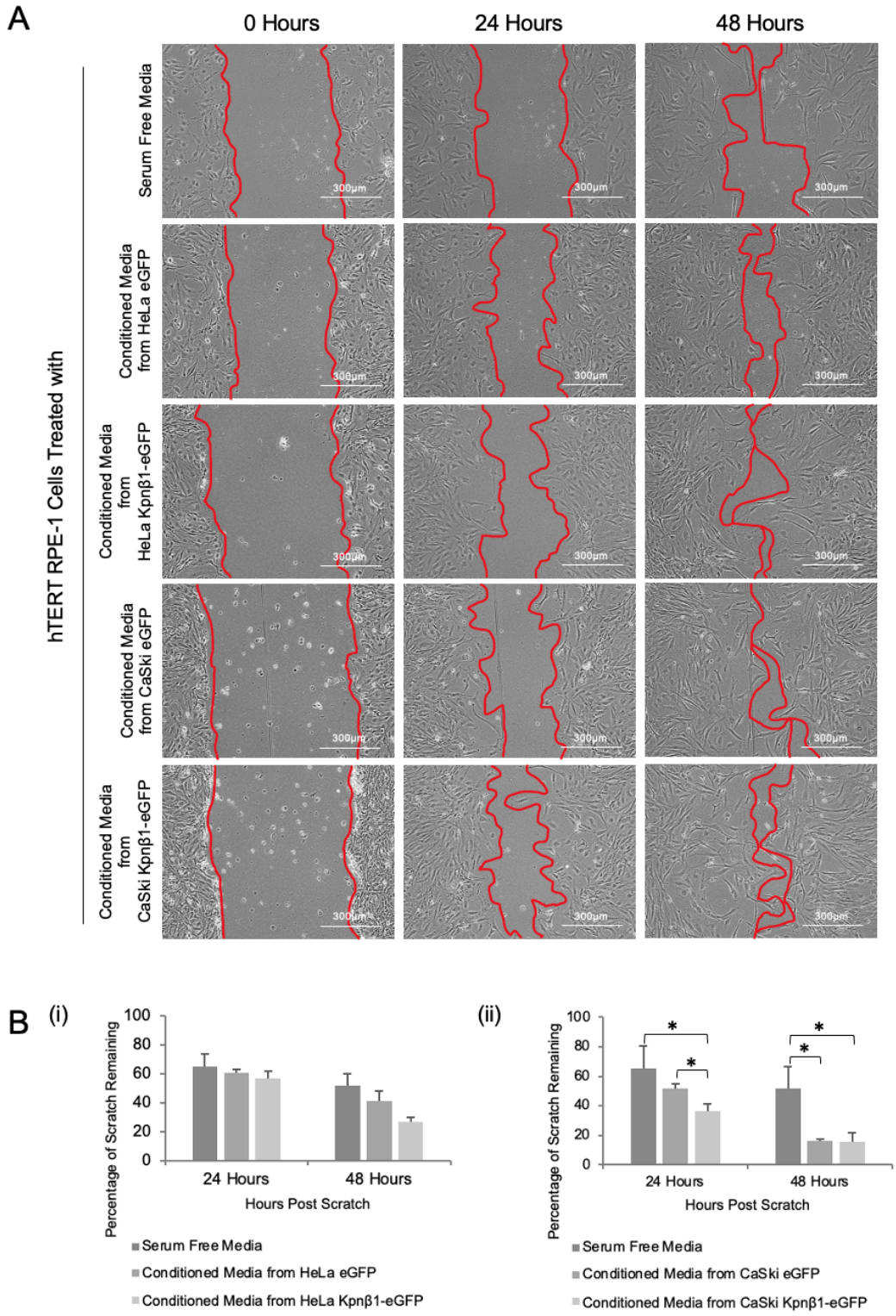

Figure 3.16: Migration of non-cancerous epithelial cells treated with eGFP and Kpnβ1-eGFP conditioned media. (A) Migration of cultured non-cancerous epithelial cells, hTERT RPE-1, after treatment with conditioned media from cervical cancer cells. Images were captured using phase contrast microscopy at a magnification of 10X. (B) Percentage of the scratch area remaining after 24 and 48 hour treatments with conditioned media originating from (i) Hela eGFP or HeLa Kpnβ1-eGFP and (ii) CaSki eGFP or CaSki Kpnβ1-eGFP. Results are represented as the mean ± SEM. Experiments were performed three independent times. Statistically significant values ($p < 0.05$) are represented with an *.

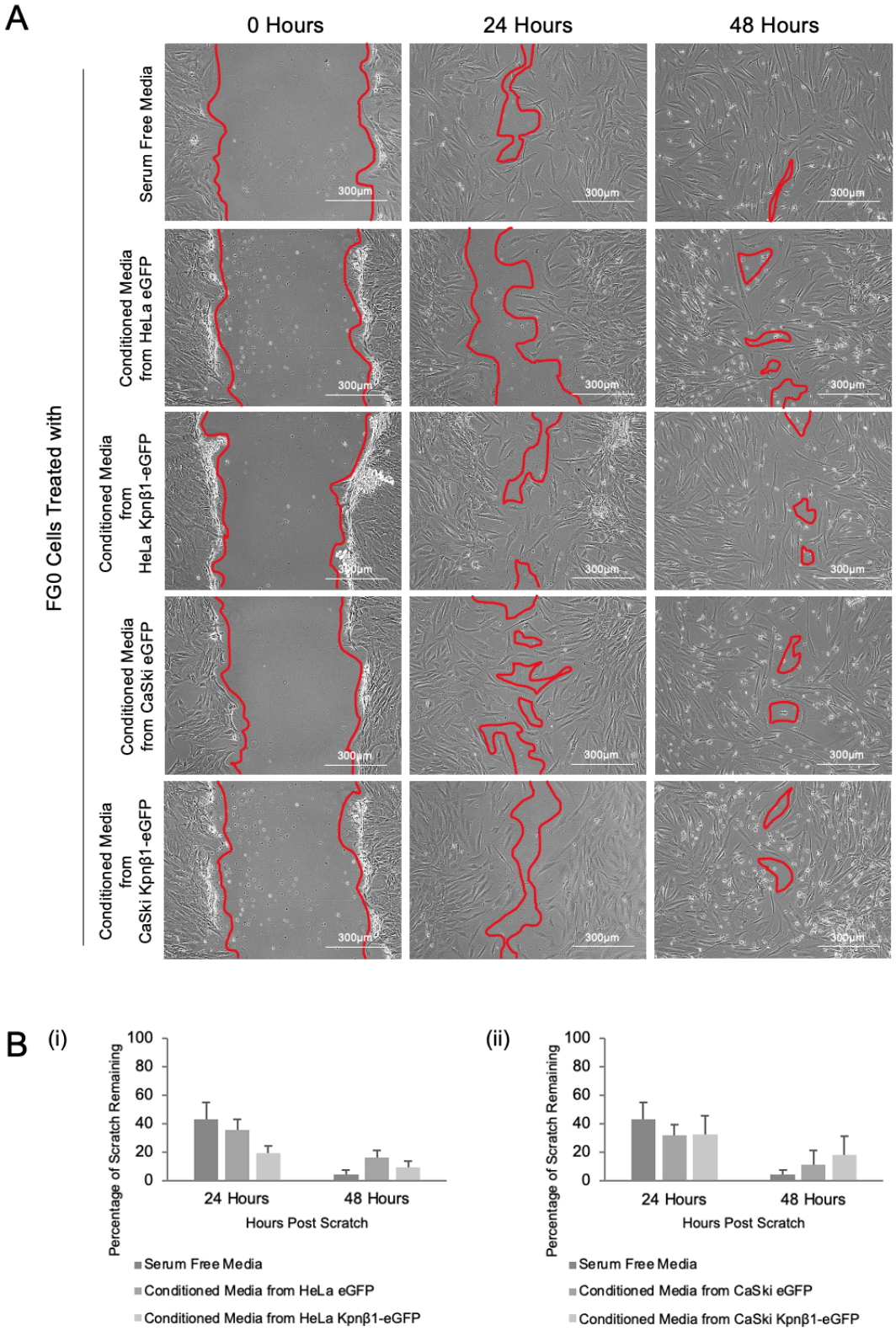

Figure 3.17: Migration of non-cancerous fibroblast cells treated with eGFP and Kpnβ1-eGFP conditioned media. (A) Migration of cultured non-cancerous fibroblast cells, FG0, after treatment with conditioned media from cervical cancer cells. Imaged using phase contrast microscopy at a magnification of 10X. (B) Percentage of the scratch area remaining after 24 and 48 hour treatments with conditioned media originating from (i) Hela eGFP or HeLa Kpnβ1-eGFP and (ii) CaSki eGFP or CaSki Kpnβ1-eGFP. Results are represented as the mean ± SEM. Experiments were performed three independent times.

3.3 Discussion

The role of intracellular Kpnβ1 has been relatively well described in the literature but its secretion into the extracellular space is a fairly recent observation [56]. Whether secreted Kpnβ1 and possibly other nuclear transport proteins can be internalised by cells in a paracrine and autocrine manner and play a role in the biology of the target cells has not been explored to date. Its potential to act in intercellular signalling represents an avenue of research that could lead to a better understanding of cancer cell functioning and enhance its potential as a drug target. This chapter used Kpnβ1-eGFP overexpressing cervical cancer cell lines to investigate the possible effects that secreted Kpnβ1 may have in an autocrine and paracrine manner on cellular phenotypes known to become altered in cancer progression.

Overexpression of Kpnβ1 has been shown to affect several biological processes[72]. To further investigate this the relative proliferation, morphology and migration of eGFP or Kpnβ1-eGFP overexpressing cells were determined. Our results show that overexpressing Kpnβ1 has cell line specific effects which are in agreement with the results presented in Carden *et al.* (2018) with the exception of HeLa proliferation [72]. The relative proliferation of HeLa Kpnβ1-eGFP and HeLa eGFP cells suggests that overexpressed Kpnβ1-eGFP increases proliferation, although this effect is not statistically significant until ninety-six hours after plating. The increase in HeLa Kpnβ1-eGFP cell proliferation in comparison to HeLa eGFP was not observed in the Carden *et al.* (2018) results, rather a reduction in relative proliferation was observed. The cause of this discrepancy is unclear but may be due to changes in cellular behaviour associated with increases in passage number. The proliferation of CaSki Kpnβ1-eGFP and CaSki eGFP indicates that overexpressing Kpnβ1-eGFP reduces the proliferation of the cells relative to eGFP-expressing cells at twenty-four hours, seventy-two hours and ninety-six hours after plating. These results suggest that the effect of overexpressing Kpnβ1-eGFP on cervical cancer cells proliferation is not consistent. The slower proliferation of CaSki cells compared to HeLa cells may have also contributed to the differential effects of overexpressed Kpnβ1 in these cell lines.

The morphology of the Kpnβ1 overexpressing Hela and CaSki cells showed a more clumped growing formation and also results in HeLa Kpnβ1-eGFP cells obtaining a more rounded morphology compared to the HeLa eGFP and wild type HeLa cells. While overexpression of Kpnβ1 has effects on cervical cancer cell proliferation and cell morphology the overexpression of Kpnβ1 in HeLa and CaSki cells does not have a significant effect on the migratory ability of the cells, suggesting that the effects that overexpressed Kpnβ1 have on cell morphology do not affect cell migration.

To target cervical cancer cells and non-cancerous cells with protein lysates secreted by cervical cancer cells in an *in vitro* setting a conditioned media transplant method was used. The conditioned media, from eGFP expressing or Kpnβ1-eGFP overexpressing cervical cancer cells, placed on the cervical cancer cell lines, HeLa and CaSki, was used to target cells originating from the same tissue and cell line in an autocrine manner, whereas the conditioned media placed on the non-cancerous cell lines, hTERT RPE-1 and FG0, was used to target cells from a different tissue in a paracrine manner. The presence of eGFP allowed for the visualisation of uptake of Kpnβ1-eGFP into cells using fluorescent microscopy. Fluorescent microscopy confirmed the uptake of eGFP or Kpnβ1-eGFP at varying levels in all of the treated cell lines, cancerous and non-cancerous. This indicates that Kpnβ1-eGFP can be acquired from the extracellular space by target cells in both an autocrine and paracrine manner. Surprisingly, the cervical cancer cell lines appeared less efficient at internalising eGFP or Kpnβ1-eGFP from the extracellular space in comparison to the non-cancerous cell lines. This suggests that the non-cancer cell lines used in the study are more receptive to internalising factors from cancer cells in a paracrine manner. Alternatively, the cervical cancer cells may be more discriminatory at internalising proteins or exosomes originating from the extracellular space, have capabilities to degrade proteins internalised that non-cancer cells may not have or do not bind the surface proteins on the exosomes facilitating the intercellular signalling[77]. The internalisation of eGFP or Kpnβ1-eGFP in the targeted cells may result in subsequent phenotypical changes but this could also be achieved though the delivery of cargo into the cell directly or into the extracellular space to bind to an extracellular receptor on the target cell [45,71], and as such the internalisation of Kpnβ1 may not be necessary for an intercellular signal to be transferred.

Kpnβ1-eGFP containing secretory protein lysates from cervical cancer cells incubated in an autocrine manner affected the morphology of HeLa cells, causing them to grow in a more clumped pattern. These results suggest that HeLa cell morphology is affected as a result of targeted conditioned media treatments dependent on Kpnβ1. The morphology and growing patterns of the non-cancerous cell line hTERT RPE-1 was not affected by conditioned media treatments from eGFP or Kpnβ1-eGFP expressing cervical cancer cells, where FG0 cells grew in a more tightly packed manner after treatment, however this may have been an artefact of increased proliferation. The differential effects of an extracellular molecule acting in an autocrine or paracrine manner has previously been observed [46]. It has also been suggested that while a specific signalling molecule can act in both an autocrine or paracrine manner there is a specific role that it plays in each [78,79]. As such a signalling molecule could affect morphology while acting in an autocrine manner but not act in a paracrine fashion at all, or not affect target cell morphology when performing this role. This may account for the differences in morphological effects due to secreted Kpnβ1 observed.

Conditioned media treatments targeted to HeLa and CaSki cells also increased proliferation when compared to control cells grown in serum free media. Increased proliferation in the conditioned media however, appeared to be independent of Kpnβ1. As this investigation used conditioned media containing the whole secretome obtained from HeLa and CaSki eGFP and Kpnβ1-eGFP cells, other molecules may be contributing factors to the increased proliferation observed. One such signalling molecule is the Autocrine Motility Factor (AMF), which has been shown to increase proliferation in endometrial cancer cells [80] and has been found in the secretome of HeLa cells [81].

Conditioned media from eGFP or Kpnβ1-eGFP expressing HeLa cells marginally increased migration in HeLa cells. As seen with the proliferation assays, the increase in migratory ability in HeLa cells appeared independent of elevated Kpnβ1 levels. One could also speculate that other factors are essential for the migration. Molecules such as AMF, amongst others may also be a possible driver in this as it has also been shown to increase motility in endometrial cancer[82] and melanoma [83]. The increase in motility may also be due to a molecule present in the secretome of eGFP or Kpnβ1-

eGFP expressing HeLa cells that is not a protein, but rather mRNAs present in extracellular vesicles (EVs), such as an exosome. EV's acting as intercellular signals originating from breast cancer cells have been shown to increase the motility of cells that have taken up those EVs [84]. Conditioned media from eGFP or Kpnβ1-eGFP expressing CaSki cells did not result in a change in migratory ability when targeted to CaSki cells, indicating that the change in migration seen in the treated HeLa cells may be cell line specific. Together, these finding using targeted conditioned media treatments on HeLa and CaSki cells in an autocrine manner showed cell line specific effects that appeared to be independent of elevated Kpnβ1 in the extracellular space.

The conditioned media treatments targeted to non-cancerous cells also had cell line specific effects. The non-cancerous epithelial cell line hTERT RPE-1 had an increase in proliferation when treated with conditioned media from either CaSki or HeLa eGFP expressing or Kpnβ1-eGFP overexpressing cells. However, similarly to the conditioned media treatments in the cervical cancer cells the increase in proliferation appeared to be Kpnβ1 independent. hTERT RPE-1 cells saw an increase in migration after treatment with Kpnβ1-eGFP overexpressing conditioned media from CaSki and Hela. Most notably there was a significant difference in the migratory ability of the hTERT RPE-1 cells between the CaSki eGFP and the CaSki Kpnβ1-eGFP conditioned media treatments after forty-eight hours. This indicates that the increase in migratory ability in the hTERT RPE-1 associates with Kpnβ1-eGFP in the conditioned media, so may be in part be linked to Kpnβ1. This differs from the effects seen in HeLa cells, indicating that the effect on migration is cell line specific. It also appeared to be specific to non-cancerous epithelial cells as the migration of FG0 fibroblast cells targeted with conditioned media from eGFP or Kpnβ1-eGFP expressing cervical cancer cells did not affect cell migration. There is evidence in the literature of cell line specific intercellular signalling, where a signalling molecule may increase motility in one cancer cell type but decrease the motility of another [81].The biological responses of the non-cancerous fibroblast cell line FG0 differed depending on the cell line from which the conditioned media originated. FG0 did not experience any significant changes in proliferation in response to conditioned media prepared from HeLa cells but saw an increase in proliferation after forty-eight hours of treatment with the CaSki conditioned

medias. A marginal but significant increase in proliferation of approximately 15% was observed after treatment with conditioned media from CaSki Kpnβ1-eGFP cells in comparison to that of CaSki eGFP conditioned media, suggesting Kpnβ1-eGFP internalised from the extracellular space could in part confer a small but significant growth advantage to fibroblasts. Cancer cells have been shown to interact with fibroblasts [85] and can stimulate fibroblast cells through intercellular signalling to affect change in the tumour microenvironment [86], all of which corroborates with this finding.

These results suggest a potential role for Kpnβ1 in conditioned media treatments targeted in a paracrine manner to non-cancerous cells as conditioned media from CaSki Kpnβ1-eGFP did increase some cancer-like traits in non-cancerous cells, including increasing proliferation and migration. We postulate that the role Kpnβ1 plays could be direct or indirect, for example by trafficking signalling molecules into the extracellular space and subsequent internalisation with possible binding partners, so requires further investigation.

Summary of Key Findings

- Overexpressing Kpnβ1 in HeLa and CaSki cells had cell line specific effects on proliferation and morphology and did not affect migration in HeLa or CaSki cells.
- The treatment of cancer and non-cancer cell lines with conditioned media in an autocrine or paracrine manner showed internalisation of eGFP or Kpnβ1-eGFP protein from the extracellular space in a cell line specific manner.
- Effects on proliferation as a result of treatments with conditioned media from eGFP or Kpnβ1-eGFP expressing cervical cancer cells in HeLa and CaSki is Kpnβ1 independent, as is the affected migration in HeLa cells.
- Treatment with conditioned media from eGFP or Kpnβ1-eGFP expressing CaSki cells increases the proliferation of FG0 cells and the migration of hTERT-RPE-1 cells and appears to be Kpnβ1 dependent.

Chapter 4: Identifying Kpnβ1 Binding Partners in the Secretome of Cancer Cells

4.1 Introduction

Karyopherin β1 (Kpnβ1), a nuclear transport protein, has been shown to be upregulated in multiple cancer types, including oesophageal and cervical cancer cells compared to non-cancerous cells and is crucial to cancer cell survival [17,24,87]. As such Kpnβ1 represents an important part of cancer cell biology and subsequent functioning, warranting further research into its role in cancer. Kpnβ1 functions to traffic cargo into the cell's nucleus [18] and also has other functions in the cell, such as playing a role in mitosis [21,22]. Kpnβ1 binds cargo proteins that contain a nuclear localisation sequence (NLS) indirectly with the assistance of the adaptor protein Karyopherin subunit alpha 2 (Kpnα2) [18] and directly binds those without a NLS. The structure of the protein contains 19 HEAT repeats in tandem and has both a convex face and a concave face, the latter of which is located just below the C terminus and is responsible for the majority of Kpnβ1's binding to its known binding partners [88]. A depiction of the Kpnβ1 structure is shown in Figure 4.1. The structure of Kpnβ1 allows it to bind a variety of cargo proteins, in an indirect or direct manner, in order to fulfil its functions and assist in cell functioning [18,89].

Figure 4.1: Structure of Kpnβ1 protein. Image was produced using ChimeraX (Version 1.6.1) [90] and developed from the structure solved by Cingolani *et al*. (1999) [91].

Our laboratory has shown that Kpnβ1 is secreted into the extracellular space of cancer cell lines and can be detected in patient serum [56]. Whether secreted Kpnβ1 is bound to any cargo and could serve as a carrier protein for secreted proteins is not known yet. We speculate that Kpnβ1 may be bound to and transport certain proteins into the extracellular space that may play a role in intercellular signalling. There is evidence in the literature that another nuclear transport protein Exportin 1 (CRM1) is responsible for trafficking Ran-GTPase to facilitate intercellular signalling [71]. Determining the binding partners of Kpnβ1 in the extracellular space after it has been secreted by cancer cells could aid in better understanding its role in cellular processes. Also, proteins trafficked into the extracellular space by Kpnβ1 in cancer cells could represent novel biomarkers that may be targeted in cancer treatment and diagnosis. Studies by Liu *et al*. (2016) and Shintani *et al.* (2008), amongst others, showed that agonists against autocrine and paracrine signalling molecules may inhibit intercellular signalling and subsequent effects, representing a potential treatment for cancer [92,93]. Secreted proteins may also be useful as biomarkers in diagnostics, whether it is a signalling molecule or not. Secreted proteins and exosomes are located in a wide variety of bodily fluids [66], allowing non-invasive liquid biopsies to be taken. Liquid biopsies allow for diagnosis of cancers otherwise inaccessible, are less painful than tissue biopsies, and represent an important tool in cancer diagnosis and management[64].

This chapter aims to analyse Kpnβ1 binding partners described in published datasets of intracellular interactions and to identify Kpnβ1 binding partners in the secretome of cervical and oesophageal cancer cells. To address these aims, an analysis of known binding partners of intracellular Kpnβ1 in three published datasets was carried out, as binding partners present intracellularly may also be present extracellularly. Secondly, extracellular protein from the conditioned media of two cervical cancer cell lines: HeLa, and CaSki, and two oesophageal cancer cell lines; WHCO5 and Kyse 30, as well as a non-cancerous cell line hTERT RPE-1 was obtained. Proteins bound to Kpnβ1 in the secretome were identified by immunoprecipitation of Kpnβ1 followed by Western blot analysis of previously described Kpnβ1 binding proteins and mass spectrometry to identify novel Kpnβ1 binding partners in the secretome.

4.2 Results

4.2.1 Analysis of intracellular Kpnβ1 binding partners described in published datasets.

Whilst there are no published reports on Kpnβ1 binding partners secreted by cancer cells, previous studies have investigated the binding partners of intracellular Kpnβ1, particularly in HeLa cells. Three studies in the literature were identified for an analysis of intracellular Kpnβ1 binding partners in HeLa cells [62,63,94]. Two of these, Di Francesco *et al*. (2018) and Okpara *et al*. (2022), used immunoprecipitation mass spectrometry (IP-MS) where Kpnβ1 and any proteins bound to it were isolated using immunoprecipitation and identified using mass spectrometry. The study by Kimura *et al*. (2017) employed a stable isotope labelling by amino acids in cell culture (SILAC) method to isolate Kpnβ1 binding partners, where proteins are labelled using normal or heavy isotope amino acids by introducing the amino acids into the cell culture medium. The isolated proteins are then distinguishable between the heavy and light groups and were subsequently identified using mass spectrometry. The results of these independent investigations were compared to identify common binding partners and subsequently analysed using STRING to determine pathway enrichment.

An analysis of the number of unique and shared intracellular Kpnβ1 binding partners in the three studies are depicted in a Venn diagram (Figure 4.2). The analysis showed that the IP-MS method appeared to yield a higher number of identified proteins, with the investigation by Di Francesco *et al*. (2018) having identified 272 and Okpara *et al*. (2022) identified 179 possible Kpnβ1 binding partners. The SILAC–MS method employed by Kimura *et al*. (2017) only yielded 63 Kpnβ1 binding partners, which is relatively low in comparison to the data obtained using IP-MS methods. Relatively few proteins were found to be common between the three investigations, showing 4 proteins in common in the Kimura, Di Francesco and Okpara studies (Figure 4.2).

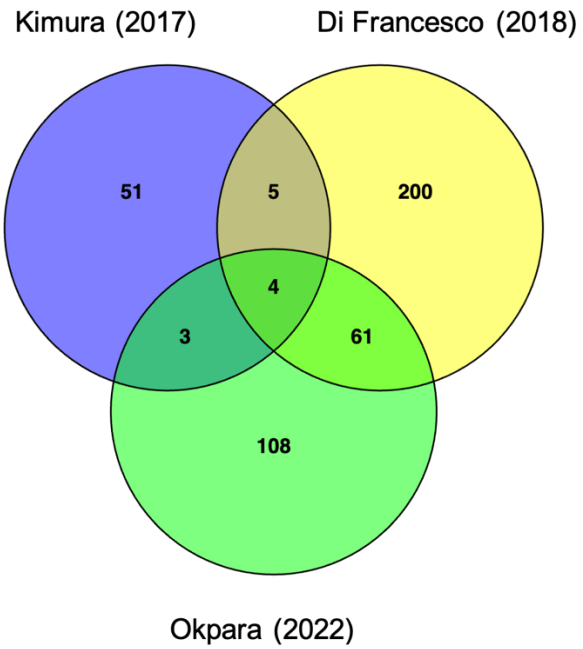

Figure 4.2: Venn diagram showing Kpnβ1 binding partners in HeLa cells identified in published literature. Kpnβ1 binding partners from HeLa cervical cancer cells, HeLa, identified in investigations by Kimura *et al*. (2017), Francesco *et al*. (2018) and Okpara *et al*. (2022). Venn diagram produced using *Venny* (Version 2.1) [95]

The four proteins found common amongst the three studies included: ATP synthase subunit alpha (ATP5F1A), SWI/SNF-related matrix-associated actin-dependent regulator of chromatin subfamily E member 1 (SMARCE1), THO complex subunit 4 (ALYREF) and Importin subunit alpha-1 (KPNA2). A STRING analysis of these four binding partners of Kpnβ1 indicated no known or predicted interactions between them, only an interaction between Kpnβ1 and KPNA2 (Figure 4.3 A). Importin subunit alpha-1 is known to bind Kpnβ1 in the classical nuclear transport pathway [18], hence it's detection as an intracellular binding partner is not surprising. The subcellular localisation of SMARCE1, ALYREF and KPNA2 proteins is primarily reported in the nucleus, whilst ATP5F1A is primarily located in the mitochondrial membrane [96]. There also did not appear to be any biological processes in which they are all involved, which is likely due to their varied roles; ATP5F1A is a metabolic protein, SMARCE1 is a transcription protein and ALYREF1, an exportin adaptor, and KPNA2, an importin adaptor, are both involved in nuclear transport.

The largest group of common binding partners between the published reports included 65 shared Kpnβ1 binding partners identified by Di Francesco *et al*. (2018) and Okpara

et al. (2022), both studies having used an IP-MS approach. The STRING analysis of the Kpnβ1 binding partners common to the Di Francesco and Okpara studies is shown in Figure 4.3 B. The proteins in this group show a large number of interactions. There is a particularly strong clustering of 17 proteins all involved in ribosomal function or mRNA binding. These Kpnβ1 binding partners also have enriched biological process, molecular function and cellular components. Functional enrichments, as determined by STRING, indicate a high presence of these characteristics in comparison to a random set of proteins so suggests that these proteins are involved in these processes or functions. Positive regulation of stress granule assembly and tRNA splicing are both enriched biological processes in this protein group.

The STRING analysis of the 9 Kpnβ1 binding partners in common between Di Francesco *et al*. (2018) and Kimura *et al*. (2017) are shown in Figure 4.3 C. There was only 1 interaction found between Kpnβ1 and KPNA2. The 7 Kpnβ1 binding partners in common between Kimura *et al*. (2017) and Okpara *et al*. (2022) are shown in Figure 4.3 D, showing an interaction between Kpnβ1 and KPNA2 and Kpnβ1 and NUP214, a component of the nuclear pore complex. In both of these groups there was an enriched RNA binding function.

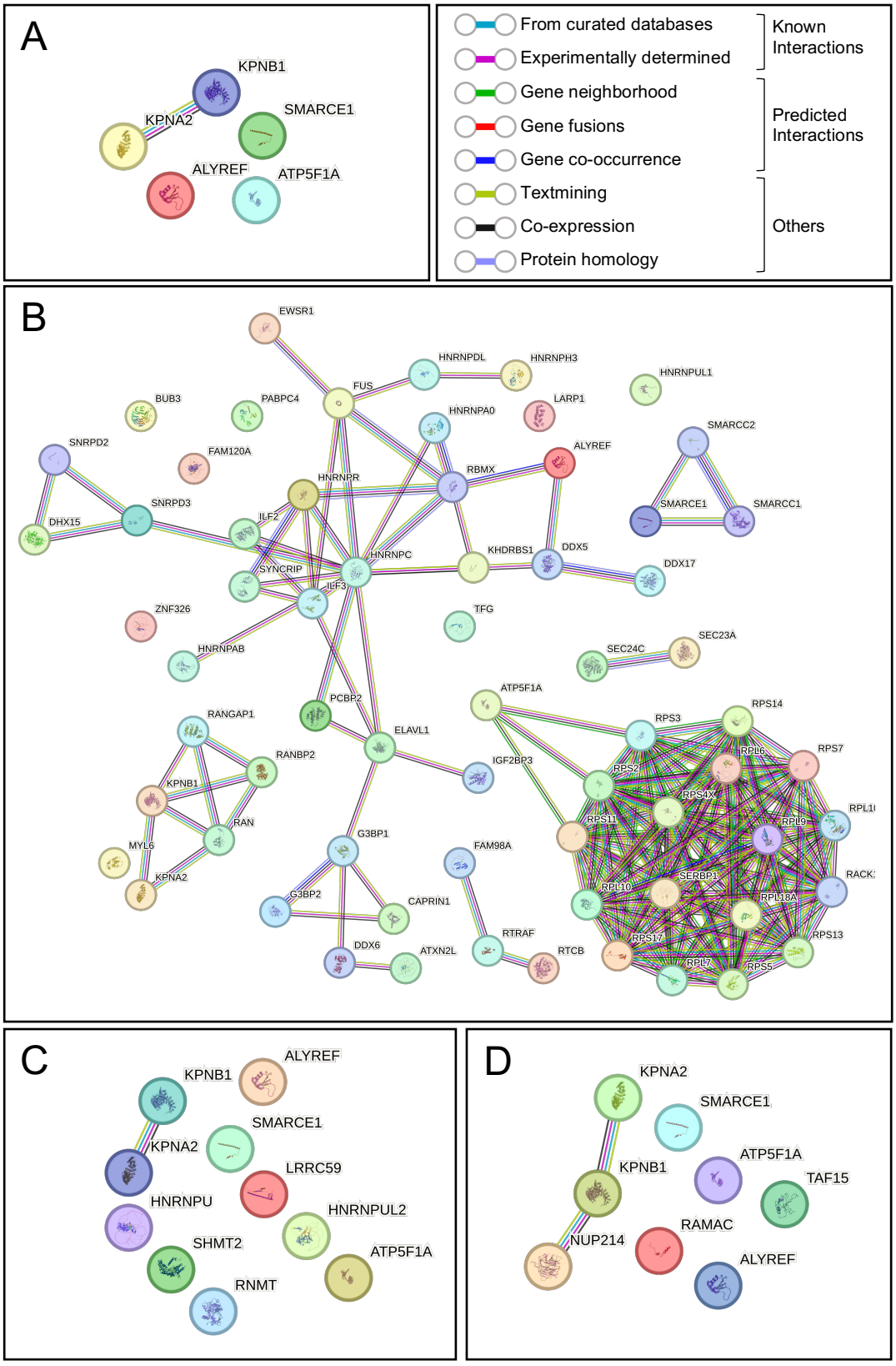

Figure 4.3: STRING protein-protein mapping of common Kpnβ1 binding partners. STRING[96] analysis of proteins shown to bind to intracellular Kpnβ1, in Homo Sapiens, in common between (A) Kimura *et al*. (2017), Di Francesco *et al*. (2018) and Okpara *et al*. (2022), (B) Di Francesco *et al*. (2018) and Okpara *et al*. (2022), (C) Kimura *et al*. (2017) and Di Francesco *et al*. (2018) and (D) Kimura *et al*. (2017) and Okpara *et al*. (2022). Interactions are colour coded and a 90% confidence level was selected for the interactions.

4.2.2 Identification of Kpnβ1 binding partners in secreted protein fractions using co-immunoprecipitation assays

In order to identify the proteins bound to secreted Kpnβ1, extracellular protein was harvested from the conditioned media of cervical cancer cell lines, HeLa and CaSki, oesophageal cancer cell lines, WHCO5 and Kyse30, and a non-cancerous epithelial cell line hTERT RPE-1. These cell lines have previously been used to identify cellular Kpnβ1 binding partners [62]. A total of 1 mg of secreted protein was collected from approximately thirty 10 cm dishes of each cell line and was used in control and Kpnβ1 immunoprecipitation assays. The samples were precleared using Protein A agarose beads then incubated with either an Anti-Karyopherin β1-agarose conjugated antibody or Protein A beads alongside an IgG antibody as a control for possible non-specific interactions. The pulled down protein was then eluted and analysed using a Western blot, probing for binding partners of intracellular Kpnβ1 previously described in the literature.

The Western blots were probed for 8 different proteins including Kpnβ1, to confirm successful immunoprecipitation, and Glyceraldehyde 3-phosphate dehydrogenase (GAPDH), which was used as a negative control, as GAPDH has not been described to bind with Kpnβ1. Six known binding partners of Kpnβ1 were also analysed, including 2 which are involved in nuclear transport and have been shown to bind to intracellular Kpnβ1, namely; CRM1 and Kpnα2 [62]. The remaining 4 known binding partners have been shown to bind intracellular Kpnβ1 in a variety of different pathways; transcription factors cJun [97] and Nuclear Factor Kappa-light-chain-enhancer of activated B cells (NF-κB) [98], a DNA binding protein Far Upstream element Binding Protein 1 (FUBP1) and a cell cycle and apoptosis regulating protein Cell division Cycle and Apoptosis Regulator 1 (CCAR1) [62].

To confirm the presence of proteins in the extracellular protein fraction 15 μg of the extracellular protein used for immunoprecipitation was loaded alongside the Kpnβ1 immunoprecipitated samples and the IgG negative control samples. This was termed the “input”. Western blot results showed that the immunoprecipitation was successful

at pulling down Kpnβ1 from the secretome of all cell lines used in the study (Figures 4.4 (Hela and CaSki), Figure 4.5 (WHCO5 and Kyse30) and Figure 4.6 (hTERT RPE1)), evidenced by the detection of a Kpnβ1 band at 97 kD in both the "Input" and "Kpnβ1" immunoprecipitated lanes and not the "IgG" control lanes.

Western blot analysis of the IP eluates of secreted protein from the cervical cancer interestingly showed that the nuclear transport protein CRM1 (115 kD) was detected in the input secreted protein samples from Hela and CaSki and in the IP Kpnβ1 elution (Figure 4.4). This shows that Kpnβ1 is bound to CRM1 in both the intracellular and extracellular space of the cervical cancer cell lines analysed. It was not detected in the IgG control lane, confirming the specificity of the interaction with Kpnβ1.

Kpnα2 (52 kD) was also detected in the extracellular input protein samples from HeLa and CaSki (Figure 4.4). However, Kpnα2 was only pulled down by Kpnβ1 in the secreted protein sample from CaSki cells, indicating that Kpnα2 was bound to Kpnβ1 in the extracellular space of CaSki cells.

CCAR1 (130 kD) was detected in the secreted protein input of CaSki cells and not in that of HeLa cells (Figure 4.4). CCAR1 was not visualised in the immunoprecipitated samples of CaSki cells, suggesting that it is not bound to Kpnβ1 in the extracellular fraction.

NF-κB (65 kD) was detected, although with faint bands, in the input lanes of HeLa and CaSki cell lines but not in the Kpnβ1 immunoprecipitated samples (Figures 4.4). This suggests that any NF-κB present in the extracellular space of the cervical cancer cell lines is likely not bound to Kpnβ1.

FUBP1 (69 kD) and cJun (39 kD) were not detected in any of the input secreted protein input fractions or immunoprecipitated with Kpnβ1 in HeLa or CaSki cell lines, suggesting that these proteins are likely not secreted by these cell lines (Figure 4.4).

GAPDH (36 kD) was found in the extracellular space of HeLa and CaSki cells, but no GAPDH bands were visualised in the IP eluates (Figure 4.4). This finding was expected as GAPDH has not been reported to bind Kpnβ1.

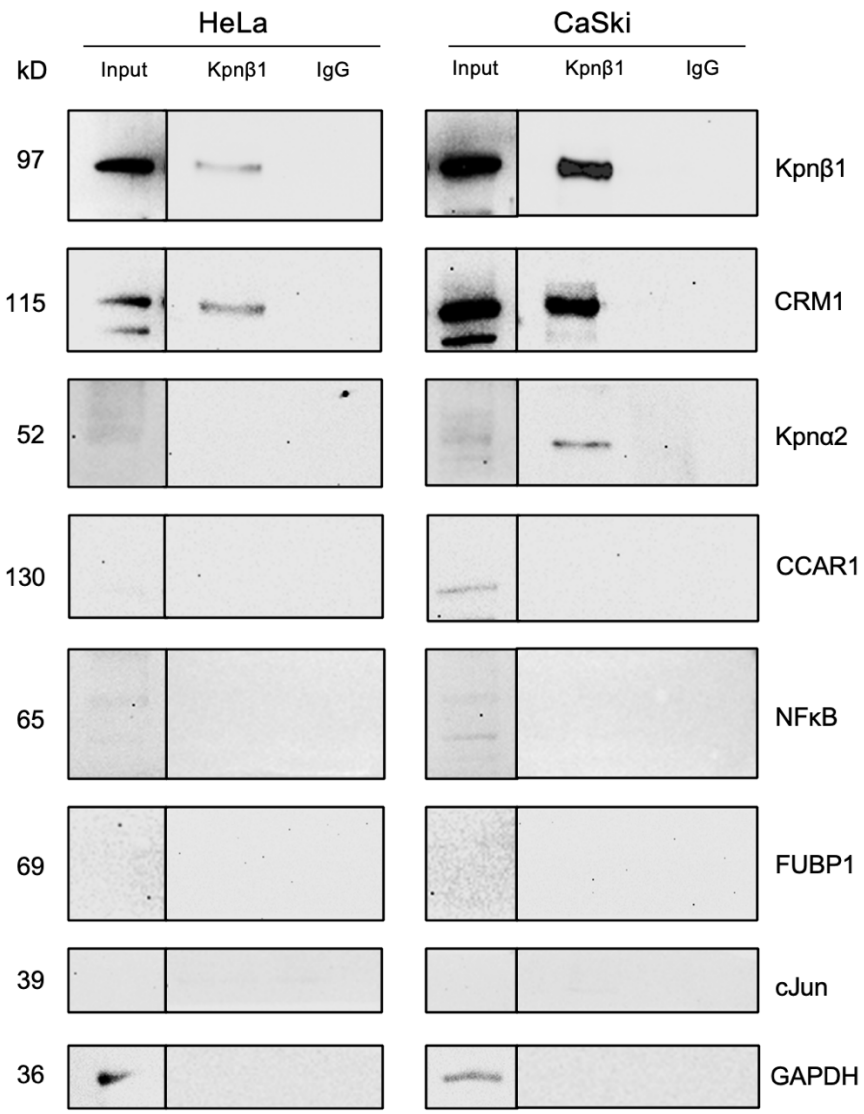

Figure 4.4: Co-Immunoprecipitated Kpnβ1 binding partners from secreted protein of cervical cancer cell lines. Western blot analysis of Kpnβ1 immunoprecipitation eluates using 500 μg of extracellular protein obtained from HeLa and CaSki cells. Immunoprecipitation pull downs using anti-Kpnβ1 bound to agarose beads and IgG control beads are shown alongside 15 μg of the input extracellular protein loaded as a control. Kpnβ1 and CRM1 were pulled down in secreted proteins from both HeLa and CaSki and Kpnα2 was pulled down from the secreted proteins of CaSki. A 12.5% acrylamide gel was used, and the bands were visualised using a Veriblot secondary antibody, which detects only antibodies in their native state.

Western blot analysis of the IP eluates of secreted protein obtained from the oesophageal cancer cell lines, WHCO5 and Kyse30, shows that the immunoprecipitation was successful as high levels of Kpnβ1 were pulled down (Figure 4.5).

CRM1 was detected in the input secreted protein samples from WHCO5 and Kyse30. As with the cervical cancer cell lines, CRM1 was detected in the Kpnβ1 pull-down eluates and not in the IgG control eluates so, interestingly, binds to Kpnβ1 in the extracellular space.

Kpnα2 was not detected in the extracellular input protein samples from WHCO5 or Kyse30 but was in the Kpnβ1 IP eluates (Figure 4.5). This may be as a result of a concentrating effect of the IP process. This indicates that Kpnα2 was likely bound to Kpnβ1 in the extracellular space of these cell lines.

CCAR1 was only detected in the secreted protein of Kyse30 cells (Figure 4.5), indicating that it is inconsistently secreted across cell lines, similarly to the cervical cancer cell lines. CCAR1 was not visualised in the Kpnβ1 immunoprecipitated samples, so is likely not bound to Kpnβ1 in the extracellular space of Kyse30 cells.

NF-κB was detected in the input lanes of both WHCO5 and Kyse30 but was not detected in the Kpnβ1 immunoprecipitated samples (Figure 4.5). As with the cervical cancer cells, this suggests that NF-κB present in the extracellular space of the oesophageal cancer cell lines is not bound to Kpnβ1.

Similar to what was seen in the cervical cancer cells, FUBP1 and cJun were not detected in the input secreted protein fractions or the Kpnβ1 IP eluates in WHCO5 and Kyse30 cells (Figure 4.5).

Additionally, GAPDH was secreted by WHCO5 and Kyse30 cells and as a negative control was not visualised in the Kpnβ1 IP eluates, as in the cervical cancer cell lines.

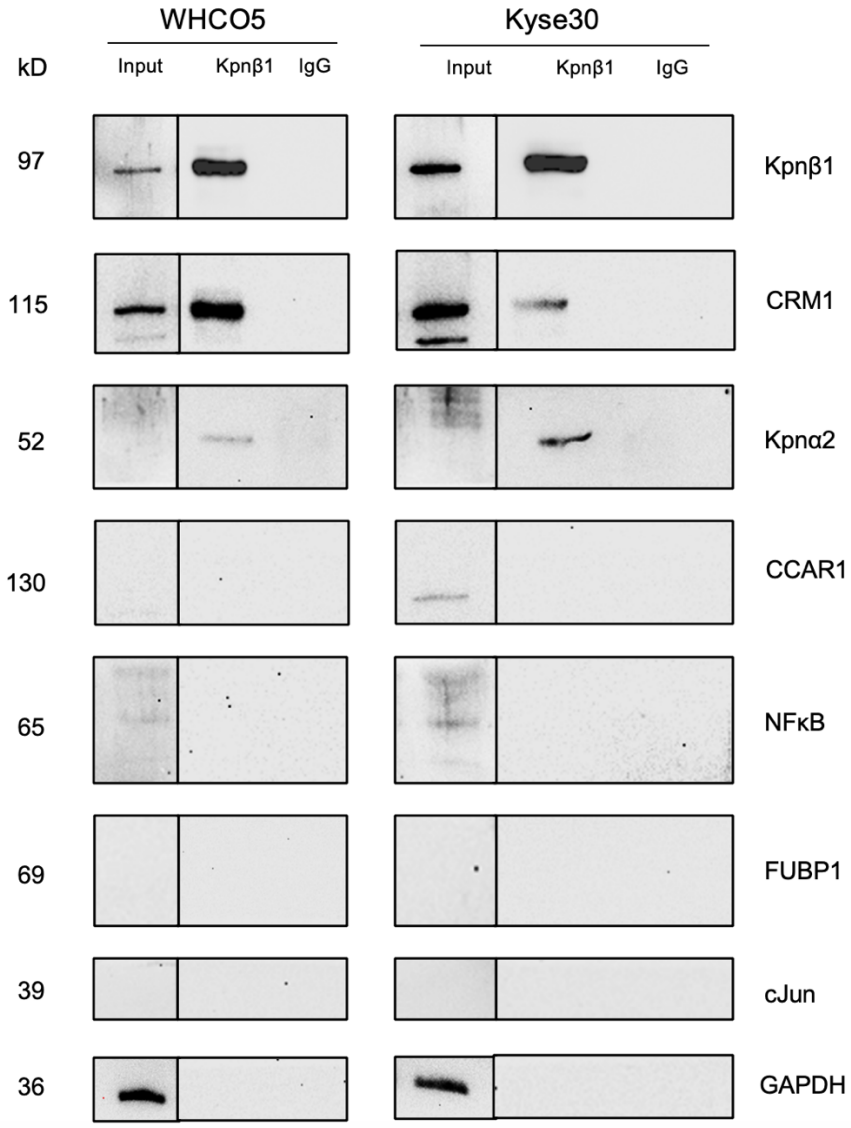

Figure 4.5: Co-Immunoprecipitated Kpnβ1 binding partners from secreted protein of oesophageal cancer cell lines. Western blot analysis of Kpnβ1 immunoprecipitation eluates using 500 μg of extracellular protein obtained from WHCO5 and Kyse30 cells. Immunoprecipitation pull downs using anti-Kpnβ1 bound to agarose beads and IgG control beads are shown alongside 15 μg of the input extracellular protein loaded as a control. Kpnβ1, CRM1 and Kpnα2 were pulled down in secreted proteins from both WHCO5 and Kyse 30. A 12.5% acrylamide gel was used and the bands were visualised using a Veriblot secondary antibody.

The Western blot analysis of the IP eluates of secreted protein from the non-cancerous epithelial cell line, hTERT RPE-1, shows Kpnβ1 was successfully pulled down, albeit at low amounts (Figure 4.6).

CRM1 was detected in the input secreted protein sample from hTERT RPE-1 and in the Kpnβ1 IP eluates so binds Kpnβ1 in the extracellular space, as was seen in the cervical and oesophageal cell lines.

Similarly to the oesophageal cancer cell lines, Kpnα2 was not detected in the input secreted protein of hTERT RPE-1 but was detected in the Kpnβ1 IP eluate (Figure 4.6), indicating that Kpnα2 was bound to Kpnβ1 in the extracellular space of hTERT RPE-1.

CCAR1 was absent from the input secreted protein and the Kpnβ1 IP eluates of hTERT RPE-1 (Figure 4.6).

NF-κB was detected in the input lane but not in the Kpnβ1 IP eluate of hTERT RPE-1 (Figure 4.6), similarly to what was seen in cervical and oesophageal cancer cell lines.

Also, in line with the results from the cervical and oesophageal cancer cell lines used, no FUBP1 or cJun was detected in the input secreted protein or was immunoprecipitated with Kpnβ1 in hTERT RPE-1 (Figure 4.6).

GAPDH was not detected in the secreted fraction of hTERT RPE-1 cells and was also not detected in the Kpnβ1 IP eluate (Figure 4.6).

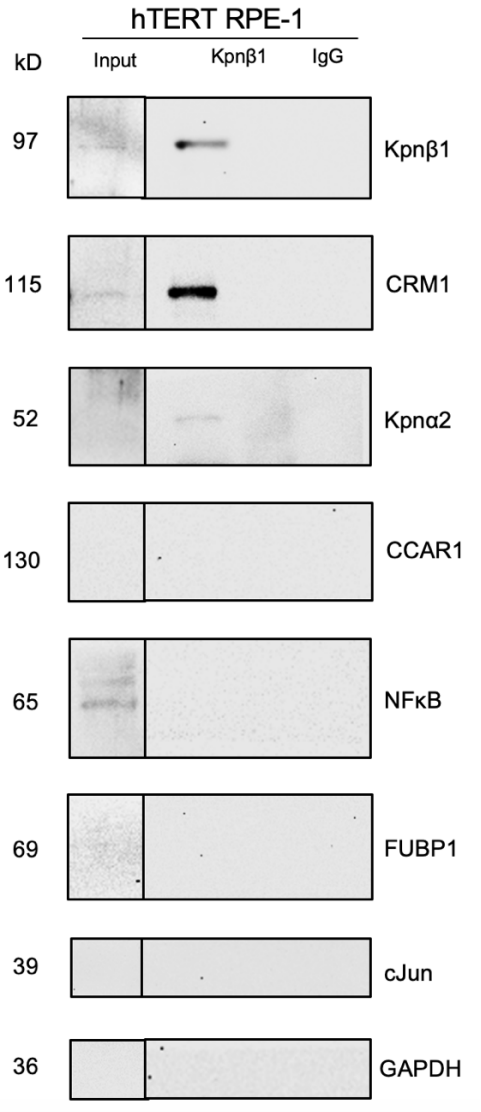

Figure 4.6: Co-Immunoprecipitated Kpnβ1 binding partners from secreted protein of a non-cancerous cell line. Western blot analysis of Kpnβ1 immunoprecipitation eluates using 500μg of extracellular protein obtained from hTERT RPE-1 cells. Immunoprecipitation pull downs using anti-Kpnβ1 bound to agarose beads and IgG control beads are shown alongside 15μg of the input extracellular protein loaded as a control. Kpnβ1, CRM1 and Kpnα2 were pulled down in secreted proteins from hTERT RPE-1 cells. A 12.5% acrylamide gel was used and the bands were visualised using a Veriblot secondary antibody.

As we could show successful pulldown of Kpnβ1 and some of its known binding partners in secreted protein fractions, we next used mass spectrometry to identify additional and possibly novel Kpnβ1 binding proteins that may be carried out of cells in a Kpnβ1-bound manner.

4.2.3 Immunoprecipitation mass spectrometry to identify Kpnβ1 binding partners in secreted protein fractions

Kpnβ1 immunoprecipitation was performed using the same protocol as described above and the samples were analysed by mass spectrometry by the proteomic core facility (D-CYPHR) based in our department.

4.2.3.1 Comparisons of IP-MS data for Kpnβ1-binding partners in protein secreted by cervical and oesophageal cancer cell lines.

The binding partners specific for Kpnβ1 were determined by selecting proteins only present in the Kpnβ1 pull down group by removing those present in the IgG pull down group, to control for non-specific binding to the agarose beads. The lists of secreted Kpnβ1 binding partners identified from HeLa, CaSki, WHCO5, Kyse30 and hTERT RPE-1 are shown in the Appendix (Tables 6.1-6.5). Whilst a number of immunoprecipitated proteins were detected, surprisingly, Kpnβ1 itself was not detected. This may be due to possible low abundance of certain proteins in the secretome combined with the highly stringent conditions used in the analysis of the IP-MS data by the proteomic core facility.

Venn diagrams comparing the proteins that were identified from the two cervical cancer cell lines, HeLa and CaSki, and the two oesophageal cancer cell lines, WHCO5 and Kyse30, is shown in Figure 4.7. The number of secreted Kpnβ1 binding partners identified for each cancer cell line was relatively low compared to those identified for intracellular Kpnβ1 in literature, with 27 in WHCO5, 25 in Kyse30, 20 in CaSki and 4 in HeLa cells. This small numbers of possible Kpnβ1 binding partners may be indicative of low concentrations of protein being present in the extracellular space, with those in smaller amounts possibly below the detection limit for IP-MS analysis, thus limiting the data that could be obtained.

Venn diagrams depicting 16 proteins in common between CaSki and WHCO5, 3 between HeLa and WHCO5 and 1 common protein between HeLa, WHCO5 and

Kyse30 (Figure 4.7). Surprisingly, no common proteins were found between all of the cancer cell lines. Also, no common secreted Kpnβ1 binding partners between the two cervical cancer cell lines and only 1 between the oesophageal cancer cell lines.

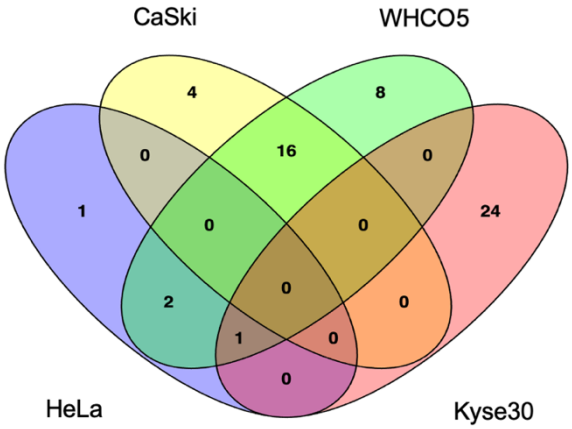

Figure 4.7: Venn diagram showing binding partners of secreted Kpnβ1 pulled down from IP-MS analysis in cancer cells. Kpnβ1 binding partners from the secreted fraction of cervical cancer cells, HeLa and CaSki, and oesophageal cancer cells WHCO5 and Kyse30. Venn diagram produced using *Venny* (Version 2.1) [95]

A STRING analysis of the 16 proteins in common between CaSki and WHCO5 cells showed strong interactions between the common proteins, which were all Histones (Figure 4.8). There was an enrichment in the biological process of nucleosome assembly and the function of chromatin assembly.

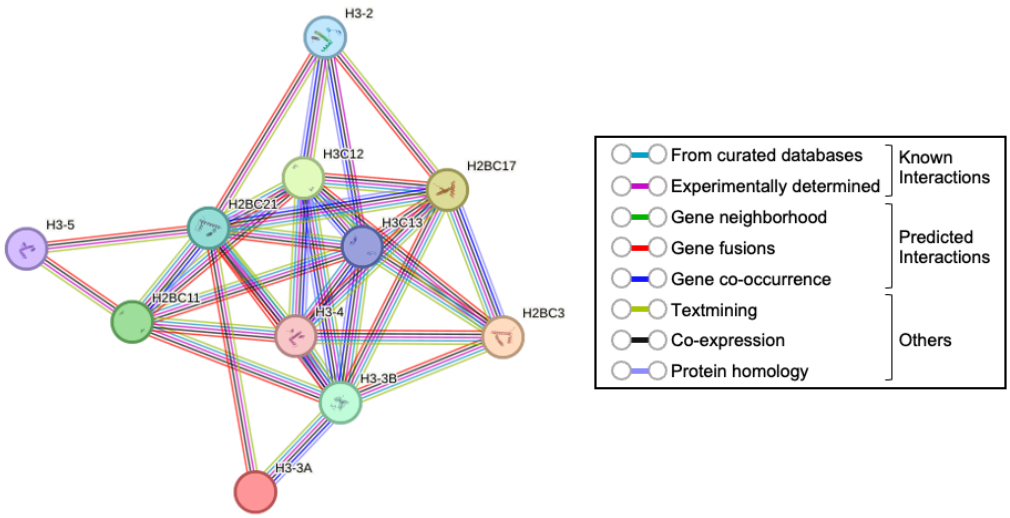

Figure 4.8: STRING protein-protein mapping of common binding partners of secreted Kpnβ1 between WHCO5 and CaSki cancer cells. Secreted Kpnβ1 binding partner proteins from IP-MS analysis in common between oesophageal cancer cells WHCO5 and cervical cancer cells CaSki were found on the STRING [96] database for homo sapiens. Interactions are colour coded and a 90% confidence level was selected for the interactions.

The three secreted Kpnβ1 binding partners in common between HeLa and WHCO5, with 1 being in common between HeLa, WHCO5 and Kyse30, are Laminin β subunits.

4.2.3.1 Comparisons of IP-MS data for Kpnβ1-binding partners in protein secreted by non-cancerous hTERT RPE-1 cells to those secreted by the cancer cells

Possible Kpnβ1 binding partners were identified in the secreted protein of the non-cancerous cell line hTERT RPE-1 in comparison to those from the cancer cell lines (Figure 4.9). Neither cervical cancer cell line had any proteins in common with the hTERT RPE-1 cells (Figure 4.9 A and B).

hTERT RPE-1 cells had 1 binding partner in common with WHCO5 cells (Figure 4.9 C), Actin cytoplasmic 1, N-terminally processed (ACTB).

Four possible binding partners in hTERT RPE-1 were found in common with Kyse30 (Figure 4.9 D). All 4 proteins were subunits of Histone 2A.

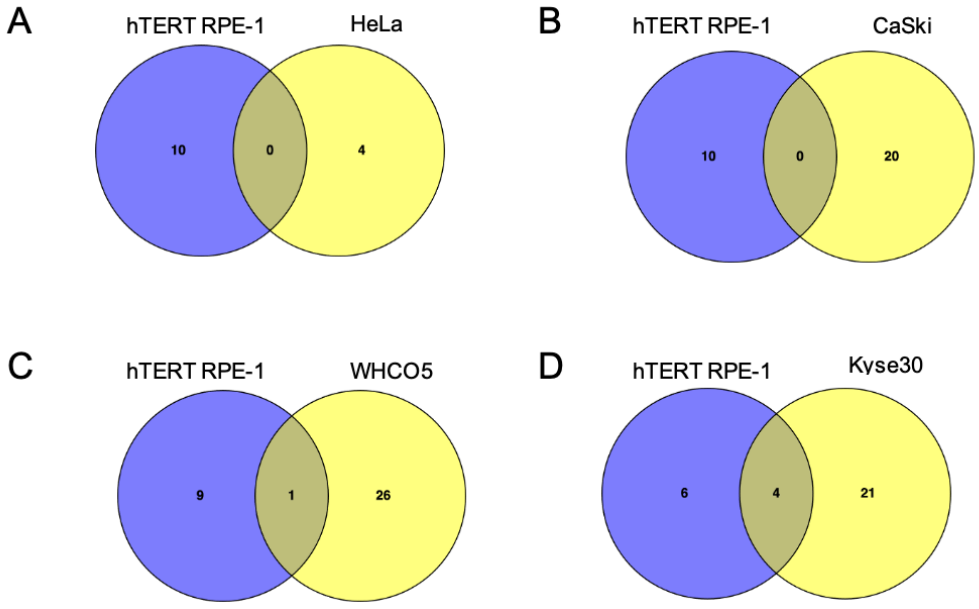

Figure 4.9: Venn diagrams showing binding partners of secreted Kpnβ1 pulled down from IP-MS analysis in non-cancerous cells compared to cancer cells. Secreted Kpnβ1 binding partners from non-cancerous epithelial cells hTERT RPE-1 compared to those from cervical cancer cells (A) HeLa and (B) CaSki and oesophageal cancer cells (C) WHCO5 and (D) Kyse30. Venn diagram produced using *Venny* (Version 2.1) [95]

4.3 Discussion

In the previous chapter, we showed that Kpnβ1 is secreted into the extracellular space and can be internalised in an autocrine and paracrine manner. It can be speculated that proteins bound to intracellular Kpnβ1 may well remain binding partners in the secretome. This chapter aimed to identify potential binding partners of secreted Kpnβ1, firstly by using published literature describing intracellular Kpnβ1 binding partners for likely candidates, as well as using IP-WB and IP-MS experiments. Knowledge of Kpnβ1 and its binding partners may aid in better understanding the function of secreted Kpnβ1 and could also identify or validate potential biomarkers for cancer diagnosis and treatment [47]. To our knowledge, this is a first study aimed at identifying nuclear transport protein binding partners in the secretome.

The role of Kpnβ1 as an intracellular protein and some of its binding partners within cells has been described [62,63,94]. Much however, is still not known regarding all of its possible binding partners. Three independent studies in the literature describing binding partners of intracellular Kpnβ1 using HeLa cervical cancer cells were compared in our study and showed that whilst many different proteins were identified the three studies had few common Kpnβ1 binding partners. The lack of many common Kpnβ1 binding partners may be due to experimental variation and technical differences and requires independent validation of some of the interactions. The IP-MS method provided a much higher yield of identified proteins when compared to the SILAC method [62,63,94] and may be a better method to use when attempting to identify a large number of binding partners, such as those of Kpnβ1. Interestingly, when comparing datasets, there was a very strong presence of proteins bound to Kpnβ1 that were involved in protein synthesis and were localised in the ribosome. The enrichment of molecular function suggests that Kpnβ1 and its binding partners are involved in small ribosomal subunit rRNA binding and mRNA 5-UTR binding, supporting protein synthesis, which is supported by evidence in the literature that shows Kpnβ1 traffics cytoplasmic proteins, including ribosomal proteins [22]. As these investigations had only a few proteins in common and were specific to HeLa cells the

findings may be useful to predict potential binding partners of secreted Kpnβ1 but may not be comprehensive.

Extracellular protein samples from cervical cancer cell lines, HeLa and CaSki, oesophageal cancer cell lines, Kyse30 and WHCO5, and a non-cancerous cell line, hTERT RPE-1, were immunoprecipitated and analysed for known Kpnβ1 binding partners using Western blot analysis and mass spectrometry to identify novel Kpnβ1 binding partners in the secretome. Our Western blot data showed that the exportin, CRM1, was bound to secreted Kpnβ1 in all of the cell lines used. To our knowledge, this is a novel finding. The adaptor protein, Kpnα2, was also found to be bound to secreted Kpnβ1 in CaSki, WHCO5, Kyse30 and hTERT RPE-1 cells, but not in HeLa cells. It is unclear why Kpnα2 was not detected in the Kpnβ1 IP eluates of HeLa cells; it may be due to cell line specific differences or that the detection assay used was not sufficiently sensitive to detect less abundant Kpnα2 in HeLa. Alternatively, it could be due to the high proliferation rate of HeLa cells, and the faster rate of nucleocytoplasmic trafficking, hence more transient Kpnβ1-Kpnα2 interactions. Western blot analysis to detect CCAR1, NF-κB, and FUBP1 proteins, previously identified to bind Kpnβ1 in intracellular cell fractions[62,97,98], indicated that these proteins are not bound to secreted Kpnβ1. However, the Western blot data showed that CaSki and Kyse 30 cells secreted CCAR1, an apoptosis and cell cycle regulator, and all of the cell lines secreted NF-κB, a transcription factor, into the extracellular space, which to our knowledge has not been shown in the literature to date.

The IP-MS experiments using secreted protein fractions yielded low numbers of potential Kpnβ1 binding partners and differed from the investigations into intracellular Kpnβ1 binding partners. The low number of binding partners is not too surprising considering that secreted protein represents a mere fraction of total cellular proteins. Whilst some of the proteins identified using IP-MS using secreted proteins agreed with previously identified endogenous Kpnβ1 binding partners, surprisingly, CRM1 and Kpnα2, which were detected in the IP-WB for all the cell lines tested were not detected by IP-MS. In addition, Kpnβ1 itself was also not detected. This discrepancy may be

due to the low abundancy of proteins in the extracellular space that could be lost in the immunoprecipitation process or as a result of more abundant proteins interfering with the MS detection of proteins of interest with relatively low abundance.

The oesophageal cancer line, WHCO5, and cervical cancer cell line, CaSki, had several common histone proteins bound to Kpnβ1 in the extracellular space. Similarly, Kyse30 and hTERT RPE-1 had a Histone bound to Kpnβ1 in common. This finding is in line with the literature as Di Francesco *et al.* (2018) and Okpara *et al.* (2022) identified subunits of Histone 1 bound to intracellular Kpnβ1, so is supportive that Kpnβ1 bind proteins in the Histone family both intracellularly and extracellularly. Histones are best known for their role in chromatin organisation but have also been shown to localise extracellularly and aid in intercellular signalling in various cell types[99]. In addition to playing a role in intercellular signalling Histone proteins present in the extracellular space appear to have anti-microbial effects, protecting the cell[99,100].

The WHCO5, Kyse30 and HeLa cell lines had Laminin β as a common binding partner of secreted Kpnβ1. Laminin β mediates basement membrane organisation and can play a role in cell migration [101]. It would be interesting to determine if secreted Kpnβ1 bound to Laminin β has a role in cell migration.

WHCO5 and the non-cancerous cell line hTERT TPE-1 had ACTB, an Actin protein, in common as a secreted Kpnβ1 binding partner, which has been shown by Di Francesco *et al.* (2018) to be bound to Kpnβ1 intracellularly, and Okpara *et al.* (2022) also found a protein from the Actin family, ACTL6A, bound to Kpnβ1. ACTB usually functions in the cell's cytoplasm to produce filaments [96,102], hence its possible role in the extracellular space is unclear. A previous study has found that Actin proteins play an important role in cell migration [103], although this was conducted in a non-human mammal cell culture model so could have a different effect in human cells.

Our results indicate that the binding partners of secreted Kpnβ1 are not consistent between the cancer cell lines, or between the cancerous cell lines and the non-cancerous cell line. Interestingly, the oesophageal cancer cell lines had more binding

partners in common with hTERT RPE-1 cells than the cervical cancer cell lines. The disparity between the cell lines may be because binding partners could be cell line specific.

The immunoprecipitated samples were analysed at a MS proteomic core facility that used a standard protocol and it is possible that the parameters of the MS protocol were too stringent and favoured more abundant proteins that may have been present at greater concentration. Indeed, Actin, Laminin and Histones are all highly abundant proteins, and these were detected in the IP-MS. One cannot exclude that there may have been technical difficulties with the IP-MS experiments. Thus, these experiments require optimisation of both experimental and data analysis conditions to arrive at a more accurate picture of Kpnβ1 binding partners in the secretome. Future experiments should include higher amounts of secreted protein, use an inclusion list of known binding partners and use a MS protocol specifically optimised for IP-MS.

Secreted proteins unique to cancer or present in larger quantities in cancer cases may be targeted in cancer treatment and diagnosis. While a intercellular signalling molecule can be targeted to slow disease progression secreted proteins may also be used as a biomarker in diagnostics [47]. As these secreted proteins can be accessed from bodily fluids, non-invasive biopsies may be performed [66], regardless of tumour size or if the tumour is physically inaccessible [64]. CRM1 and KPNα2 secreted by cancer cells have been suggested to be potential biomarkers for cancer diagnosis in cervical and oesophageal cancer [56]. This study validates the presence of these proteins in secreted protein collected from cervical and oesophageal cancer cells. Whilst some were also detected in the secreted protein fraction of the non-cancerous cell line, hTERT RPE-1, a study by van der Watt *et al*. (2022) showed that their levels were significantly higher in the cancer cell lines compared to non-cancer, and in cancer patient serum compared to non-cancer patient serum [56].

Future work into potential cancer biomarkers based on this study may include investigations into the relative expression of secreted CCAR1, NF-κB, Laminin β and Histone 1 and 2 proteins of cervical and oesophageal cancer cells compared to non-

cancerous cells could indicate if they have the potential to act as cancer biomarkers. A protein from the Histone family, Citrullinated histone H3, has been suggested to be a biomarker for advanced cancer in patients [104–106], so supports the use of a Histone as a biomarker, but secreted Histone 1 and 2 proteins are not yet being used as biomarkers for cancer. Future work from this study may also include an investigation into the role of secreted CRM1 and KPNα2, which were shown to associate with Kpnβ1 in the secreted fraction of cancerous and non-cancerous cells, as this is a novel finding.

Summary of Key Findings:

- A comparison of independent studies identifying Kpnβ1 binding partners in HeLa cells showed many binding partners involved in protein synthesis.
- IP-WB showed that secreted Kpnβ1 from HeLa, CaSki, WHCO5, Kyse30 and hTERT RPE-1 is bound to CRM1. It also showed that secreted Kpnβ1 from CaSki, WHCO5, Kyse30 and hTERT RPE-1 is bound to Kpnα2.
- IP-WB showed that CaSki and Kyse 30 cells secreted CCAR1 and HeLa, CaSki, WHCO5, Kyse30 and hTERT RPE-1 secreted NF-κB.
- IP-MS showed secreted binding partners of Kpnβ1 from cancerous cell lines include Histones, ACTB and Laminin β. These proteins may play a role in intercellular signalling and cell migration.

Chapter Five: Conclusion

Previous work in our lab identified Kpnβ1 as upregulated in cancer cells and necessary for cancer cell survival. In addition Kpnβ1 was identified in the secretome of cancer and non-cancer cells [56]. Secreted proteins may act as intercellular signalling molecules, which may affect the functioning of its original cell or the cells surrounding it through autocrine or paracrine signalling [46,47,78,80–83]. The functioning and specific roles of intracellular Kpnβ1 in non-cancer and cancer cells has been relatively well defined but little is known of its extracellular role. To the best of our knowledge this study is a first to investigate a potential the role for Kpnβ1 secreted by cancer cells in the extracellular space.

A model comparing eGFP-expressing and Kpnβ1-eGFP overexpressing cervical cancer cell lines was employed to determine the effects of Kpnβ1 secreted by cancer cells on cells targeted in an autocrine or paracrine manner. The effect of the overexpressed Kpnβ1-eGFP on the phenotypic traits of the cervical cancer cells was also investigated. Kpnβ1-eGFP overexpressing HeLa cells saw an increase in proliferation when compared to the eGFP expressing HeLa cells after ninety-six hours, where the Kpnβ1-eGFP overexpressing CaSki cells saw a reduction in proliferation in comparison to the GFP expressing cells from twenty-four hours post plating. The Kpnβ1-eGFP overexpressing HeLa cells had an altered morphology and both the Kpnβ1-eGFP overexpressing HeLa and CaSki cells saw an altered growing pattern. Neither Kpnβ1-eGFP expressing HeLa cells or CaSki cells showed differed migratory ability in comparison to their respective eGFP expressing HeLa or CaSki cells. These results show that overexpressing Kpnβ1 may alter phenotypical traits in cervical cancer cells, but these effects are cell line specific.

An *in vitro* conditioned media treatment method was used to target cells in an autocrine and paracrine manner. This was evidenced by the internalisation of eGFP by HeLa, CaSki, h-TERT RPE-1 and FG0 cells from conditioned media originating from the eGFP-expressing and Kpnβ1-eGFP expressing cervical cancer cells.

Conditioned media treatments targeted in an autocrine manner to cervical cancer cells increased cell proliferation of the parental HeLa and CaSki cells as well as increased the migratory ability of HeLa cells, but appeared independent of Kpnβ1.

The non-cancerous hTERT RPE-1 cells showed increased cell migration and the non-cancerous FG0 cells showed an increase in proliferation after treatment with conditioned media from CaSki Kpnβ1-eGFP. These changes in biological processes in the non-cancerous cells although cell line specific appeared Kpnβ1 dependent. These results suggest that factors secreted by cervical cancer cells, including Kpnβ1, may alter aspects of the cell biology of non-cancerous cells in a paracrine manner.

Kpnβ1 is able to bind a variety of cargo proteins as a result of its shape and use of adaptor proteins [59,88]. We thus speculated that Kpnβ1 may be bound to and transport cargo proteins into the extracellular space that could have a potential role in intercellular signalling. There have been a few studies investigating the binding partners of cellular Kpnβ1 [62,63,94]. In this study, these published findings were compared and analysed to determine the most likely binding partners and most effective methods to identify binding partners. The IP-MS method used in two of these three studies yielded far more binding partners of Kpnβ1 than the SILAC method used in the third. Comparisons of these studies showed very few endogenous Kpnβ1 binding partners in common. Of the proteins found in common many were involved in protein synthesis, specifically mRNA transport or ribosomal proteins. These studies and others in the literature [97,98] presented possible binding partners of secreted Kpnβ1 and were used to inform the IP-WB experiment performed in this study. IP was used to identify proteins bound to Kpnβ1 in the extracellular space. The isolated binding partners of secreted Kpnβ1 from cervical cancer cells, oesophageal cancer cells and non-cancerous cells were then analysed using both a Western blot and mass spectrometry.

The Western blot analysis showed secreted Kpnβ1 from all the cell lines analysed bound to CRM1 and Kpnβ1 secreted by CaSki, WHCO5, Kyse30 and hTERT RPE-1 was bound to Kpnα2. CCAR1, FUBP1, Ran, cJun and NF-κB, all documented binding partners of endogenous Kpnβ1 [62,97,98], were not found bound to Kpnβ1 secreted by

any of the cell lines tested. The mass spectrometer analysis of the IP eluates yielded relatively few binding partners in comparison to the studies on endogenous Kpnβ1 in the literature. This may be indicative of the low abundance of proteins in the extracellular space and stringent IP-MS methodology and data analysis used. Of those binding partners of secreted Kpnβ1 that were identified using mass spectrometry very few were found to be common between the cancer types, or between the cancerous cells and the non-cancerous cells, suggesting that the binding partners of secreted Kpnβ1 may be cell line specific. The Histones and Actin protein found bound to secreted Kpnβ1 in cancerous and non-cancerous cells are in agreement with the literature as studies on the cellular binding partners of Kpnβ1 have found these proteins or proteins in the same family [62,63]. Histones' functions in the extracellular space include playing a role in intercellular signalling and having antimicrobial effects where Actin is involved in fiber synthesis with a possible role in cell migration[99,100,102,103]. The IP-MS also identified Laminin β as a binding partner of Kpnβ1 secreted by cervical and oesophageal cancer cells. Laminin β plays a role in basement membrane organization and cell migration [101]. The investigation into Kpnβ1 mediated intercellular signalling showed cell line specific effects on cell migration, both Actin and Laminin β may play a mechanistic role in this as they are bound to secreted Kpnβ1 and function in cell migration pathways.

In conclusion, Kpnβ1 secreted by cancer cells may play a role in paracrine intercellular communication, conferring subtle changes to the biological phenotype of non-cancerous cells. In addition, Kpnβ1 in the secretome of cancer and non-cancer cells interacts with several proteins with varied cellular function. The exact nature and purpose of these interactions in the secretome requires further investigation.

5.1 Limitations and Future Perspectives

The IP-MS experiments identified few Kpnβ1 interacting partners in secretory protein fractions and did not detect Kpnβ1, CRM1 or Kpnα2, all of which were identified in the IP-WB. This may be due to low concentrations of Kpnβ1 and other proteins present in the extracellular space. The relatively low abundance of extracellular proteins required

a large number of plated cells hence the culturing of cells in large numbers of tissue culture plates to harvest sufficient secreted proteins for IP experiments was a time-consuming and laborious process. Additionally, the mass spectrometry execution and analysis using the D-CYPHR proteomic core facility in our department, used a standard and stringent protocol and had a considerably long waiting period to have time on the Q-Exactive quadrupole-Orbitrap Mass Spectrometer, hence the MS experiments could not be reproduced in the time frame for this master's study. Ideally, the MS protocol requires optimisation to obtain the best and reproducible results.

To assay biological endpoints such as cell migration in the presence of conditioned media, scratch assays were used. Whilst useful data can be generated using the scratch assay as a proxy for migration, alternative assays such as the trans-well migration assay could in future provide supportive and more conclusive data to what is presented in this study.

One must keep in mind, that the study used cancer and non-cancer cell lines grown in a 2-dimensional cell culture module. This in itself has certain limitations, as the results obtained using 2-D models may not necessarily be reflect in 3-D models and *in vivo* models. Future work will include investigating the effects of Kpnβ1 containing conditioned media in 3-D models such as cancer spheroids.

Future studies could also include the generation and subsequent investigation of overexpressing Kpnβ1-eGFP oesophageal and non-cancerous cell lines to build upon the work with overexpressing cervical cancer lines presented here.

References

1. Basu, A. K. DNA damage, mutagenesis and cancer. *Int. J. Mol. Sci.* **19**, 970 (2018).

2. WHO. The Global Cancer Observatory - All cancers. *Int. Agency Res. Cancer - WHO* **419**, 199–200 (2020).

3. WHO. Cervix uteri Source: Globocan 2020. *Int. Agency Res. Cancer* **419**, 1–10 (2020).

4. Sung, H. *et al.* Global cancer statistics 2020: GLOBOCAN estimates of incidence and mortality worldwide for 36 cancers in 185 countries. *CA. Cancer J. Clin.* **0**, 1–41 (2021).

5. Bruni, L. *et al.* Cervical human papillomavirus prevalence in 5 continents: Meta-analysis of 1 million women with normal cytological findings. *J. Infect. Dis.* **202**, 1789–1799 (2010).

6. WHO & INTERNATIONAL AGENCY FOR RESEARCH ON CANCER. *IARC Monographs on the Evaluation of Carcinogenic Risks to Humans: Human Papillomaviruses*. *Iarc Monographs On The Evaluation Of Carcinogenic Risks To Humans* **90** (2007).

7. Walboomers, J. *et al.* Human Papillomavirus Is a Necessary Cause. *J. Pathol.* **189**, 12–19 (1999).

8. de Martel, C. *et al*. Global burden of cancer attributable to infections in 2018: a worldwide incidence analysis. *Lancet Glob. Heal.* **8**, e180–e190 (2020).

9. WHO. HIV Statistics, globally and by WHO region, 2024. 1–8 (2024).

10. Stelzle, D. *et al.* Estimates of the global burden of cervical cancer associated with HIV. *Lancet Glob. Heal.* **9**, e161–e169 (2021).

11. Goldie, S. J. *et al.* Projected clinical benefits and cost-effectiveness of a human papillomavirus 16/18 vaccine. *J. Natl. Cancer Inst.* **96**, 604–615 (2004).

12. International Agency for Research / World Health Organization (IARC/WHO). Oesophagus (GLOBOCAN 2020). *Int. Agency Res. / World Heal. Organ.* **419**, 2–3 (2021).

13. Toh, Y. *et al.* Alcohol drinking, cigarette smoking, and the development of squamous cell carcinoma of the esophagus: Molecular mechanisms of carcinogenesis. *Int. J. Clin. Oncol.* **15**, 135–144 (2010).

14. Pacella-Norman, R. *et al.* Risk factors for oesophageal, lung, oral and laryngeal cancers in black South Africans. *Br. J. Cancer* **86**, 1751–1756 (2002).

15. Ferndale, L. & Aldous, C. Oesophageal cancer in South Africa: A scoping review. *South African J. Oncol.* **6**, 1–9 (2022).

16. Joo, W. D. *et al.* Targeted cancer therapy – Are the days of systemic chemotherapy numbered? *Maturitas* **76**, 308–314 (2013).

17. Van Der Watt, P. J. *et al.* The karyopherin proteins, Crm1 and Karyopherin β1, are overexpressed in cervical cancer and are critical for cancer cell survival and proliferation. *Int. J. Cancer* **124**, 1829–1840 (2009).

18. Marfori, M. *et al.* Molecular basis for specificity of nuclear import and prediction of nuclear localization. *Biochim. Biophys. Acta - Mol. Cell Res.* **1813**, 1562–1577 (2011).

19. Stelma, T. *et al.* Targeting nuclear transporters in cancer: Diagnostic, prognostic and therapeutic potential. *IUBMB Life* **68**, 268–280 (2016).

20. Sekimoto, T. & Yoneda, Y. Intrinsic and extrinsic negative regulators of nuclear protein transport processes. *Genes to Cells* **17**, 525–535 (2012).

21. Ciciarello, M. *et al.* Importin β is transported to spindle poles during mitosis and regulates Ran-dependent spindle assembly factors in mammalian cells. *J. Cell Sci.* **117**, 6511–6522 (2004).

22. Harel, A. & Forbes, D. J. Importin Beta. *Mol. Cell* **16**, 319–330 (2004).

23. Yang, W. & Musser, S. M. Nuclear import time and transport efficiency depend on importin β concentration. *J. Cell Biol.* **174**, 951–961 (2006).

24. van der Watt, P. J. *et al.*Overexpression of Kpnβ1 and Kpnα2 importin proteins in cancer derives from deregulated E2F activity. *PLoS One* **6**, 1–10 (2011).

25. Weinstein, B. & Joe, A. Oncogene Addiction. *Cancer Res.* **68**, 3080 (2008).

26. Hanahan, D. & Weinberg, R. A. Hallmarks of cancer: The next generation. *Cell* **144**, 646–674 (2011).

27. Stelma, T. & Leaner, V. D. KPNB1-mediated nuclear import is required for motility and inflammatory transcription factor activity in cervical cancer cells. *Oncotarget* **8**, 32833–32847 (2017).

28. Azmi, A. S. *et al.* Exportin 1 (XPO1) inhibition leads to restoration of tumor suppressor miR-145 and consequent suppression of pancreatic cancer cell proliferation and migration. *Oncotarget* **8**, 82144–82155 (2017).

29. Okpara, M. O. Investigating Nuclear Transport Proteins as Secreted Cancer Biomarkers. (2018).

30. Wishart, A. L. Investigating secreted biomarkers for cancer : the potential of nuclear transport proteins. (2017).

31. Cooper, G. Pathways of Intracellular Signal Transduction. in *The Cell: A Molecular Approach. 2nd edition* (2000).

32. Thompson, E. B. & Bradshaw, R. A. Overview of Cell – Cell and Cell – Matrix Interactions. in *Handbook of Cell Signalling* 11–12 (2021).

33. Madeo, M. *et al.* Cancer exosomes induce tumor innervation. *Nat. Commun.* **9**, 4284 (2018).

34. Raposo, G. & Stoorvogel, W. Extracellular vesicles: Exosomes, microvesicles, and friends. *J. Cell Biol.* **200**, 373–383 (2013).

35. Azmi, A. S. *et al.* Exosomes in cancer development, metastasis, and drug resistance: A comprehensive review. *Cancer Metastasis Rev.* **32**, 623–642 (2013).

36. Choi, J. U. *et al.* The biological function and therapeutic potential of exosomes in cancer: Exosomes as efficient nanocommunicators for cancer therapy. *Int. J. Mol. Sci.* **21**, 1–23 (2020).

37. Maas, S. L. N. *et al.* Extracellular Vesicles: Unique Intercellular Delivery Vehicles. *Trends Cell Biol.* **27**, 172–188 (2017).

38. Iraci, N. *et al.* Focus on extracellular vesicles: Physiological role and signalling properties of extracellular membrane vesicles. *Int. J. Mol. Sci.* **17**, (2016).

39. Tian, T. *et al.* Exosome uptake through clathrin-mediated endocytosis and macropinocytosis and mediating miR-21 delivery. *J. Biol. Chem.* **289**, 22258–22267 (2014).

40. Fitzner, D. *et al.* Selective transfer of exosomes from oligodendrocytes to microglia by macropinocytosis. *J. Cell Sci.* **124**, 447–458 (2011).

41. Nanbo, A. *et al.* Exosomes Derived from Epstein-Barr Virus-Infected Cells Are Internalized via Caveola-Dependent Endocytosis and Promote Phenotypic Modulation in Target Cells. *J. Virol.* **87**, 10334–10347 (2013).

42. Valapala, M. & Vishwanatha, J. K. Lipid raft endocytosis and exosomal transport facilitate extracellular trafficking of annexin A2. *J. Biol. Chem.* **286**, 30911–30925 (2011).

43. Zhang, Y. & Wang, X. F. A niche role for cancer exosomes in metastasis. *Nature Cell Biology* **17**, 709–711 (2015).

44. Peinado, H. *et al.* Melanoma exosomes educate bone marrow progenitor cells toward a pro-metastatic phenotype through MET. *Nat. Med.* **18**, 883–891 (2012).

45. Dilsiz, N. Role of exosomes and exosomal microRNAs in cancer. *Futur. Sci. OA* **6**, 4 (2020).

46. Lázár-Molnár, E. *et al.* Autocrine and paracrine regulation by cytokines and growth factors in melanoma. *Cytokine* **12**, 547–554 (2000).

47. Heasley, L. E. Autocrine and paracrine signaling through neuropeptide receptors in human cancer. *Oncogene* **20**, 1563–1569 (2001).

48. Becker, A. *et al.* Extracellular vesicles in cancer: cell-to-cell mediators of metastasis. *Cancer Cell* **30**, 836–848 (2016).

49. Ribeiro, M. F. *et al.* Exosomes function in pro- and anti-angiogenesis. *Curr. Angiogenes.* **2**, 54–59 (2013).

50. Whiteside, T. L. Exosomes and tumor-mediated immune suppression. *J. Clin. Invest.* **126**, 1216–1223 (2016).

51. Park, J. E. *et al.* Hypoxic tumor cell modulates its microenvironment to enhance angiogenic and metastatic potential by secretion of proteins and exosomes. *Mol. Cell. Proteomics* **9**, 1085–1099 (2010).

52. Camussi, G. *et al.* Exosomes/microvesicles as a mechanism of cell-to-cell communication. *Kidney Int.* **78**, 838–848 (2010).

53. Costa-Silva, B. & Lyden, D. Pancreatic cancer exosomes initiate pre-metastatic niche formation in the liver. *Nat. Cell Biol.* **17**, 816–826 (2015).

54. Webber, J. *et al.* Proteomics analysis of cancer exosomes using a novel modified aptamer-based array (somascantm) platform. *Mol. Cell. Proteomics* **13**, 1050–1064 (2014).

55. Van Der Watt, P. J. *et al.* Targeting the nuclear import receptor Kpnβ1 as an anticancer therapeutic. *Mol. Cancer Ther.* **15**, 560–573 (2016).

56. van der Watt, P. J. *et al.* Nuclear transport proteins are secreted by cancer cells and identified as potential novel cancer biomarkers. *Int. J. Cancer* **150**, 347–361 (2022).

57. Mattaj, I. W. & Englmeier, L. Nucleocytoplasmic transport: The soluble phase. *Annu. Rev. Biochem.* **67**, 265–306 (1998).

58. Macara, I. G. Transport into and out of the Nucleus. *Microbiol. Mol. Biol. Rev.* **65**, 570–594 (2001).

59. Pemberton, L. F. & Paschal, B. M. Mechanisms of receptor-mediated nuclear import and nuclear export. *Traffic* **6**, 187–198 (2005).

60. Yuh, M. C. & Blobel, G. Karyopherins and nuclear import. *Curr. Opin. Struct. Biol.* **11**, 703–715 (2001).

61. Cimica, V. *et al.* Dynamics of the STAT3 transcription factor: Nuclear import dependent on ran and importin-β1. *PLoS One* **6**, 5 (2011).

62. Okpara, M. O. *et al.* A mass spectrometry-based approach for the identification of Kpnβ1 binding partners in cancer cells. *Sci. Rep.* **12**, 1–14 (2022).

63. Di Francesco, L. *et al.* Visualization of human karyopherin beta-1/importin beta-1 interactions with protein partners in mitotic cells by co-immunoprecipitation and proximity ligation assays. *Sci. Rep.* **8**, 1–15 (2018).

64. Sheridan, C. Exosome cancer diagnostic reaches market. *Nature biotechnology* **34**, 359–360 (2016).

65. Yang, Y. *et al.* Liquid biopsies in the management of bladder cancer: Next-generation biomarkers for diagnosis, surveillance, and treatment-response prediction. *Crit. Rev. Oncog.* **22**, 389–401 (2017).

66. Caby, M. P. *et al.* Exosomal-like vesicles are present in human blood plasma. *Int. Immunol.* **17**, 879–887 (2005).

67. Brady, P. N. & Macnaughtan, M. A. Evaluation of Colorimetric Assays for Analyzing Reductively Methylated Proteins: Biases and: Biases and Mechanistic Insights. *Physiol. Behav.* **176**, 139–148 (2017).

68. Grela, E. *et al.* Current methodology of MTT assay in bacteria – A review. *Acta Histochem.* **120**, 303–311 (2018).

69. Vang Mouritzen, M. & Jenssen, H. Optimized scratch assay for in vitro testing of cell migration with an automated optical camera. *J. Vis. Exp.* **2018**, 1–6 (2018).

70. van der Watt, P. J. *et al.* The nuclear import receptor Kpnß1 and its potential as an anticancer therapeutic target. *Crit. Rev. Eukaryot. Gene Expr.* **23**, 1–10 (2013).

71. Khuperkar, D. *et al.* Inter-cellular transport of Ran GTPase. *PLoS One* **10**, 1–15 (2015).

72. Carden, S. *et al.* A tight balance of Karyopherin β1 expression is required in cervical cancer cells. *BMC Cancer* **18**, 1–15 (2018).

73. Angus, L. *et al.* Inhibition of the nuclear transporter, Kpnß1, results in prolonged mitotic arrest and activation of the intrinsic apoptotic pathway in cervical cancer cells. *Carcinogenesis* **35**, 1121–1131 (2014).

74. Luther, D. C. *et al.* Protein Delivery: If Your GFP (or Other Small Protein) Is in the Cytosol, It Will Also Be in the Nucleus. *Bioconjug. Chem.* **32**, 891–896 (2021).

75. Kawada, M. *et al.* Stromal cells positively and negatively modulate the growth of cancer cells: Stimulation via the PGE2-TNFα-IL-6 pathway and inhibition via secreted GAPDH-E-cadherin interaction. *PLoS One* **10**, 1–26 (2015).

76. Yang, J. Identification of novel biomarkers, MUC5AC, MUC1, KRT7, GAPDH, CD44 for gastric cancer. *Med. Oncol.* **37**, 1–10 (2020).

77. Christianson, H. C. *et al.* Cancer cell exosomes depend on cell-surface heparan sulfate proteoglycans for their internalization and functional activity. *Proc. Natl. Acad. Sci. U. S. A.* **110**, 17380–17385 (2013).

78. Shih, I. M. & Herlyn, M. Role of growth factors and their receptors in the development and progression of melanoma. *J. Invest. Dermatol.* **100**, S196–S203 (1993).

79. Lu, C. & Kerbel, R. S. Interleukin-6 undergoes transition from paracrine growth inhibitor to autocrine stimulator during human melanoma progression. *J. Cell Biol.* **120**, 1281–1288 (1993).

80. Li, Y. *et al.* Autocrine motility factor promotes endometrial cancer progression by targeting GPER-1. *Cell Commun. Signal.* **17**, 22 (2019).

81. Park, H. S. & Jeoung, N. H. Autocrine motility factor secreted by HeLa cells inhibits the growth of many cancer cells by regulating AKT/ERK signaling. *Biochem. Biophys. Res. Commun.* **525**, 557–562 (2020).

82. Li, Y. *et al.* Autocrine motility factor promotes epithelial-mesenchymal transition in endometrial cancer via MAPK signaling pathway. *Int. J. Oncol.* **47**, 1017–1024 (2015).

83. Silletti, S. *et al.* Autocrine Motility Factor Induces Differential 12-Lipoxygenase. *Cancer Res.* **54**, 5752–5756 (1994).

84. Zomer, A. *et al.* In vivo imaging reveals extracellular vesicle-mediated phenocopying of metastatic behavior. *Cell* **161**, 1046–1057 (2015).

85. Kalluri, R. The biology and function of fibroblasts in cancer. *Nat. Rev. Cancer* **16**, 582–598 (2016).

86. Sever, R. & Brugge, J. S. Signal Transduction in Cancer. *Cold Spring Harb. Perspect. Med.* **5**, (2015).

87. Van Der Watt, P. Expression and regulation of the nuclear transport proteins, Crm1 and Kpnß1, in cervical cancer and transformed cells. (University of Cape Town, 2009).

88. Christie, M. *et al.* Structural Biology and Regulation of Protein Import into the Nucleus. *J. Mol. Biol.* **428**, 2060–2090 (2016).

89. Chook, Y. M. & Süel, K. E. Nuclear import by karyopherin-βs: Recognition and inhibition. *Biochim. Biophys. Acta - Mol. Cell Res.* **1813**, 1593–1606 (2011).

90. Pettersen, E. F. *et al.* UCSF ChimeraX: Structure visualization for researchers, educators, and developers. *Protein Sci.* **30**, 70–82 (2021).

91. Cingolani, G. *et al.* Structure of importin-β bound to the IBB domain of importin-α. *Nature* **399**, 221–229 (1999).

92. Liu, T. *et al.* Capsaicin mediates caspases activation and induces apoptosis through P38 and JNK MAPK pathways in human renal carcinoma. *BMC Cancer* **16**, 1–13 (2016).

93. Shintani, Y. *et al.* ADH-1 suppresses N-cadherin-dependent pancreatic cancer progression. *Int. J. Cancer* **122**, 71–77 (2008).

94. Kimura, M. *et al.* Extensive cargo identification reveals distinct biological roles of the 12 importin pathways. *Elife* **6**, 1–31 (2017).

95. Oliveros, J. C. Venny. An interactive tool for comparing lists with Venn's diagrams. *Version 2.1*

96. STRING. *Version 12.0* Available at: https://string-db.org.

97. Waldmann, I. *et al.* Nuclear import of c-Jun is mediated by multiple transport receptors. *J. Biol. Chem.* **282**, 27685–27692 (2007).

98. Stelma, T. & Leaner, V. D. KPNB1-mediated nuclear import is required for motility and inflammatory transcription factor activity in cervical cancer cells. *Oncotarget* **8**, 32833–32847 (2017).

99. Parseghian, M. & Luhrs, K. Beyond the walls of the nucleus: the role of histones in cellular signaling and innate immunity. *Biochem. Cell Biol.* **84**, 589–604 (2006).

100. Moiana, M. *et al.* A focus on the roles of histones in health and diseases. *Clin. Biochem.* **94**, 12–19 (2021).

101. Ekblom, P. *et al.* Expression and biological role of laminin-1. *Matrix Biol.* **22**, 35–47 (2003).

102. Pollard, T. D. Actin and actin-binding proteins. *Cold Spring Harb. Perspect. Biol.* **8**, 1–17 (2016).

103. Burnette, D. T. *et al.* A role for actin arcs in the leading-edge advance of migrating cells. *Nat. Cell Biol.* **13**, 371–382 (2011).

104. Mauracher, L. M. *et al.* Citrullinated histone H3, a biomarker of neutrophil extracellular trap formation, predicts the risk of venous thromboembolism in cancer patients. *J. Thromb. Haemost.* **16**, 508–518 (2018).

105. Grilz, E. *et al.* Citrullinated histone H3, a biomarker for neutrophil extracellular trap formation, predicts the risk of mortality in patients with cancer. *Br. J. Haematol.* **186**, 311–320 (2019).

106. Thålin, C. *et al.* Citrullinated histone H3 as a novel prognostic blood marker in patients with advanced cancer. *PLoS One* **13**, 1–17 (2018).

Appendix I: Solutions

10% SDS

20g SDS

100ml dH_2O

1M Tris (pH 6.8, 7.5 or 8.8)

60.57g Tris

500ml dH_2O

HCl or NaOH

5M NaCl

146.1g NaCl

500ml dH_2O

1M Glycine

37.5g Glycine

500ml dH2O

10X Transfer buffer

72g Glycine

19g Tris

500ml dH_2O

1X Transfer buffer

100ml 10X Transfer buffer

200ml Isopropanol

700ml dH_2O

10X Running buffer

20g Glycine

31.6g Tris

5g SDS

500ml dH_2O

1X Running buffer

100ml 10x Running buffer

900ml dH_2O

4X loading dye

2.5ml 1M Tris (pH 6.8)

4ml Glycerol

3ml 20% SDS

0.2ml 0.25% bromophenol blue

Make up to 10ml with dH_2O

RIPA Buffer

3ml 5M NaCl

1ml Triton X-100

1g Sodium deoxycholate

1ml 10% SDS

1ml M Tris (pH 7.4)

94ml dH_2O

Complete RIPA Buffer

25ul RIPA

5ul 10X PI

0.5ul 1M NaVO3

10X PBS

17.8g Na2HPO4.2H2O

2.4g KH2PO4

80g NaCl

2g KCl

Make up to 1L with dH_2O

TBST

920ml dH_2O

50ml 1M Tris (pH7.5)

500ul Tween

30ml NaCl

7.5% Resolving gel

3.62ml dH_2O

4ml 1M Tris (pH8.8)

106.7ul 10% SDS

2.88ml 30% Acrylamide

213.3ul 10% APS

21.3ul TEMED

4% Stacking gel

3.65ml dH2O

0.625ml 1M Tris (pH6.8)

50ul 10% SDS

0.650ml 30% Acrylamide

60ul 10% APS

6ul TEMED

Appendix II: Additional Tables

Table 6.1: Kpnβ1 binding partners secreted from HeLa cells identified by IP-MS

Molecular Function	Protein ID	Protein Name	Gene Name	Molecular Weight (kDa)
Basement Membrane	A0A7I2V2T9	Laminin subunit beta-1	LAMB1	155
	A0A7I2V5X5	Laminin subunit beta-1	LAMB1	185
	A0A7I2V3I5	Laminin subunit beta-1	LAMB1	139
Blood Coagulation	D6REL8	Fibrinogen beta chain	FGB	31

Table 6.2: Kpnβ1 binding partners secreted from CaSki cells identified by IP-MS

Molecular Function	Protein ID	Protein Name	Gene Name	Molecular Weight (kDa)
Small molecule binding	H0Y5A1	Prostaglandin-H2 D-isomerase	PTGDS	14
	Q5SQ11	Prostaglandin-H2 D-isomerase	PTGDS	21
Blood Coagulation	P02671	Fibrinogen alpha chain	FGA	95
Antibiotic	Q16778	Histone H2B type 2-E	H2BC21	14
	P06899	Histone H2B type 1-J	H2BC11	14
DNA Binding	P33778	Histone H2B type 1-B	H2BC3	14
	P23527	Histone H2B type 1-O	H2BC17	14
	Q8N257	Histone H2B type 3-B	H2BC26	14
	B4DEB1	Histone H3	H3-3A	14
	K7EMV3	Histone H3	H3-3B	10
	A0A590UJJ6	Histone H3	H3-3A	14
	K7EK07	Histone H3	H3-3B	15
	P68431	Histone H3.1	H3C1	15
	Q16695	Histone H3.1t	H3-4	15
	Q71DI3	Histone H3.2	H3C15	15
	P84243	Histone H3.3	H3-3A	15
	K7ES00	H3.3 Histone B	H3-3B	17
	K7EP01	H3.3 Histone B	H3-3B	13
	Q6NXT2	Histone H3.3C	H3-5	15
	Q5TEC6	Histone H3-7	H3-7	15

Table 6.3: Kpnβ1 binding partners secreted from WHCO5 cells identified by IP-MS

Molecular Function	Protein ID	Protein Name	Gene Name	Molecular Weight (kDa)
Oxygen Transport	P68871	Haemoglobin subunit beta	HBB	16
Hydrolase	E7EVS6	Actin beta	ACTB	37
Basement Membrane	A0A7I2V2T9	Laminin subunit beta-1	LAMB1	155
	A0A7I2V5X5	Laminin subunit beta-1	LAMB1	185
	A0A7I2V3I5	Laminin subunit beta-1	LAMB1	139
Protein biosynthesis	A0A2U3TZH3	Elongation factor 1-alpha	EEF1A2	54
	Q05639	Elongation factor 1-alpha 2	EEF1A2	50
Protein binding	E9PG15	Tyrosine 3-monooxygenase	YWHAQ	17
	A2IDB2	Tyrosine 3-monooxygenase	YWHAH	19
	E7ESK7	14-3-3 protein zeta/delta	YWHAZ	16
Antibiotic	Q16778	Histone H2B type 2-E	H2BC21	14
	P06899	Histone H2B type 1-J	H2BC11	14
DNA Binding	Q96A08	Histone H2B type 1-A	H2BC1	14
	P33778	Histone H2B type 1-B	H2BC3	14
	P23527	Histone H2B type 1-O	H2BC17	14
	B4DEB1	Histone H3	H3-3A	14
	A0A590UJJ6	Histone H3	H3-3A	14
	K7EK07	Histone H3	H3-3B	15
	K7EMV3	Histone H3	H3-3B	10
	P68431	Histone H3.1	H3C1	15
	Q16695	Histone H3.1t	H3-4	15
	Q71DI3	Histone H3.2	H3C15	15
	P84243	Histone H3.3	H3-3A	15
	Q6NXT2	Histone H3.3C	H3-5	15
	K7ES00	H3.3 Histone B	H3-3B	17
	K7EP01	H3.3 Histone B	H3-3B	13
	Q5TEC6	Histone H3-7	H3-7	15

Table 6.4: Kpnβ1 binding partners secreted from Kyse30 cells identified by IP-MS

Molecular Function	Protein ID	Protein Name	Gene Name	Molecular Weight (kDa)
Basement membrane	A0A7I2V5X5	Laminin subunit beta-1	LAMB1	185
Protein biosynthesis	P26641	Elongation factor 1-gamma	EEF1G	50
	P13639	Elongation factor 2	EEF2	95
Cell Adhesion	P14543	Nidogen-1	NID1	136
DNA Binding	A0A0U1RRH7	Histone H2A	H2A	19
	C9J0D1	Histone H2A	H2AZ2	13
	A0A494C189	Histone H2A	H2AZ1	13
	A0A0U1RR32	Histone H2A	H2A	18
	A0A3B3IS11	Histone H2A	H2A	15
	Q9BTM1	Histone H2A.J	H2AJ	14
	Q71UI9	Histone H2A.V	H2AZ2	14
	P16104	Histone H2AX	H2AX	15
	P0C0S5	Histone H2A.Z	H2AZ1	14
	P0C0S8	Histone H2A type 1	H2AC11	14
	Q96QV6	Histone H2A type 1-A	H2AC1	14
	P04908	Histone H2A type 1-B/E	H2AC4	14
	Q93077	Histone H2A type 1-C	H2AC6	14
	P20671	Histone H2A type 1-D	H2AC7	14
	Q99878	Histone H2A type 1-J	H2AC14	14
	Q96KK5	Histone H2A type 1-H	H2AC12	14
	Q6FI13	Histone H2A type 2-A	H2AC18	14
	Q16777	Histone H2A type 2-C	H2AC20	14
	Q7L7L0	Histone H2A type 3	H2AC25	14
Immunity	P07911	Uromodulin	UMOD	70
	X6RBG4	Uromodulin	UMOD	76

Table 6.5: Kpnβ1 binding partners secreted from hTERT RPE-1 identified by IP-MS

Molecular Function	Protein ID	Protein Name	Gene Name	Molecular Weight (kDa)
Hydrolase	E7EVS6	Actin beta	ACTB	37
Protein Biosynthesis	A0A7I2V3H3	Elongation factor 1-alpha	EEF1A1	41
	A0A7I2V5N4	Elongation factor 1-alpha	EEF1A1	47
DNA Binding	C9J0D1	Histone H2A	H2AZ2	13
	A0A494C189	Histone H2A	H2AZ1	13
	Q71UI9	Histone H2A.V	H2AZ2	14
	P0C0S5	Histone H2A.Z	H2AZ1	14
Immunity	A0A087WW87	Immunoglobulin kappa variable 2-40	IGKV2-40	13
	A0A087X0Q4	Immunoglobulin kappa variable 2-40	IGKV2-40	13
	P01614	Immunoglobulin kappa variable 2D-40	IGKV2D-40	13